Expanding Frontiers with Standard Radioisotope Power Systems

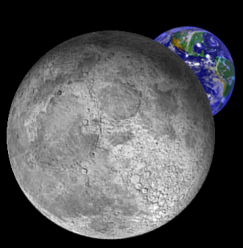

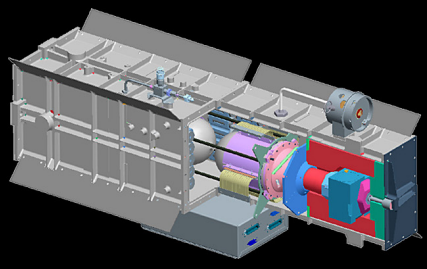

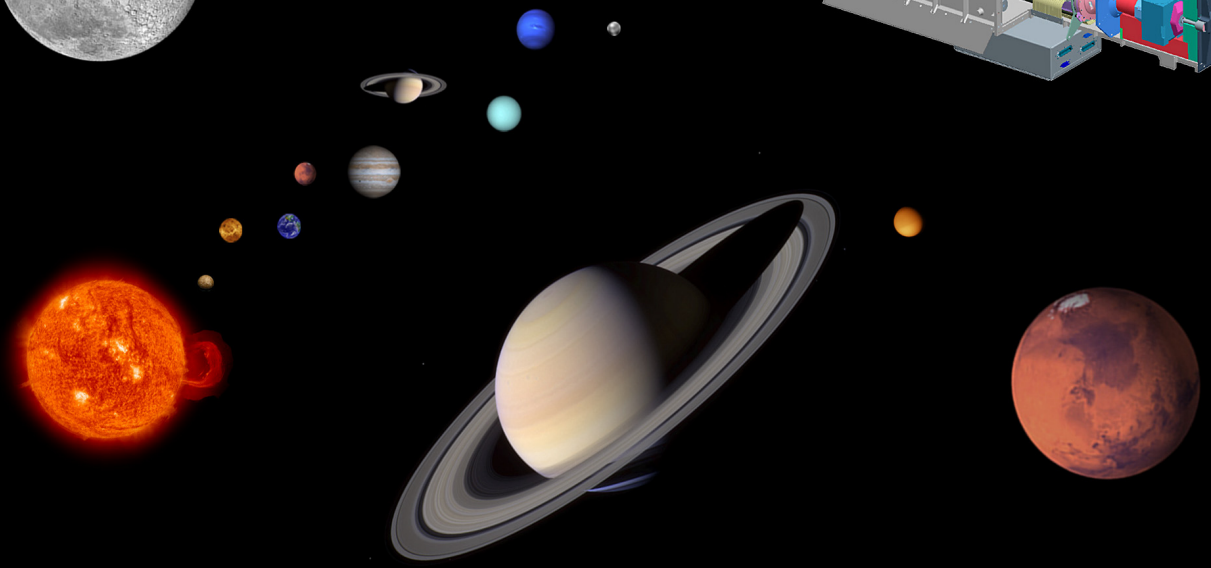

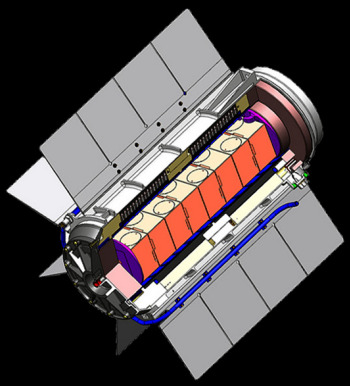

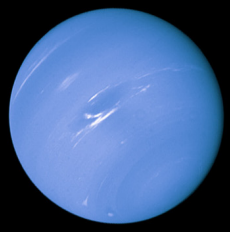

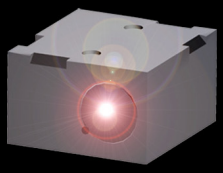

JPL NASA GRC

JPL D-28902
PP-266 0332

Expanding Frontiers with Standard Radioisotope Power Systems

Prepared for the

NASA Science Mission Directorate

Written by

Robert D. Abelson (Editor)	JPL/Caltech
Tibor S. Balint	JPL/Caltech
Keith Coste	JPL/Caltech
John O. Elliott	JPL/Caltech
James E. Randolph	JPL/Caltech
George R. Schmidt	NASA HQ
Timothy Schriener	JPL/Caltech
James H. Shirley	JPL/Caltech
Thomas R. Spilker	JPL/Caltech

January 12, 2005

JPL

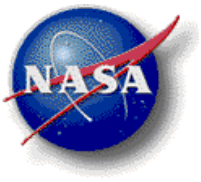

GRC
GLENN RESEARCH CENTER
at Lewis Field

Prepared by the Jet Propulsion Laboratory, California Institute of Technology through an agreement with the National Aeronautics and Space Administration.

Cover Art (Front Left to Right, Top to Bottom): Moon with rising Earth in background, Stirling Radioisotope Generator (SRG), Our Solar System, Saturn and Titan, Mars, Multi-Mission Radioisotope Thermoelectric Generator (MMRTG), Neptune and Triton, General Purpose Heat Source (GPHS) module.

TABLE OF CONTENTS

LIST OF FIGURES

LIST OF TABLES

This page is intentionally blank

1 SUMMARY

1.1 BACKGROUND

Nuclear power has played a significant role in the exploration of the solar system, in many cases enabling missions that could not have been achieved otherwise. First flown by the United States in 1961, radioisotope power systems (RPSs) have consistently demonstrated unique capabilities over other types of space power systems. RPSs generate electrical power by converting the heat released from the nuclear decay of radioactive isotopes (typically plutonium-238) into electricity via one of many conversion processes. The key advantages of RPSs are their long life, robustness, compact size, and high reliability. They are able to operate continuously, independent of orientation to and distance from the Sun, and are relatively insensitive to radiation and other environmental effects. These properties have made RPSs ideally suitable for autonomous missions in the extreme environments of outer space and on planetary surfaces.

The current standard RPS unit used in the United States is the General Purpose Heat Source (GPHS) – Radioisotope Thermoelectric Generator (RTG). These units have been used with great success on the Galileo, Ulysses and Cassini missions, and nominally generate 285 watts of electrical power (from 18 GPHS modules) at the time of their assembly, defined as beginning of life (BOL). However, no new GPHS-RTGs are being produced, and one of two remaining units (a spare from the Cassini and Galileo projects) is slated for the 2006-2007 New Horizons Mission to Pluto and the Kuiper belt. The next generation RPSs are the Multi-Mission Radioisotope Thermoelectric Generator (MMRTG) and the Stirling Radioisotope Generator (SRG). Both of these units are currently in development and would replace the GPHS-RTG as NASA's standard radioisotope power systems. The MMRTG and SRG possess enhanced multi-mission capability over recent RPS designs in their ability to operate both in the vacuum of space and in a range of planetary environments. The MMRTG represents NASA and DOE's low developmental risk approach to next generation RPS development by using flight-proven technologies. The SRG represents a significant evolution in power conversion efficiency, but is the higher developmental risk approach to RPS development due to reduced flight heritage. The MMRTG and SRG would each generate $\geq$110 We at BOM, and both are expected to be available by 2009.

The MMRTG is expected to have a conversion efficiency of >6% at BOM, and use eight GPHS module heat sources and thermoelectric elements made from Lead Telluride (PbTe) / Tellurides of Antimony, Germanium and Silver (TAGS). RTGs have been successfully flown on twenty four previous U.S. space missions (Table 1-1), and the heat source and conversion technology on the MMRTG have significant design heritage from previously flown RPS units. The SRG would use the dynamic Stirling cycle, operating a linear alternator to generate an electrical conversion efficiency of over 20% at BOM using two GPHS module heat sources to generate approximately the same electrical power output as the MMRTG. Though no Stirling convertors have yet flown in space for power generation, twenty-four Stirling units have flown for cryocooler applications on spacecraft for both industry and government.

The requirements for the MMRTG and SRG were developed in 2002 based on the power requirements of five representative proposed missions including the Mars Science Laboratory (MSL), Solar Probe, Europa Orbiter, Pluto Kuiper-Belt, and Titan Explorer [1]. While the Europa Orbiter mission was cancelled, the proposed MSL mission is currently considering the use of one standard RPS, and the Solar Probe mission has baselined three standard RPSs [2]. The Titan Explorer mission is still in the conceptual design phase, and the New Horizons Pluto mission to Pluto and the Kuiper belt has baselined one of the two remaining GPHS-RTGs [3].

Table 1-1. Previous U.S. Space Missions Using Nuclear Power [1-3, 47]

Spacecraft	Principal Energy Source (#)	Destination/ Application	Launch Year	Status
Transit 4A	SNAP-3B7 RTG (1)	Earth Orbit/ Navigation Satellite	1961	RTG operated for 15 yrs. Satellite now shut down.
Transit 4B	SNAP-3B8 RTG (1)	Earth Orbit/ Navigation Satellite	1961	RTG operated for 9 yrs. Operation intermittent after 1962 high alt test. Last signal in 1971.
Transit 5BN-1	SNAP-9A RTG (1)	Earth Orbit/ Navigation Satellite	1963	RTG operated as planned. Non-RTG electrical problems on satellite caused failure after 9 months.
Transit 5BN-2	SNAP-9A RTG (1)	Earth Orbit/ Navigation Satellite	1963	RTG operated for over 6 yrs. Satellite lost navigational capability after 1.5 yrs.
Transit 5BN-3[1]	SNAP-9A RTG (1)	Earth Orbit/ Navigation Satellite	1964	Mission aborted because of launch vehicle failure.
Nimbus B-1[2]	SNAP-19B2 RTG (2)	Earth Orbit/ Navigation Satellite	1968	Mission aborted because of range safety destruct. RTG heat sources recovered and recycled.
Nimbus III	SNAP-19B3 RTG (2)	Earth Orbit/ Navigation Satellite	1969	RTGs operated for over 2.5 yrs. No data taken after that.
Apollo 11	ALRH Heater	Lunar Surface/ Science Payload	1969	Heater units for seismic experimental package. Station shut down Aug 3, 1969.
Apollo 12	SNAP-27 RTG (1)	Lunar Surface/ Science Payload	1969	RTG operated for about 8 years until station was shut down.
Apollo 13[3]	SNAP-27 RTG (1)	Lunar Surface/ Science Payload	1970	Mission aborted. RTG reentered intact with no release of Pu-238. Currently located at bottom of Tonga Trench.
Apollo 14	SNAP-27 RTG (1)	Lunar Surface / Science Payload	1971	RTG operated for over 6.5 years until station was shut down.
Apollo 15	SNAP-27 RTG (1)	Lunar Surface / Science Payload	1971	RTG operated for over 6 years until station was shut down.
Pioneer 10	SNAP-19 RTG (4)	Planetary / Payload & Spacecraft	1972	Spacecraft now well beyond Pluto. Last signal received January 23, 2003.
Apollo 16	SNAP-27 RTG (1)	Planetary / Payload & Spacecraft	1972	RTG operated for about 5.5 years until station was shut down.
Triad-01-1X	Transit-RTG (1)	Earth Orbit/ Navigation Satellite	1972	RTG still operating as of mid-1990s.
Apollo 17	SNAP-27 RTG (1)	Planetary / Payload & Spacecraft	1972	RTG operated for almost 5 years until station was shut down.
Pioneer 11	SNAP-19 RTG (4)	Planetary / Payload & Spacecraft	1973	Spacecraft traveled to Jupiter, Saturn and beyond. Last signal received September 30, 1995.
Viking 1	SNAP-19 RTG (2)	Planetary / Payload & Spacecraft	1975	RTGs operated for over 6 years until lander was shut down.
Viking 2	SNAP-19 RTG (2)	Planetary / Payload & Spacecraft	1975	RTGs operated for over 4 years until relay link was lost.
LES 8, LES 9[4]	MHW-RTG (4)	Earth Orbit / Com Satellites	1976	LES 8 was shutdown in 2004. LES 9 continues to operate.
Voyager 2	MHW-RTG (3)	Planetary / Payload & Spacecraft	1977	RTGs still operating. Spacecraft successfully operated to Jupiter, Saturn, Uranus, Neptune, and beyond.
Voyager 1	MHW-RTG (3)	Planetary / Payload & Spacecraft	1977	RTGs still operating. Spacecraft successfully operated to Jupiter, Saturn, and beyond.
Galileo	GPHS-RTG (2) RHU Heater (120)	Planetary / Payload & Spacecraft	1989	RTGs continued to operate until 2003, when spacecraft was intentionally deorbited into Jupiter atmosphere.
Ulysses	GPHS-RTG (1)	Planetary / Payload & Spacecraft	1990	RTG continues to operate successfully after 14 years. Spacecraft conducting polar solar orbits.
Mars Pathfinder	RHU Heater (3)	Mars Surface Rover Electronics	1996	Heater units used to maintain payload temperature. Units still presumed active.
Cassini	GPHS-RTG (3) RHU Heater (117)	Planetary / Payload & Spacecraft	1997	RTGs continue to operate successfully after 7 years. Spacecraft entered Saturn orbit in 2004.
Mars MER Spirit	RHU Heater (8)	Mars Surface Rover Electronics	2003	Heater units still operational and used to maintain payload temperature.
Mars MER Opportunity	RHU Heater (8)	Mars Surface Rover Electronics	2003	Heater units still operational and used to maintain payload temperature.

1. Mission was aborted due to launch vehicle failure. RTG burned up on reentry as designed.
2. Mission was aborted due to launch vehicle failure. RTG heat sources recovered, recycled and used on subsequent mission.
3. Mission aborted on way to Moon. RTG reentered Earth atmosphere intact with no release of Pu-238. It is currently located deep in the Tonga Trench in the South Pacific Ocean.
4. Mission consisted of two RPS-powered communications satellites (LES 8 and 9) launched on a single launch vehicle.

1.2 PURPOSE

The purpose of this report is to identify the range of mission concepts and applications that could be enabled by the newest generation of standard multi-mission radioisotope power systems, the MMRTG and SRG. It describes the results of the most recent set of JPL mission studies using realistic estimates of RPS performance, and provides information for review by potential users that may benefit from these types of power systems. The report also identifies the possible advantages of each type of standard RPS unit as a function of mission category and application. Also identified are the potential operating environments (pressure, temperature, atmospheric composition and g-load) that future spacecraft, and thus the standard RPSs, may encounter. This data is meant to benefit the RPS technology community in assessing the environmental operating requirements of the MMRTG and SRG units. This report also provides a current set of top-level performance requirements for each standard RPS type to assist the mission studies community in performing realistic system trades using radioisotope power systems.

This report is divided into three sections. Section 1 summarizes the results of the activities to date and lists the space science and human precursor missions that could potentially be enabled by standard RPSs. Section 2 presents the detailed results of four mission concept studies that demonstrate the overall feasibility of standard RPS-powered missions and summarizes the top-level goals and objectives of the remaining missions identified in this study. Section 3 summarizes the current technical performance characteristics of the MMRTG and SRG units for mission planning purposes.

1.3 RESULTS

Twenty-seven potential missions and applications were identified in this study (Table 1-2) that could potentially be enabled by standard RPS technology. These concepts were, in many cases, based on the priorities defined in the Decadal Surveys of the National Academies [8], or support the goals and objectives outlined in the Vision for Space Exploration [9]. Nine concepts are space missions, eight are mobility missions (e.g., aerobots and surface rovers), five are lander missions, and five are human base infrastructure support applications. Two flight projects are also included in the table (MSL and Solar Probe) as they are currently baselining the standard RPS power source.

Detailed studies were performed for four mission concepts, including a Triton lander, a Dual-Mode Lunar Rover Vehicle (DMLRV), a Titan Aerobot, and a Saturn Ring Observer. The results of the mission studies indicate that the MMRTG and SRG each have distinct benefits with regards to their use on deep space missions. The following paragraphs identify the potential benefits of each RPS system for a given set of mission parameters, and suggest the favored RPS unit for a given mission configuration.

The MMRTG would be well suited for missions able to utilize the excess heat (~1900 Wt at BOM) generated by its eight GPHS modules, compared with the SRG's two GPHS modules (~400 Wt of excess heat at BOM). Missions that could potentially benefit from the excess RPS heat are those that would operate in extremely cold environments such as the surface of Europa, Titan, and permanently shadowed areas of the Moon. These concepts could potentially use the excess RPS heat to maintain spacecraft operating temperatures (i.e., via heat pipe systems, etc.) in place of electric heaters, potentially freeing up electrical power for instruments and other subsystems.

The MMRTG utilizes thermoelectric conversion, which is a vibration-free process. This would potentially make the MMRTG better suited for missions using vibration-sensitive instruments (e.g., seismometers) that measure low-amplitude motions (such as seismic activity from tectonic motions or volcanic events). Though the SRG uses synchronous opposed Stirling converters [10] to minimize vibration, it remains a dynamic conversion process and could have residual motion that might impact sensitive seismic measurements.

The MMRTG would be favored from the perspective of proven reliability and lower technical risk. MMRTG technology is very mature, sharing significant design heritage with the SNAP-19 RTGs used on the Viking surface missions, with the MHW-RTGs used on the Voyager deep-space missions, and with the GPHS-RTGs used on the Galileo, Ulysses and Cassini deep space missions. The failure modes of the MMRTG are well understood, and are more likely to provide graceful degradation than the SRG.

Initially, the MMRTG could have an advantage from a mass perspective, as current NASA/DOE guidelines recommend that early missions using SRGs carry at least one redundant SRG unit until its reliability has been verified [11]. This means that early missions using SRGs would need to carry a minimum of two SRG units. Thus, for early missions (where a redundant SRG would be required), the MMRTG (at $\leq$45 kg [10]) would be the lighter option for spacecraft requiring one or two RPS units. At three RPSs, the mass difference between using MMRTGs and SRGs (including a mandatory fourth spare unit) becomes minimal, representing a breakpoint from a mass perspective (i.e., the mass of three MMRTGs is nearly the same as four SRG units). Missions requiring more than three RPSs would benefit overall from the SRG's lighter mass (~34 kg [10]), even with the addition of one redundant unit. However, the redundant SRG would not simply be a "dead weight", and could be used to enhance mission performance, if the spacecraft was able to use the additional power to exceed its baseline performance values. Rover missions, for example, would be well suited to use the added power of the redundant SRG to increase the rover's speed and range beyond the "nominal" mission goal. In the event that an SRG were to fail during the mission, the rover would simply return to its "nominal" power level, having already capitalized on the excess power to achieve enhanced mobility. Once the early SRG-powered missions have flown and the SRG's reliability successfully demonstrated, the redundant-SRG policy would likely be relaxed making this RPS the lightest option overall.

Both the MMRTG and SRG are specified to have an electrical power output of $\geq$110 We at BOM. However, the MMRTG is currently predicted to generate ~125 We in deep space (BOM), and 123 We on the surface of Mars (BOM) [12]. The SRG, on the other hand, is currently predicted to generate 116 We in deep space (BOM), and 103 We on Mars (BOM) [13]. The higher BOM power output of the MMRTG (particularly on Mars) would be preferred from a total power perspective. Note, however, that both standard RPS units are in development, and thus their power outputs continue to evolve as their designs mature.

The SRG could be favored for missions where there would be difficulty in rejecting excess heat to the environment. The SRG generates 25% of the thermal power of the MMRTG, which could be a significant benefit for missions that require the RPS to be housed within an aeroshell (e.g., for atmospheric entry, performing an aerocapture maneuver, etc.) or integrated within a spacecraft fuselage where the heat could not be directly radiated to space. Both the MMRTG and SRG have fluid lines that could be used to cool the RPS in addition to their radiator fins; however, an external pump would be required to operate the fluid loop, and the greater quantity of waste heat from the MMRTG could result in a larger, more complicated pumping system being required relative to that for the SRG.

The radiation levels of the MMRTG and SRG are both relatively low, and not expected to pose any significant issues for most mission concepts. However, for missions that require minimal radiation dose, the SRG has the advantage of generating only 25% of the radiation of the MMRTG due to the SRG's higher conversion efficiency. The radiation dose from the MMRTG and SRG can be further reduced by using additional shielding (with an additional mass penalty) or by physically separating the RPS from the payload or crew.

The higher efficiency of the SRG would also make this RPS favored from the standpoint of fuel conservation. Each SRG contains two GPHS modules corresponding to about 1 kg of Pu-238, while each MMRTG contains eight GPHS modules, corresponding to about 4 kg of Pu-238. Plutonium is an expensive component of the RPS in terms of cost and the time it takes to acquire and manufacture the fuel. The fact that the United States currently does not have the capability to produce its own Pu-238, and must purchase it from foreign sources, makes the more efficient SRG an attractive option from the perspective of making future missions less susceptible to potential fuel shortages.

All missions identified in this study had a maximum g-load requirement expected to be achievable with the existing MMRTG and SRG designs. The greatest accelerations would be expected to occur during launch, atmospheric entry, and landing, and would require an appropriate method (e.g., parachutes, airbags, or Sky Cranes in an atmosphere environment; soft landers in vacuum environment) to reduce the deceleration load below the 30g design requirement. Were the MMRTG and SRG capable of withstanding larger acceleration loads (hundreds of g's), then airbag landings on the Moon, Europa, Triton, and other bodies with minimal or no atmosphere might be possible. System-level trades would need to be performed to assess the relative mass and cost penalties of a reinforced RPS and whether they were offset by the simpler airbag landing system relative to a soft lander approach.

The minimum lifetime requirement of both RPSs is specified as 14 years from BOM [7]. However, the MMRTG and SRG are expected to be robust units, and there is nothing intrinsic in their design that would prevent them from running longer, albeit at decreasing power levels. The fact that the RTGs on both Voyager spacecraft are still operating nearly 30 years after launch demonstrates this robustness. The thermal and electrical power output from the standard RPSs is expected to gradually and predictably decrease due primarily to 1) Pu-238 decay (MMRTG and SRG), 2) sublimation of the thermoelectrics within the MMRTG, and 3) degradation of the thermal insulation within the SRG.

Both standard RPS designs include integrated radiator fins to reject their excess heat to the ambient environment. These fins make up a sizable fraction of the total physical envelope of the MMRTG, and to a lesser degree with the SRG, and must be properly oriented to the environment to be effective. Both RPS designs also include cooling tubes that could be charged with a working fluid and externally pumped by the spacecraft to reject the excess heat via alternate pathways. For spacecraft concepts having significant size and configuration constraints (e.g., the DMLRV concept of Section 2.4), this study suggests that a variant of the MMRTG or SRG without integrated radiator fins could be beneficial. Heat removal would be performed by an external pumping system using the RPSs cooling tubes and a separate radiator optimized for the overall spacecraft design. The removal of the fins could permit the RPS unit to be closely spaced to

Table 1-2. Mission Concepts Potentially Enabled by Standard RPSs

#	Mission / Application	Power Level (Preliminary)	Pressure[1] (Ambient)	Atmospheric Composition	Temperature[2] (Min Ambient)	Temperature[3] (Max Ambient)
Spacecraft / Satellite Concepts						
1	Saturn Ring Observer*	300 We	Vacuum	N/A	4K	>4K
2	Solar Probe - Flight Project	300 We	Vacuum	N/A	4K	TBD
3	Jovian Magnetospheric Remote Sounder	200 We	Vacuum	N/A	4K	>4K
4	Jovian Magnetospheric In-Situ Constellation	100 We	Vacuum	N/A	4K	>4K
5	Europa Orbiter	300 We	Vacuum	N/A	4K	>4K
6	Saturn Magnetospheric Remote Sounder	200 We	Vacuum	N/A	4K	>4K
7	Saturn Magnetospheric In-Situ Constellation	100 We	Vacuum	N/A	4K	>4K
8	Neptune Orbiter	300 We	Vacuum	N/A	4K	>4K
9	Triton Orbiter	300 We	Vacuum	N/A	4K	>4K
10	Pluto and Charon Orbiter	300 We	Vacuum	N/A	4K	>4K
Mobility Concepts (Aero, Surface, Subsurface)						
11	Dual-Mode Lunar Rover Vehicle*	300 We	Vacuum	N/A	-190°C	110°C
12	Titan Aerobot*	100 We	1.5 atm	N_2, CH_4	-179°C	-179°C
13	Mercury Polar Rover	100 We	Vacuum	N/A	-183°C	427°C (-183°C)[3]
14	Mercury Night-Side Rover	100 We	Vacuum	N/A	-183°C	427°C (-183°C)[3]
15	Venus Aerobot	100 We	0.01 atm[5]	CO_2, N_2, Ar	-45°C[5]	-45°C[5]
16	Lunar Surface Rover**	100 We	Vacuum	N/A	-190°C	110°C
17	Mars Science Laboratory - Flight Project	300 We	0.01 atm	CO_2, N_2, Ar	-133°C	27°C
18	Mars Surface Rover	100 We	0.01 atm	CO_2, N_2, Ar	-133°C	27°C
19	Triton Rover	100 to 200 We	15E-6 atm	N_2, CH_4	-235°C	-235°C
Lander Concepts						
20	Triton Lander*	100 We	15E-6 atm	N_2, CH_4	-235°C	-235°C
21	Mercury Polar Lander	100 We	Vacuum	N/A	-183°C	427°C (-183°C)[4]
22	Mercury Night-Side Lander	100 We	Vacuum	N/A	-183°C	427°C (-183°C)[4]
23	Mars Deep Drill	100 We	0.01 atm	CO_2, N_2, Ar	-133°C	27°C
24	Europa Lander	100 We	Vacuum	N/A	-223°C	-133°C
Human Base Infrastructure Support						
25	Life Support System	≥100 We	Moon: Pressure=Vacuum, Tmin=-190°C, Tmax=110°C Mars: Pressure=0.01 atm, Tmin=-133°C, Tmax=27°C			
26	In-Situ Resource Utilization	≥100 We				
27	Base Construction Tools	≥100 We				
28	Base Site Preparation	≥100 We				
29	Generic Power Source	≥100 We				

Notes
1. Values represent surface pressure levels where applicable. Vacuum defined here as < 1E-8 atm.
2. Estimate of the minimum terrestrial body surface temperature [References 5-7] or the temperature of deep space (for satellite missions). Does not account for planetary fly-bys, planetary albedo or solar reflection which may increase the maximum ambient temperature value.
3. Estimate of the maximum terrestrial body surface temperature [References 5-7] or the temperature of deep space (satellite missions). Actual mission parameters will detemine the realized minimum temperature.
4. Mercury maximum temperature is 427°C on Sun-facing side. The night-side and inside permanently shadowed craters is expected to be closer to the minimum temperature of -183°C.
5. Venus atmospheric temperature and pressure representative of environmental conditions at an altitude of ~65 km.

* Mission study conducted by JPL RPS Mission Studies Team and documented in this report.
** Mission study performed by JPL Team-X and not presented in this report.

other spacecraft subsystems or tightly packed against other RPSs. This would permit greater flexibility in designing the spacecraft, in optimizing the heat rejection system, and could result in a vehicle that is smaller overall. In addition, missions to extremely cold bodies with convective atmospheres (e.g., Titan) may require the fins be significantly shortened or removed completely.

The MMRTG and SRG have each been designed to operate in a range of environments that includes Earth (for assembly, storage, and launch), Mars (surface operations) and deep space. This requires that the MMRTG and SRG operate over a pressure range of at least one atmosphere down to vacuum, over a sink temperature range of -269 to 31°C (4 to 304K), and within atmospheres rich in oxygen (O_2), carbon dioxide (CO_2) and nitrogen (N_2). These RPS requirements represent a broad range of environments that cover the majority of the mission destinations identified within this study. Venus surface missions, however, are beyond the capabilities of either standard RPS unit due to the extreme temperatures (464°C) and pressures (90 bar) existing there [17-19], and thus are not considered in this report.

Missions to the surface of the Moon, Mercury and Titan need additional thermal analysis to assess their overall feasibility and any additional spacecraft/RPS requirements. A Moon surface mission in direct view of the sun could expose the RPS to temperatures as high as 110°C. Though both RPS units could operate at this temperature, their conversion efficiency could be decreased due to the higher heat rejection temperature. Using a sunshade to shield the RPS from direct solar exposure could be one mitigating option for missions where the reduction in efficiency was deemed unacceptable. A mission to a permanently shadowed crater at the pole of Mercury, or to Mercury's dark side, could expose the spacecraft to temperatures as low as -183°C in the shade. This low temperature is not an issue for either RPS design; however, the RPS would need to be shielded to prevent direct exposure to the Sun during approach and landing, where the temperature could exceed 400°C. Judicious spacecraft design (e.g., using thermal shields) and orientation relative to the Sun could potentially mitigate this issue and allow the RPS to maintain its nominal operating temperatures. The extremely cold environment of Titan also may pose a challenge for the baseline RPS designs, and NASA and DOE are planning studies to assess any potential RPS impacts and approaches to withstanding Titan's atmosphere [10].

Mission concepts that would likely require a modified MMRTG or SRG design include a Europa orbiter or lander. A mission to Europa would expose the spacecraft to intense levels of radiation (potentially several Mrads (Si) behind 100 mils of aluminum), which could damage key components of the MMRTG and SRG. Future analyses will be performed by NASA and DOE to assess the radiation impacts to the RPSs and possible mitigation strategies for tolerating a total dose up to 4 Mrads [10].

1.4 CONCLUSIONS

The MMRTG and SRG are the next generation of multi-mission radioisotope power systems expected to be available by 2009. Both units represent a significant new capability for the mission design community in their ability to operate both in deep space (vacuum) and within an atmosphere. Twenty-seven mission concepts and applications have been identified within this study that could potentially be enabled by the MMRTG and SRG, and two flight missions (MSL and Solar Probe) are currently baselining the standard RPS as their power source. The mission concepts and applications identified in this study are, in many cases, based on the priority missions outlined in the Decadal Surveys and the Vision for Space Exploration. Four mission concepts, covering a broad range of goals and objectives, were analyzed in detail to demonstrate the overall feasibility of MMRTG and SRG-powered missions, to identify the mission benefits of each type of RPS system, and to assess their preliminary power requirements. The concepts include a Triton Lander, Dual-Mode Lunar Rover Vehicle, Titan Aerobot, and Saturn Ring Observer. Key benefits of the MMRTG include its higher predicted electrical power output at BOM, significant flight heritage (e.g., SNAP-19, MHW-RTG, and GPHS-RTG), and vibration-free operation (important for experiments involving seismometers, microphones, etc.) The potential benefits of the SRG are its significantly higher conversion efficiency ($\geq$20% at BOM) requiring only a fraction (25%) of the Pu-238 fuel used by the MMRTG, the associated lower radiation dose (potentially important for manned missions to the Moon and Mars), and the lower unit mass. Both RPS units were identified as potentially able to support all missions identified in this study, with the exception of two concepts with extreme radiation environments (Europa Lander and Europa Orbiter concepts) that would require modifications to the current RPS designs. In summary, the MMRTG and SRG promise to extend the boundaries of exploration by enabling missions that would otherwise not be possible.

2 MISSION CONCEPTS AND APPLICATIONS

2.1 INTRODUCTION AND PURPOSE

The Jet Propulsion Laboratory (JPL) performed a set of studies to identify and assess mission concepts that could be enabled by the new generation of standard RPSs currently in development by NASA and DOE. The MMRTG and SRG have specified power outputs of ≥110 We (BOM), and both units are expected to be available to the mission community starting in 2009. The goal of this study was to identify high-value missions and applications that could be enabled by this new RPS technology, to perform detailed analyses on selected concepts to demonstrate feasibility and assess preliminary power requirements, and to identify the potential benefits and RPS preference as a function of key mission parameters.

2.2 DESCRIPTION OF THE MISSION CATEGORIES

Studies were performed to identify and assess the range of missions that could be enabled by the MMRTG and SRG for four types of deep space vehicles, comprised of landers, rovers, aerobots, and satellites. Integrated mission design teams were formed that included scientists, RPS technologists, and mission design architects. The scientists were responsible for defining the a preliminary set of science goals of each mission based on NASA and National Research Council (NRC) roadmaps [8], and the Vision for Space Exploration [9]. The RPS technologists provided accurate technical data for the RPSs, including performance and environmental requirements. The mission architects worked with the scientists, RPS technologists, and a host of subsystem experts to design and integrate each mission concept.

Twenty-seven mission concepts and applications were identified in the study (Table 2-1) in addition to two flight projects (MSL and Solar Probe) currently baselining the standard RPS power source. Four mission concepts were selected for detailed investigation and assessment; these include a Triton lander, Dual-Mode Lunar Rover Vehicle, Titan Aerobot, and a Saturn Ring Observer. Additional RPS-enabled missions were identified based on modifications and extrapolations of the point designs and from mission studies performed by other design teams including JPL's Team X. More RPS-enabled mission concepts undoubtedly exist in the larger mission community, and this report serves to solicit those concepts for inclusion in future appendices to this document. Each of the flight missions and mission concepts identified herein belongs to one of four categories as defined by their function, operating location and mobility. The categories are *Landers*, *Mobility Concepts* (Rovers, Aerobots, etc.), *Spacecraft and Satellites*, and *Human Base Infrastructure Support*. *Landers* are defined as all vehicles that land on another solar system body, including planets, moons, asteroids or comets, to perform their mission from a fixed location (e.g., Viking and Ranger). The category of *Mobility Concepts* includes all mobile vehicles that can operate on a surface (e.g., rovers such as Pathfinder and MER), above the surface (e.g., aerobots) and below the surface (e.g., cryobots and submarines). The category of *Spacecraft and Satellites* includes missions using orbiting spacecraft (e.g., Cassini, Galileo) or fly-by missions (e.g., Voyager). The fourth category relates to the infrastructure support elements required to support human exploration as specified in the Vision for Space Exploration. This category includes applications that could use RPS power to provide infrastructure support such elements as in-situ resource utilization, life support, scientific instruments, tools, machinery, and other equipment needed to pave the way for permanent human habitation on the Moon and Mars.

The top-level science and mission goals for each of the twenty-nine missions and applications identified in this study are listed in Table 2-1. Preliminary power requirements and expected operating environments for each mission concept are provided in Table 1-2.

Table 2-1. Mission Concepts Potentially Enabled by Standard RPS Power Sources (Part 1 of 2)

#	Mission / Application	Goals
Spacecraft / Satellite Concepts		
1	Saturn Ring Observer[1]	Spacecraft would enter orbit about Saturn starting just above the B-ring to perform extremely close-in observations of ring particles, their dynamics, and to take local field measurements. The spacecraft would perform ring "hops" every quarter orbit to prevent collision with the ring, and would translate radially-outwards approximately once a week out to the A-ring.
2	Solar Probe – Flight Project	Mission proposed for 2012 and is baselining three MMRTGs. Would characterize the solar wind within a high-speed stream and measure changes during the cruise from Jupiter to the Sun. Would measure the plasma in a closed coronal structure, probe the sub-sonic solar wind, and image the longitudinal structure of the white-light corona from the poles.
3	Jovian Magnetospheric Remote Sounder	Mission to map magnetosphere particle distributions and field configuration, and characterizing magnetospheric processes (e.g., wave-particle interactions). Would receive echos from low-frequency RF waves transmitted into the Jovian magnetosphere.
4	Jovian Magnetospheric In-Situ Constellation	Would use multiple-satellites, at different inclinations and relative positions, to perform in-situ fields and particles measurements to characterize the Jovian environment and its interaction with the solar wind.
5	Europa Orbiter	Would perform detailed multispectral surface mapping, subsurface radar and gravity mapping, and magnetometry. Would require extensive radiation shielding for spacecraft and instruments.
6	Saturn Magnetospheric Remote Sounder	Mission to map magnetosphere particle distributions and field configuration, and characterizing magentospheric processes (e.g., wave-particle interactions). Would receive echoes from low-frequency RF waves transmitted into the Saturn's magnetosphere.
7	Saturn Magnetospheric In-Situ Constellation	Would use multiple-satellites, at different inclinations and relative positions, to perform in-situ fields and particles measurements to characterize the Saturn environment and its interaction with the solar wind.
8	Neptune Orbiter	Would perform Cassini-level exploration of the Neptune system. Would characterize Neptune's interior, atmosphere, and magnetosphere; Triton's interior, surface, atmosphere, and interactions with Neptune's magnetosphere; other satellites including Nereid and ring-associated satellites; and Neptune's ring system. Would include Neptune entry probes.
9	Triton Orbiter	Would perform remote measurements of Triton's structure, geysers, composition, and verify the existence of organic matter. Would map Triton's highly varied surface, ranging from smooth to very bumpy, potentially for a future Triton lander or rover mission. Would require three or more standard RPSs for a direct communications to Earth architecture. Could potentially reduce the Triton satellite power level to one standard RPS were a Neptune orbiter used as a relay satellite.
10	Pluto and Charon Orbiter	Would perform extended duration imaging of the surface of Pluto and Charon to characterize the global geology and geomorphology of both bodies, map the composition of Pluto's surface; and determine the composition and structure of Pluto's atmosphere. Would also make magnetic field extensive measurement, and perform gravitational field mapping.
Note 1. Detailed design study was performed for this mission concept and is documented in this report.		

Table 2-2. Missions Potentially Enabled by Standard RS Power Sources (Part 2 of 2)

#	Mission / Application	Goals
Mobility Concepts (Aero, Surface, Subsurface)		
11	Dual-Mode Lunar Rover Vehicle[1]	A mobile lunar infrastructure element that would facilitate manned exploration and allow long-duration and long-range telerobotic science surveys.
12	Titan Aerobot[1]	Titan airborne platform would make in-situ atmospheric and surface measurements of compositions, conditions, and processes, especially as pertaining to the organic environment. Would employ sondes for in-situ surface and/or liquid body measurements. Orbiter's synergy greatly enhances science, and relay satellite could be used to reduce aerobot power requirements.
13	Mercury Polar Rover	Could land in permanently shadowed crater to look for water ice at poles, perform surface composition and mineralogy, take surface imagery, perform magnetometry. Could be a long duration mission (months to years).
14	Mercury Night-Side Rover	Would land in night-side of Mercury to perform surface composition and mineralogy, take surface imagery, perform magnetometry. Mission would last the duration of one Mercury night (~88 Earth days).
15	Venus Aerobot	Would perform in-situ atmospheric measurements above the upper cloud layer (>60km altitude) where ambient temperature and pressure are Earth-like. Would also perform remote sensing of surface and deeper atmosphere.
16	Lunar Surface Rover	A long-duration, long-distance remote-operated science platform. Could support a sample return mission by collecting samples from multiple locations and bringing them to a separate sample-return vehicle.
17	Mars Science Laboratory - Flight Project	Long-duration and long-distance science platform designed to perform an astrobiological mission to 1) search for life, 2) understanding the environment, and 3) perform geological characterization in line with the MEPAG science goals.
18	Mars Surface Rover	A mobile Mars infrastructure element that would facilitate manned exploration and allow long-duration, long-distance tele-robotic science surveys.
19	Triton Rover	Perform in-situ measurements of Triton's interior structure and geomorphology, geysers, composition (organic and inorganic), and atmosphere including surface-atmosphere interactions.
Lander Concepts		
20	Triton Lander[1]	Perform in-situ measurements of Triton's interior structure and geomorphology, geysers, composition (organic and inorganic), and atmosphere including surface-atmosphere interactions.
21	Mercury Polar Lander	Would land in permenantly shadowed crater to look for water ice at poles, perform surface composition and mineralogy, take surface imagery, perform magnetometry. Could be a long duration mission (months to years).
22	Mercury Night-Side Lander	Would land in night-side of Mercury to perform surface composition and mineralogy, take surface imagery, perform magnetometry. Mission would last the duration of one Mercury night (~88 Earth days).
23	Mars Deep Drill	Lander vehicle would contain a drill designed to penetrate up to 50-m deep into the Martian surface to perform characterization of the subsurface and stratification, and to search for signs of water.
24	Europa Lander	Would look for the presence of a subsurface ocean, signs of life and prebiotic chemistry. Would make detailed measurements of surface composition and properties, monitor seismic activity, search for possible signs of cryovolcanism, and provide ground truth for remote measurements made by orbiting space craft.
Human Base Infrastructure Support		
25	Life Support System	Could use the heat and electricity generated by one or more RPSs to produce / recycle oxygen and water to support and/or extend the surface mission of an expeditionary human crew on the Moon. Could power a greenhouse or hydroponic garden to generate food for crew. Infrastructure support element.
26	In-Situ Resource Utilization	Could use RPS electrical power for exploting local resources for infrastructure development, reducing amount of material needing to be brought from Earth.
27	Base Construction Tools	Could use the RPS as a heat source for installing thermosetting materials (e.g., Lunar Lumber™) used for building human shelters/structures on the Moon or Mars. Would be an infrastructure support element.
28	Base Site Preparation	RPS-powered vehicles could provide regolith-moving and excavation capability in support of establishing a human base. See DPLRV concept above.
29	Generic Power Source	Could use RPS electrical power to operate tools, equipment or instruments (e.g., similar to ALSEP unit) and would be brought by human precursor / colonization missions to the Moon or Mars. Could also use the thermal power to keep instruments and crew warm. Infrastructure support element.
Note 1. Detailed design study was performed for this mission concept and is documented in this report.		

2.3 LANDER MISSIONS

2.3.1 Triton Lander Mission Concept

The Vision for Space Exploration [9] identifies three major exploration pathways, targeting Mars, the Moon and the Outer Planets. Within this roadmap the first planned science mission to the Outer Planets is the Jupiter Icy Moons Orbiter (JIMO) mission. Potential JIMO follow-on missions could target other outer planetary destinations, such as Saturn, Neptune or Pluto. This section describes a landed mission concept to Neptune's largest moon, Triton, with the aim of expanding our incomplete knowledge of the Neptunian system, which is based on the August 25, 1989 flyby of the Voyager 2 spacecraft, and on more recent Earth and space-based observations (Figs. 2.3.1-1 and 2.3.1-2).

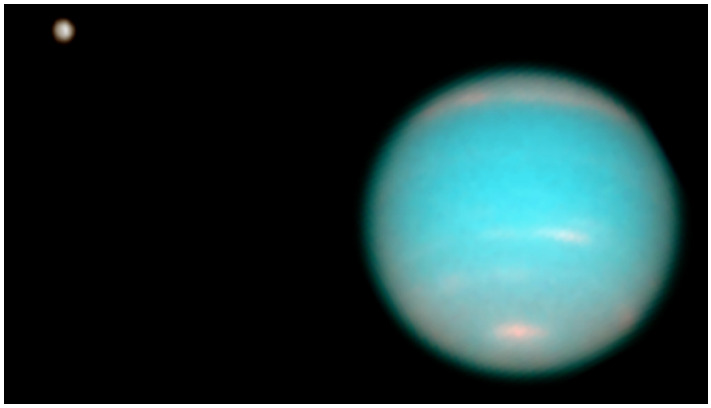

Figure 2.3.1-1. Neptune and Triton as Captured by the Hubble Space Telescope [NASA]

2.3.1.2 Science Goals

Triton is a target of great interest for outer solar system studies. The potential science objectives for a Triton lander mission would include a more complete characterization of the composition and circulation of the atmosphere; investigation of the physical processes responsible for plume formation; surface composition measurements; and geophysical monitoring. In particular, seismological measurements could potentially refine our knowledge of the physics of plume eruptions, and could detect Triton-quakes, if such are occurring at the present time.

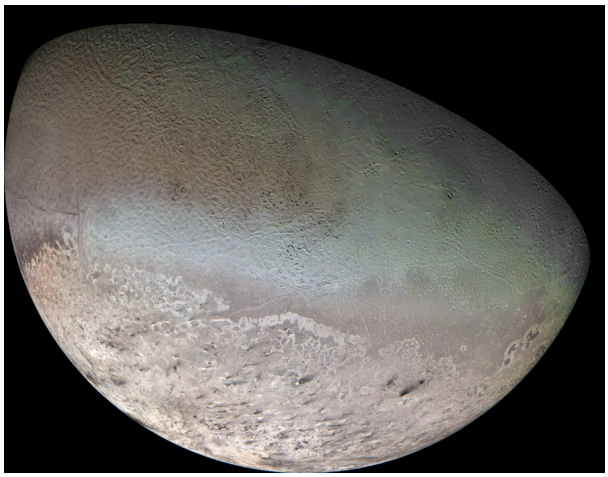

Figure 2.3.1-2. Triton Captured by Voyager 2 [NASA/JPL]

A pair of landers, one located in the summer hemisphere and the other in the winter hemisphere, could collect complementary information on atmospheric processes and on the interior structure. It would be very desirable to land atop one of the dark streaks (Fig. 2.3.1-3), in order to perform in-situ compositional analyses. This information would help constrain models of the physics of plume eruptions (Fig. 2.3.1-4) on this exceedingly cold, icy body.

The complement of instruments for such a landed mission could include a sophisticated weather station (pressure, wind, and temperature measurements), along with an imaging system and a micro-seismometer system. Remote or contact instruments for determining the compositions of surface materials would also have high priority. Last but not least, a separate instrument for determining the atmospheric composition (a mass spectrometer of some type) should be included.

Although not described here in detail, the accompanying orbiter should likewise carry instrumentation to measure Triton's magnetic field (if any) and to determine the internal structure through gravity measurements. (The latter would be a radio science investigation employing the communications signal from the spacecraft to the Earth). Imaging, remote sensing of surface composition, and fields and particles instruments appropriate for Neptune's magnetospheric environment should also be considered. Remote measurements of surface composition may be difficult due to the extremely low surface temperature; active illumination of the surface might be required. For completeness, Table 2.3.1-1 provides a summary of Triton's key statistics.

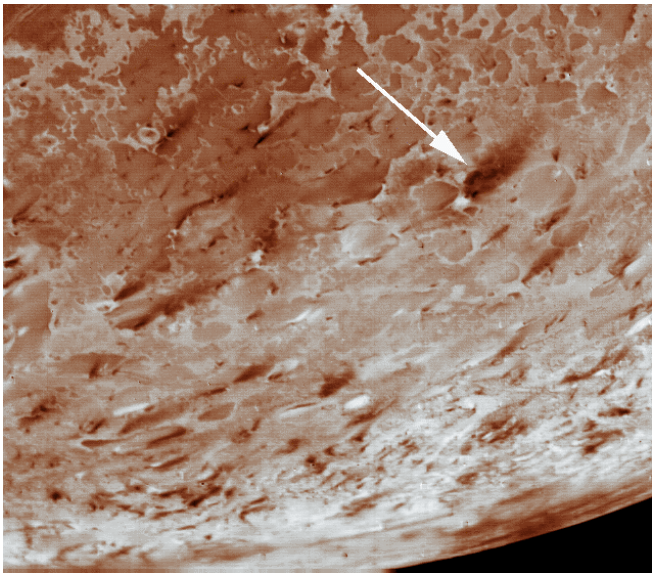

Figure 2.3.1-3. Triton's South Pole and Dark Streaks Caused by Volcano Ejecta, [NASA]

2.3.1.3 Mission Goals

The mission goals for this Triton lander mission would include a successful landing of at least one, but preferably two, spacecraft on the surface followed by a nominal three year surface science mission to characterize the environment and to extend our knowledge base on the Neptunian system. Measurements would be taken to identify mineral composition in the vicinity of the landing site. Seismic activity and geyser eruptions would be monitored as well. Visual observations would be taken and local meteorological conditions could be monitored over a long duty cycle in order to characterize seasonal changes through a small portion of a Neptunian year.

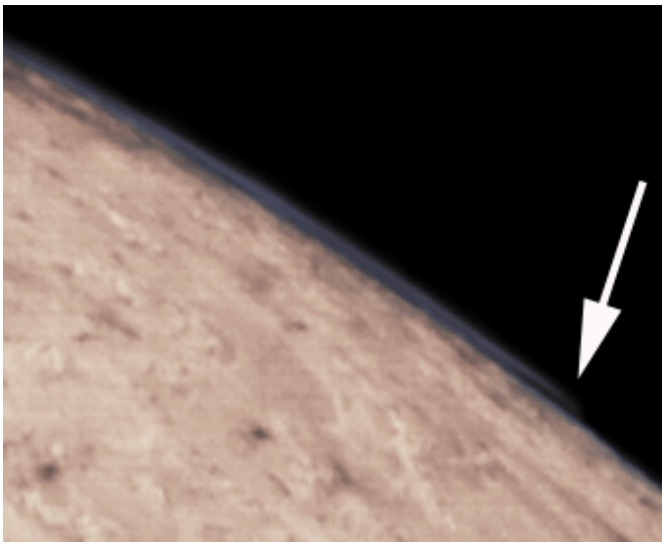

Figure 2.3.1-4. Plume Cloud on Triton (©1999 Hamilton)

2.3.1.4 Mission Architecture Overview

The primary architecture assumes a JIMO follow-on configuration utilizing a low thrust nuclear electric propulsion (NEP) system, with the mission referred to as the Neptune Icy Moon Orbiter or NIMO. The NIMO spacecraft, just as its predecessor, would require a heavy launch capability that does not exists at this time. The various launch vehicle (LV) options could include a number of Delta IV-H LVs and in-orbit assembly or a single heavy LV with a Saturn LV capability. Although this study will focus on the NIMO-based configuration, a second high thrust trajectory based architecture will be also mentioned for comparison purposes in Section 2.3.2.

It is assumed that the NIMO "mothership" would be powered by a 300-kWe nuclear reactor, built upon the proposed 100-kWe JIMO design. NEP enables the highest mass delivery, but results in the longest transfer time when compared against high thrust trajectories. Venus and Jupiter gravity assists could further reduce the trip time to Neptune. A NEP-enabled mission to Neptune would take about 15 years, which includes spiraling out of Earth and spiraling in to Neptune. It would take an additional 3 years to reach orbit around Triton. JIMO's currently proposed payload allocation is 1500 kg. Since the NIMO spacecraft would only pass Jupiter during a gravity assist flyby, the high radiation environment of the Jovian system would not have a significant effect on it. Thus, the mass allocated on JIMO for shielding could, in part, be reallocated as payload on NIMO. (Note that mass differences will in part be a function of the size of the power system, and more importantly will reflect differences in the propellant needs to account for traveling about 6 times farther from the Sun to Neptune than JIMO's journey to Jupiter.) The current mission concept assumes the payload envelope can be increased to 3000 kg, which would effectively support two Triton landers and additional science instruments on the NIMO orbiter for remote sensing / mapping of Triton and for observing Neptune from Triton's orbit. Since the present mission concept focuses on the landers, it is assumed that NIMO is already in a 1500 km circular orbit around Triton with a suitable payload allocation for two landers. Therefore, details of the NEP-enabled low thrust trajectory from launch to arrival are not addressed here due to the limited scope of this study.

Table 2.3.1-1. Triton Statistics [20-23]

Parameter	Value
Discovered by	William Lassell
Date of discovery	1846
Mass (kg)	2.14E+22
Mass (Earth = 1)	3.5810E-03
Equatorial radius (km)	1,350
Equatorial radius (Earth = 1)	2.1167E-01
Mean density (gm/cm^3)	2.066
Mean distance from Neptune (km)	354,800
Rotational period (days)	5.87685
Orbital period (days)	5.87685
Mean orbital velocity (km/s)	4.39
Orbital eccentricity	~1.65E-5
Orbital inclination (degrees)	157.35
Escape velocity (km/s)	1.45
Visual geometric albedo	0.7
Star magnitude (brightness)	13.47
Mean surface temperature	-235°C / 38 K

According to the primary mission configuration, NIMO would achieve a 1500 km circular orbit around Triton and spend the first weeks mapping the surface. The returned data would enable the science team on Earth to select suitable landing locations for the two landers for a "stop-and-drop" type landing. Each lander would de-orbit to the surface using the lander's own propulsion system. An initial 137 m/s small de-orbit burn would lower the lander's periapsis to about 20 km, where a large 1200 m/s burn would remove all horizontal velocity. Soft landing would require a small 195 m/s throttled burn from the bi-propellant system, assisted further by a Sky Crane, which would be based on 2009 Mars Science Laboratory (MSL) concept. Lowering the landing platform from a Sky Crane could help minimize surface contamination from the impinging exhaust of the thrusters.

Once the lander was released, the Sky Crane platform would disengage and crash land at a safe distance from the payload base. Soft landing was selected for two reasons. First, when landing on an airless body the option for an aeroshell and parachutes is not feasible; thus, all or at least most of the velocity must be removed through propulsive means. (From the aspects of descent and landing, Triton, with its very thin atmosphere, can be considered an airless body.) Furthermore, the savings in fuel mass from cutting off the engine at a few kilometers altitude, free falling and landing with airbags is significantly less than the additional mass required for an second landing system, such as the Sky Crane concept discussed here. Therefore, as demonstrated by Balint [24] adding a second landing system, such as airbags similar to the landing configuration of the Mars Exploration Rovers [25], or crushable materials such as proposed for the Mars Net Landers [26] would potentially decrease the landed payload mass. Second, the power source used for this mission, a standard RPS, is currently specified for a maximum acceleration load tolerance of about 30g. Therefore, on Triton soft landing presents the only viable mass effective landing configuration with the given power source. A conceptual design of the Triton lander with the Sky Crane, thrusters and propulsion system is shown in Figure 2.3.1-5.

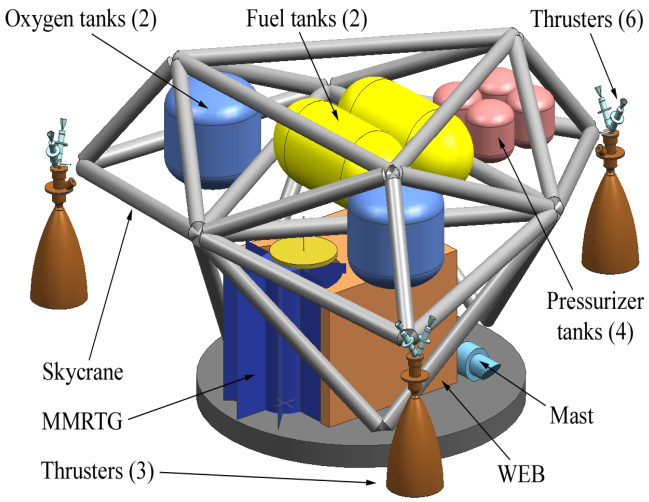

Figure 2.3.1-5. Conceptual Illustration of the Triton Lander with a Sky Crane Platform

As previously discussed, the first lander would touch down on the illuminated side of Triton, such as the South Pole shown in Figure 2.3.1-3. The landing location could be either inside or outside of the dark streaks. Another potential landing location could be inside the remains of an ancient impact crater that is thought to be filled with ice, probably formed by eruptions of water or water-ammonia slurry (Fig. 2.3.1-6).

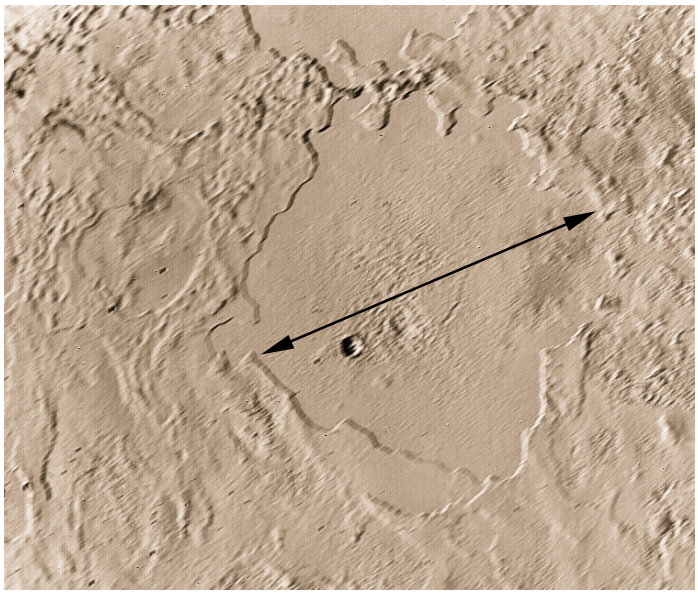

Figure 2.3.1-6. Icy-Slurry Filled Crater on Triton, [NASA]

The second lander would touch down on the opposite side of the moon, which would allow for studying atmospheric processes such as potential migration of atmospheric constituents from the illuminated side to the dark side of Triton.

The environment on the surface of Triton is harsh. Therefore, the lander concept is designed with the philosophy of simplicity and reliability in mind to meet mission lifetime requirements using an appropriate combination of high-reliability components and dual-string design.

The very long 18 years cruise phase combined with the 38K surface temperature makes mobility with a rover or even an articulating robotic arm undesirable. Thermal cycling or freezing could cause an early end to a long awaited mission. Upon arrival at the surface, the lander would initiate investigations of science targets. First it would deploy its only mobile component, the mast, on which the panoramic camera (Pancam) and remote sensing instruments (Raman Spectroscope / Laser Induced Breakdown Spectroscope or LIBS) are located. Good contact with the surface would allow for seismic measurements. A meteorology sensor suite would monitor the temperature and pressure changes in the atmosphere, while a Gas Chromatograph / Mass Spectrometer (GC/MS) would make compositional measurements. Details on the instruments and their operations are given in the relevant sections below. To minimize risk to mission success, the lander design would use as much design and flight mission heritage as possible from previous outer planets orbiters and landers.

2.3.1.5 Power Source Trade Study

Insolation decreases with distance squared from the Sun. In fact, at Neptune (30 AU from the Sun) solar radiation is only about 0.1% of that at Earth. It is generally acknowledged that beyond 3 to 4 AU, solar power generation is effectively impractical with current technology – future Low Intensity Low Temperature (LILT) technology could theoretically work, but would likely be mass prohibitive for a Triton lander mission. Consequently, missions to Jupiter and beyond (such as to the Neptunian system) require a different kind of power source, independent from the Sun. Batteries may support limited duration mission operations; however, longer missions require nuclear fission or radioisotope decay-based power systems. The current study baselines an MMRTG, but a lander mission to the Neptunian system could potentially utilize a Stirling Radioisotope Generator (SRG) or a small fission reactor. The SRG is powered by two GPHS modules [27], resulting in a significantly lower Pu^{238} fuel requirement than the 8 GPHS module-based MMRTG [28]. With fewer GPHS modules, the thermal output of the SRG would also be reduced by 75%, to about 500 Wt (BOM). Due to the extreme cold temperatures expected at Triton, this mission considered the MMRTG as its preliminary baseline due to its greater amount of excess heat, which could be needed to maintain spacecraft operating temperatures. Though the SRG could potentially generate enough heat to affect the same result, not enough information was available at the time of this study to evaluate an SRG-baselined version of this mission. Small fission reactors, for example a conceptual HOMER type reactor, could potentially generate ~3 kWe of power using a Stirling power converter, and weigh ~ 775 kg [29]. An advantage of fission reactors is that they could remain inactive until the beginning of the surface operation. During the inactive "cold" phase, these reactors would produce negligible radiation and would not be affected by the long cruise phase. However, the power and mass configuration of a HOMER-type reactor exceeds the power requirements and mass limits of a Triton lander mission, and therefore was not considered a viable power source alternative for this mission concept.

Although not the focus of this study nor detailed here, the NIMO orbiter would perform remote sensing measurements to characterize Triton and Neptune. On NIMO, the onboard 300 kWe nuclear reactor would power the science instruments. Other subsystems such as telecom and command and data handling would also be supported. Thus, the baseline mission architecture would rely on a nuclear reactor on the NIMO orbiter and one MMRTG in each of the two landers.

2.3.1.6 RPS Characteristics

A mission requirement is that the power system should operate continuously during the entire mission, which includes ~15 years of cruise phase to Neptune and about 3 additional years to reach Triton's orbit. Though the standard RPS lifetime requirement is a minimum of 14 years from BOM, both the MMRTG and SRG are robust units and are expected to continue to generate power with a gradual and predictable decline in output over time. The power generated by the MMRTG is assumed to degrade by about 1.7% per year. Approximately half of this decrease would be due to the natural decay of the plutonium fuel and the other half would be due to the degradation of the thermoelectrics. Thus, at the beginning of the science mission, defined by landing on Triton (18 years after BOM), the generated electrical and thermal power would be ~81.5 We and ~1735 Wt, respectively (Section 3 - Table 3-6). Soft landing on Triton would be used to impart acceleration loads on the MMRTG within design limits. Excess RPS heat would be utilized through radiation from the MMRTG to a hot plate of the warm electronic box (WEB), and through conduction along the MMRTG fins and thermal straps from the power source to the WEB. Consequently, the present design would benefit from two of the advantages of an RPS, namely continuous electrical power generation and utilization of its excess heat.

2.3.1.7 Science Instruments

The lander concept shown in Figure 2.3.1-7 was designed to fulfill the key science objectives of the mission, given in Section 2.3.1.1. Potential instruments on the lander can be broken down to three categories, including remote sensing, contact and analytical suites. Remote sensing instruments are located on the mast and include a panoramic camera (Pancam), an illumination source and sensors for a Raman spectroscope and Laser Induced Breakdown Spectroscope (LIBS). Contact instruments are the seismometer and, to a certain extent, the meteorology station. The Gas Chromatograph / Mass Spectrometer (GC/MS) is an analytical instrument. All of these instruments must have sufficient sensitivity to measure the relevant environmental conditions listed in Section 2.3.1.1. After describing the instruments shown in the Triton lander concept drawing (Fig. 2.3.1-7), additional potential instruments will be considered. These might be placed either on the lander or on the NIMO orbiter.

The imaging system, a MER derivative panoramic camera, is located at the top of the mast. The high-resolution stereoscopic camera provides needed context and aids in characterizing the geomorphology of the surface through the generation of terrain maps, slope maps and ranging. It can generate 360° panoramas and multi-spectral images of the surface, which helps to characterize the nature of the materials sampled with other instruments. Thus, in effect, the Pancam would work in conjunction with the Raman spectroscope and with the LIBS. The Pancam camera is at TRL9.

The combined Raman spectroscope and LIBS system could measure elemental abundance and mineralogy of surface materials. By actively stimulating the target these instruments would avoid the negative consequences of the low Triton surface temperature that would reduce the capabilities of TES and other IR-sensitive instruments. The Raman spectroscope fulfills the astrobiology-driven science goals by performing mineral characterization and assisting in the detection of water, organic and inorganic forms of carbon. It identifies many major, minor and trace minerals and their relative proportions (i.e., Mg/Fe ratios), and carbon ratios. Sharp Raman spectral features and statistical point counting help identify minerals in complex mixtures and morphologies. LIBS would use a higher energy excitation of the surface than Raman, consequently

ablating the studied surface. Compositional information would be drawn from spectral analysis of the resulting plasma. The instrument is based on the Mars Microbeam Raman Spectroscope, currently at TRL 4. LIBS is proposed for upcoming Mars missions and is at TRL 5.

The lander would be equipped with a two-component seismometer measuring both high and low frequencies. The 2-axis very broad-band seismometer would capture tidal and long period motions up to 10 Hz. The 3-axis short period micro-seismometer would measure high frequency movements from 1 Hz to 50 Hz. The two sets of seismometers would achieve the highest sensitivity in an ultra broad band from $5x10^{-5}$ Hz to 50 Hz. In addition, a partial redundancy would be achieved due to their significant overlap in frequency band. Triton's geysers produce plumes rising several kilometers in height. Like geysers on Earth, these must produce seismic waves within crustal materials, which could be measured with this seismometer assuming the lander is located within a reasonable distance from the source. Detection and analysis of seismic energy can provide information on the eruptive processes (their energy, frequency, time evolution) and on the properties of crustal materials traversed by the waves. This proposed seismometer is currently at TRL 4.

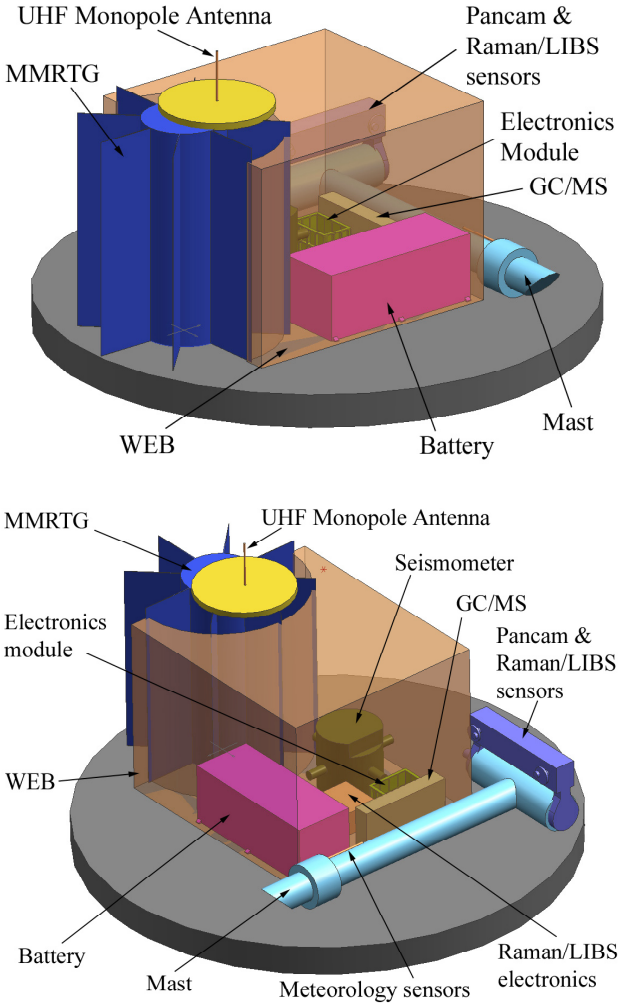

Figure 2.3.1-7. Triton Lander Instrumentation

Triton is one of only two satellites in the solar system (along with Titan) that has an appreciable atmosphere. Every aspect of this frigid atmosphere is of scientific interest: its composition, its circulation, its exchange processes with the surface, its evolution with time. A pair of sophisticated weather stations situated in opposite hemispheres could yield a very significant science return. The very cold environment and thin atmosphere requires significant modifications to the sensitivity of existing weather monitoring equipment. Such instruments are at TRL 5.

The GC/MS measures isotopic gas ratios of trace atmospheric components. If a sampling mechanism were implemented, the GC/MS could be used to identify the presence of organics as well as mass spectra and isotopic ratios of evolved gas constituents from rock and soil samples. The instrument is proposed for upcoming Mars missions and is currently at TRL 5 / TRL 6.

Although not included in this concept, additional instruments on the lander and NIMO orbiter could also be considered. For example on the lander a small sampling mechanism in the form of a robotic arm with a scoop could be used to position the contact instruments (Raman, LIBS) closer to the target objects. If a sample acquisition (e.g., scoop) is included, then the collected sample could be analyzed by a Thermal and Evolved Gas Analyzer (TEGA). TEGA offers a more complete characterization of the volatile component of surface materials than is possible with Raman and LIBS. However, TEGA is heavier and more complex than a simple oven to heat the samples and analyze them by the GC/MS. Sample handling introduces additional complexities especially in a cold environment such as Triton, hence this is not included in the present concept. Beside LIBS, a heat lamp or conducting fins could warm the surface near the lander. Heating or thawing the surface could potentially initiate small geyser-like eruptions after creating a sub-surface greenhouse effect.

On the NIMO orbiter, an Ion and Neutral Mass Spectrometer (INMS) could directly sample the tenuous atmosphere surrounding Triton. It could confirm the presence of the major gases and could detect other, as yet unknown, gases in the atmosphere. The NIMO orbiter could carry additional atmospheric remote sensing instruments to fully characterize the composition of the atmosphere, such as LIDAR, ground penetrating radar, cameras, and a Thermal Emission Spectrometer (TES). (Note that thermal emissions at 38K are very low, compared to the ~150K on Mars. Therefore, TES at Triton may not have the sensitivity to perform meaningful measurements.)

Table 2.3.1-2. Instrument List of the Proposed Triton Lander Mission

Instrument	What It Does	Science Objective Addressed
Panoramic Camera (Pancam)	Obtain near and far field images; high resolution 360° panorama stereoscopic imaging.	Surface characterization and geomorphology of the landing site, terrain mapping, multi-spectral images, works with Raman and LIBS.
Raman Spectroscope	Measure backscattered light to determine composition and concentration of minerals and chemical species present, including organics.	Elemental abundance and mineralogy of surface materials. Astrobiology driven science goals, detection of water & organic materials.
LIBS (combined with Raman)	Pulsed laser focused on surface ice produces an ionized plasma whose emissions are characteristic of the elemental composition of the surface material.	Searches for signatures of biological activity. Characterize the chemical and physical habitability. Describes the composition of non-ice materials.
Seismometer	2-axis seismometer for long period movement, and 3-axis measurements for high frequency events.	Measure seismic activities due to geysers, quakes or potential gravity induced tidal movements.
Meteorology sensors	Measure pressure, temperature, wind velocity and direction.	Characterize Triton's environment.
GC/MS	Measures isotopic gas ratios of trace atmospheric components (mass spectra of surface sample).	Characterization of the atmosphere (and the soil).

2.3.1.8 Data

The command and data handling (C&DH) system, assumed to be a dual string Harris RH3000 unit with radiation tolerance exceeding 100 krads, is sized by the data collected from the science instruments and communicated to NIMO during the telecom opportunities. The highest data volume would be generated by the seismometer, which would collect up to 16.6 kbits/s and would operate continuously (Table 2.3.1-3). The collected data would include both high and low frequency measurements. This data volume could be significantly reduced by data compression and by stand-by monitoring of the activities. For time periods without seismic activity, the data handling system would simply discard the data. In case of an activity, a memory loop would retain the immediate time period prior to the event and record throughout the activity. The Pancam would take 12 frames for a full panorama, where each frame would use 50.4 Mbits of raw data. This data could be compressed at a ratio of 3 to 1. After taking the initial 360° panoramic image, the Pancam would enter standby mode where it would remain until the on-board seismometer detected a seismic event with specific characteristics (e.g., indicative of a nearby erupting geyser, etc.) The Pancam would then be activated, taking another 360° panoramic image with the hope of capturing a view of an eruption plume, etc. The Raman spectroscope and LIBS would each generate less than 1 Mbit of data per measurement. The GC/MS would perform only a limited number of measurements; therefore, the data obtained by these instruments would not have an impact on the C&DH system.

Table 2.3.1-3. Data Rate for the Triton Lander

Instrument / Subsystem	Data rate
Panoramic Camera	50.4 Mbits/frame raw. Average compression ~3:1; 12 frames required for a full panorama
Raman Spectroscope	17 kbits / spectra (raw), 50 Raman spectra per hour
Laser Induced Breakdown Spectroscopy	Similar to Raman
Seismometer	16.6 kbits/s
Meteorology sensors	Few kbits / hour
GC/MS	~10 kbits per mass spectra (MS); ~200 kbits per evolved gas sample (GC)

The lander operation would include two modes, based on operation time frames. The initial mode, following the landing, would include a full set of measurements. The second mode would switch most of the instruments into standby mode, keeping only the seismometer and meteorology sensors operational. This second mode would generate only a small amount of data, which would reduce data transfer from the surface to NIMO and back to Earth. For the second mode only a reduced staff would be required to operate the landers, and to analyze the data.

2.3.1.9 Communications

The distance of Neptune from the Sun is 30 AU; therefore, direct to Earth (DTE) communication from the landers is not likely. Because of the limited power availability from the MMRTG and potential visibility issues, the data to Earth would nominally be relayed through NIMO. Each lander would utilize redundant ElectraLite UHF radios with a 5 W transmitter to communicate with NIMO. This telecom system would support a data rate up to 500 kbits/s. (The UHF system could transfer data at rates between 1 kbits/s and 2048 kbits/s, while the receive data rate would correspond to a range between 1 kbits/s and 8 kbits/s). Based on the telecom opportunities for an

assumed 1500 km orbit the daily data volume could be over 200 Mbits, transmitted through the lander's monopole antenna. The ElectraLite UHF radio would be placed inside the warm electronics box, while the base plate of the UHF monopole antenna would be positioned above the MMRTG, utilizing its waste heat through conduction and radiation to prevent the antenna temperature from dropping below its survival temperature (Fig. 2.3.1-7).

2.3.1.10 Thermal

Thermal design of the landers requires maintaining them at an appropriate operating temperature during all phases of the mission. It would also be desirable to reduce and potentially eliminate the number of moving components on the landers in order to minimize the potential for thermal-mechanical failures. To prevent thermal cycling, the thermal environment could be sustained by utilizing excess heat from the MMRTG.

Thermal control for the Triton landers would be accomplished by a combination of passive and active components. Both landers would have the same thermal design. The Pancam camera would require a 2.5-We resistance heater. To maintain the temperature of the WEB, two possible options could be considered, including covering each of the exposed surfaces with a 1/16 inch layer of Aerogel (a high performance, lightweight thermal insulator) or by covering them with MLI in addition to two 2-We resistance heaters to compensate for the less efficient thermal blanket design. The MMRTG would generate about 1700 Wt of heat at EOM, of which ~520 Wt would be conducted to the WEB using a high performance thermal strap (e.g., K1000 heat strap.) The remaining MMRTG heat (~1280 Wt) would be radiatively dissipated from the MMRTG fins. A doubler plate could also be used to help remove a portion of the heat and to minimize the hot spots located along the mounting plate. Analysis indicates that the MMRTG waste heat would be sufficient to maintain the operating temperature of the components within the WEB. For components outside of the WEB (e.g., Pancam), resistance heaters would be used.

2.3.1.11 Power

Each lander would baseline one MMRTG power source and a secondary 25 A-hr Li-Ion battery that would provide load leveling during high power operations (e.g., telecom events). Power calculations for a 3-day repeatable mission scenario, assuming an 80 We continuous power source, demonstrated that the present hybrid system would provide sufficient power to the lander and would keep the secondary battery power positive. This would permit repeatable cycle lander operations through the whole mission lifetime. In the power analysis, three operational modes were considered. In high power mode, all science instruments and support subsystems would work simultaneously. In low power mode, some of the instruments would not be operated, such as the Raman spectroscope, LIBS and the GC/MS. In telecom mode, the UHF transmitter would operate in conjunction with the power, electronics and thermal subsystems. Science instruments designated as "Always on" would be also operational throughout all three modes, as shown in Table 2.3.1-4. The electronics subsystem would provide permanent support to the instruments, by processing the collected information, storing it and sending it to NIMO through the telecom system (10.4 We). The power subsystem would use 15.4 We to power the peripheral control unit (PCU), the power distribution unit (PDU), the battery control, the universal switch and the shunt limiter. Thermal heaters, drawing 5.9 We, would be used continuously to maintain the operating temperatures of the Pancam and the WEB. The telecom system would use 52 We of power during telecom opportunities.

In summary, the power analysis performed for this mission concept confirmed that an MMRTG-powered Triton lander would be feasible.

Table 2.3.1-4. Power Estimates for the Triton Lander (Includes 30% Contingency)

Electrical Load	Power (We)	Subsystem/Instrument Duty cycle
Instruments		
Panoramic Camera	5.6	1 hour on demand
Raman Spectroscope	23.4	2-3 hours
LIBS	23.4	2-3 hours
Seismometer	3.5	Always on
Meteorology sensors	1.4	Always on
GC/MS	11	8 hours total
Subsystems		
Harris Electronics	10.4	Always on
Power subsystem	15.4	Always on
Telecom	52	1 hr / day (max)
Thermal heaters	5.9	Always on

2.3.1.12 Mass

It is assumed within this study that NIMO could deliver up to 3000 kg of payload mass to Triton's orbit. The payload allocation on the NIMO orbiter is assumed to be higher than that of JIMO due to two factors. First, the 300 kWe NIMO reactor would allow for larger electric propulsion thrusters, thus increasing the deliverable mass to the Neptunian system. Second, as will be explained in Section 2.3.1.13, Neptune's radiation environment is benign compared to that of Jupiter. Thus, NIMO's shielding requirement would be much lower than JIMO's, resulting in a mass savings that could be re-assigned to the science payload. The larger payload mass would, in effect, allow for two landers in addition to science instruments allocated on the orbiter for remote sensing and data relay. The mass breakdown is shown in Table 2.3.1-5. The mass of the propulsion system accounts for about 57% of the lander mass at the time it detaches from the orbiter. This includes the propellant wet mass (bi-propellant and pressurant) and the propulsion system dry mass (thrusters, tanks, valves). The structures and mechanisms, about 24% of the total mass, account for the lander base plate, WEB housing, mast, Sky Crane and miscellaneous items such as cabling. The power system is almost 14% of the total mass, and includes the MMRTG power source, the batteries and other components such as PCU, PDU, shunt limiter and battery control boards. The thermal, avionics and telecom systems account for less than 3.3% of the mass. Finally, the science instruments utilize about 2.2% of the total lander mass. With 30% mass margin, required by design principles for conceptual designs, the Triton lander mass at the time it detaches from NIMO would be about 740 kg, while two landers would be less than 1500 kg, leaving half of NIMO's assumed payload for orbiter-based science instruments.

Table 2.3.1-5. Mass Estimates for the Triton Lander

Subsystems	Mass (kg)	Mass with 30% Margin (kg)
Propulsion System	321.5	418
Structures & Mechanisms	135	175.5
Power System	82.1	106.7
Thermal System	7.9	10.3
Avionics	2.2	2.9
Telecom	8.3	10.8
Science Instruments	12.4	16.2
Total	**569.5**	**740.3**

2.3.1.13 Radiation

During the total mission lifetime, the NIMO spacecraft and Triton landers would be exposed to various radiation sources. These include the Van Allen radiation belts near Earth, cosmic radiation through the cruise phase, Jupiter's radiation during the flyby, and radiation from the NIMO reactor and the landers' MMRTGs. A calculation was performed comparing the radiation environment for this mission against the preliminary calculations for the proposed JIMO mission. The calculations assumed 100 mil of aluminum shielding to protect NIMO and its landers. During the spiraling out phase from an 1000 km Earth orbit, the Van Allen radiation belt would expose both NIMO and the landers to about 100 krads of total ionizing dose (TID) radiation. The Jupiter flyby could add about 40 to 60 krads, based on the flyby distance (the above values assumed 10 and 6 Jupiter radii at 0° inclination). The NIMO reactor would add ~40 krads TID. The radiation dose from the MMRTGs is dependent on the distance from the radiation source and was extrapolated from calculations performed for the Mars Science Laboratory mission [30]. The resulting TID for the 18-year cruise phase is estimated at <250 krads. The natural radiation environment at Neptune results in an additional 0.003 krads/year, which is relatively negligible.

It is evident that such a mission would not require the amount of shielding seen on JIMO. Since the shield mass per unit area for 100 mils of aluminum is 0.686 gm/cm^2, the mass savings due to shielding could be significant, accommodating an equally larger payload. The currently projected JIMO payload allocation envelope is 1500 kg. The JIMO follow-on spacecraft assumed for this Triton lander mission is assumed to accommodate a payload of ~3000 kg.

2.3.1.14 Alternate RPS Power System

Small radioisotope power systems with thermoelectric (TE) conversion, in a modular configuration, could be considered for a Triton lander mission. However, the minimum number of small-RPSs required to support a Triton lander mission would be close to the number of GPHS modules in an MMRTG. The mission could also consider SRGs, providing approximately the same electric power output as the MMRTG. However, an MMRTG would generate four times more heat than an SRG, providing an advantage in the cold Triton environment through excess RPS heat utilization. Therefore, the MMRTG is currently considered the best choice for a Triton lander mission in order to reduce complexity and potentially lower cost through the use of a single system.

2.3.2 Additional RPS–Enabled Lander Mission Concepts

In comparison with the baseline concept using NEP, a chemical propulsion system combined with a 30 kWe solar electric propulsion (SEP) system, could reduce the trip time from ~15 years to ~10.25 years. Due to the distance between Earth and Neptune, the trajectory would require a high C_3. Since Triton's gravity is very small, Neptune's gravity field would be used to capture the spacecraft. From there, the orbit would be changed to an orbit around Triton, still with the propulsion system of the mother spacecraft. Such a mission is expected to utilize a significantly sized propulsion system for the orbiter/mother spacecraft. For this baseline trajectory, the spacecraft would be launched on a C_3 of 18.4 km^2/s^2, followed by a Venus and Jupiter Gravity Assist (VJGA). The inertial entry velocity for a Neptune aerocapture, in the range of 28-30 km/s, would offer the best combination of highest delivered mass to a Neptunian orbit with the lowest entry heating. Although this second option would cut the trip time by about a third, only 790 kg could be placed into orbit around Triton [31, 32], which is insufficient to support both an orbiter and lander.

Table 2.3.2-1. Mass Allocation and Delta V Requirements for a Chemical / SEP system [33]

Item	Delta V (m/s)	Required Mass (kg)	Total Mass (kg)
Initial payload mass at launch to C_3			**7250**
Mass to place into Neptune orbit		**3460**	**3790**
SEP module (wet mass) (ejected before aerocapture)	n/a	2800	
Cruise propellant	25	70	
Neptune aerocapture aeroshell / TPS (discarded after aeropassage)	n/a	400	
Aerocapture control	30	40	
Neptune Perineps Raise to ~4000 km (including 3% gravity loss)	110	120	
Neptune Aponeps Correction (358,000 km Neptune orbit)	40	30	
From Neptune orbit to Triton orbit			
Insert to 1500 km circular Triton orbit	2800	**1850**	**1940**
Orbiter mass at lander-orbiter separation; & mass available for lander	n/a	**1000**	**940**
From Triton Orbit to surface (propellant only to land ~300 kg payload, including the propulsion system dry mass for tanks, thrusters etc., and 30% contingency)			
Lander de-orbit burn (to a 1500 km by 20 km orbit)	137	37	
Triton Pericenter Burn (including 2% gravity loss)	1200	241	
Soft landing (incl. 10% gravity loss)	195	28	
Attitude Control Allotment (total)	n/a	15	
Propulsion system dry mass	n/a	97	

Table 2.3.2-2. Mission Architecture Options for a Triton Lander Mission

Option	Comments
Baseline (NIMO)	300 kWe fission reactor; Low thrust through all stages; Payload: ~3000 kg; Trip time: ~15 years to Neptune (+3 years orbit transfer to Triton)
Chemical / SEP (Low C_3 / High mass)	C_3=12.1 km^2/s^2; SEP: 50 kWe; Payload: ~1940 kg; Trip time: ~12.5 years
Chemical / SEP (High C_3 / Low mass)	C_3=18.4 km^2/s^2; SEP: 30 kWe; Payload: ~790 kg; Trip time: ~10.25 years
JIMO class launcher for the baseline option	(a) multiple launches plus in orbit assembly (b) Saturn class launch vehicle

With the reduction of C_3 velocity from 18.4 km^2/s^2 to 12.1 km^2/s^2 (with V_{inf}=12.8 km/s) and scaling up to a 50 kWe SEP stage (with 2800 kg wet mass), about 3330 kg could be inserted into Neptune's orbit on a 2017 launch opportunity. This is based on a Delta IV-H launch vehicle with a 7250 kg payload mass inserted to a C_3 of 12.1 km^2/s^2; a 12.5-year VJGA trajectory; and an advanced aerocapture vehicle (< 1250 kg). (Note that for this C_3 the maximum payload on a Delta IV 4050-H launch vehicle is 7510 kg [34].) Following an orbit transfer to Triton the total mass of the spacecraft would be around 1940 kg. Assuming a ~900 kg lander, the spacecraft in orbit could only support one lander and a ~1000 kg orbiter. This configuration would not fully satisfy the science goals of the mission given in Section 2.3.1.1. Although this option was not selected, the velocity and propellant mass calculations for the lander shown in Table 2.3.2-1 would be the same as for the primary mission configuration.

Note that this second mission architecture would be more power limited. Due to an average 30 AU distance from Triton to Earth, telecommunication would present a significant challenge, requiring power in the multi hundred-watt range. For example, three MMRTGs could provide about ~245 We power to the orbiter after an 18 year mission duration. In summary, this second architecture would require a total of four MMRTGs to power the orbiter and a single lander.

A summary of the various mission architectures is provided in Table 2.3.2-2. For the chemical / SEP options, the SEP stage would be ejected at Jupiter and the spacecraft would utilize aerocapture at Neptune. The baseline (NIMO) option would require a Saturn-class LV or multiple launches with in-orbit assembly using existing heavy LVs. The chemical/SEP options would use a single Delta IV-H launch vehicle.

2.3.3 Triton Lander Summary and Conclusions

A study has been performed to demonstrate the feasibility of a landed mission to Neptune's moon Triton with two landers, deployed from a JIMO follow–on orbiter called NIMO. Each lander was designed to use a standard RPS as its power source, with the MMRTG baselined. The power levels of the MMRTG are assumed to be ~2000 Wt and ~110 We at BOM; however, due to natural decay of the plutonium power source, and degradation of the TE converters, the power would drop to about ~1735 Wt and 81.5 We after the 18 year transfer from Earth to Triton. Since Triton is considered to be the coldest place in our solar system with a mean surface temperature of -235°C, the lander was designed with no moving parts (other than the mast and mechanical components of the panoramic camera), and with arrangements to utilize the excess heat generated by the MMRTG. An MMRTG would provide sufficient electric power to support science instruments fulfilling the science objectives of this mission. It was also concluded that radioisotope-

based power systems would provide the best solution for a landed mission to Triton, since a solar energy power source at this distance would be mass prohibitive for power generation, and a fission reactor would be oversized for this type of mission.

2.4 MOBILITY CONCEPTS

2.4.1 Dual Mode Lunar Rover Vehicle (DMLRV) Concept

The Dual Mode Lunar Roving Vehicle developed in this study extends a concept originally investigated during the Apollo program [35, 36]. For extended lunar exploration it was recognized that the manned transportation rovers that had been used to such good effect on the later Apollo missions could, with modification, provide a telerobotic exploration platform allowing long-range surveys of the lunar terrain between manned landings. These early studies (Fig. 2.4.1-1) indicated the feasibility of such a vehicle, but the demise of the Apollo program meant that the design studies were never given the opportunity to proceed to flight units.

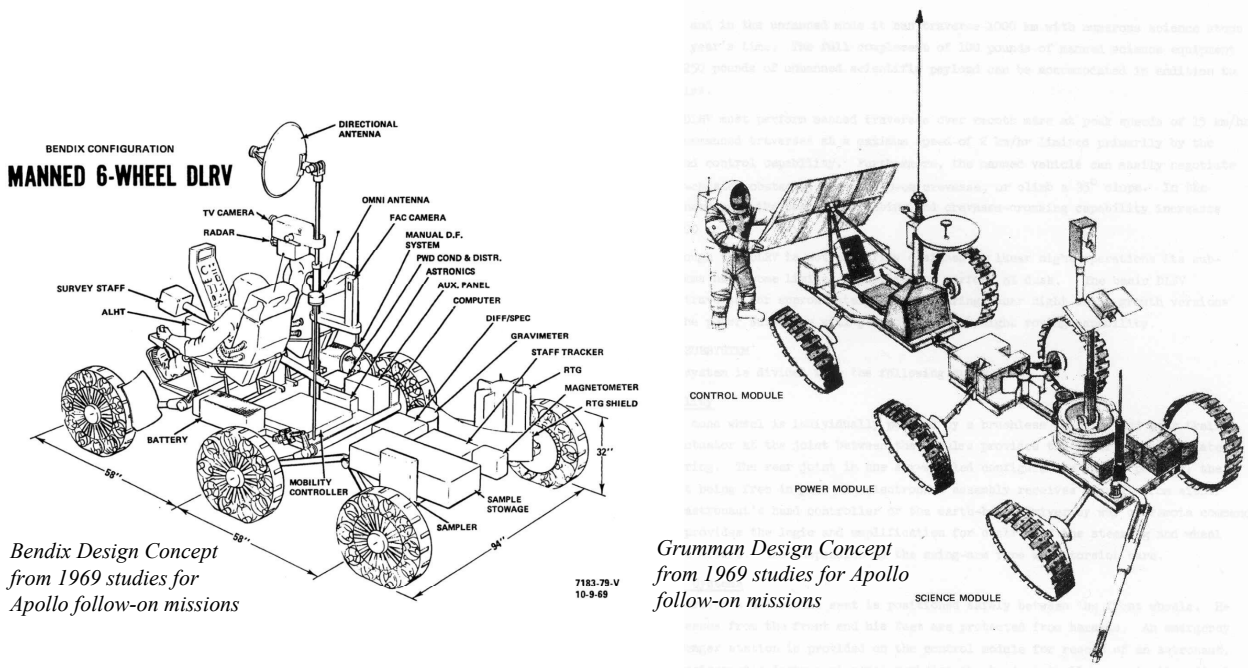

Bendix Design Concept from 1969 studies for Apollo follow-on missions

Grumman Design Concept from 1969 studies for Apollo follow-on missions

Figure 2.4.1-1. 1969 DLRV Design Studies

Three decades later the utility of this original concept appears especially timely. The Apollo missions manifestly demonstrated the value of the manned lunar rover to the astronaut's exploration activities. The stated plan of the Vision for Space Exploration [9] to establish a permanent presence on the moon in the next decades gives new impetus to providing long range roving and exploration capability in support of the siting, construction, and maintenance of future human bases. The addition of radioisotope power systems to the design further extends the capability of such a rover, allowing operation during the full lunar day/night cycle, as well as enabling exploration in permanently shadowed regions that may be of interest to humans for the resources they may hold.

2.4.1.2 Science Goals

In its manned mode, the rover would be used primarily as a means of transportation for the human crew. As such it would act to further the science that the humans are able to perform. In its teleoperated mode however, the rover would become a long-range exploration platform, carrying a variety of science payloads that would be used to thoroughly characterize the regions over which it traverses.

The present study has developed a strawman science payload design aimed at geologic exploration activities to characterize the large area accessible during the telerobotic portion of the mission. A particular focus of this science mission would be on prospecting to identify minerals and other resources that could be exploited by subsequent expeditions or provide a suitable site for a permanent human base. Rock and soil samples, as well as rock cores could be collected at sites of interest during the teleoperated traverse and stored on board the rover for recovery and return to Earth by the next human crew. Many of the instruments in the science suite are tuned to finding sources of water ice on and under the surface, as water is seen as a key resource for sustained presence on the Moon.

In addition to mineral resources, the prospective science package would allow for the detection of organic compounds deposited by comet impacts in the Moon's past. This could give greater insight into the organics inventory carried by comets.

2.4.1.3 Mission Goals

The goal of the Dual Mode Lunar Roving Vehicle (DMLRV) would be to provide a multipurpose infrastructure element and remote science platform for the exploration of the moon. The DMLRV would be essential for extending the productivity of human exploration crews, and would provide a unique capability for diverse long-range, long-duration science exploration between human visits. An additional goal of the DMLRV would be to provide a reconfigurable vehicle system capable of conducting surveying and a range of site preparation activities in support of the establishment of a permanent human presence on the moon.

The DMLRV's systems would be designed to operate over a nominal lifetime of 5 years. In telerobotic operation, the rover would be capable of traversing over 1000 km of the lunar surface. Operating in conjunction with astronauts would enable the DMLRV to be serviced in the event of component failure, and also allows for simplified deployment and instrument/payload flexibility throughout its life. These features would provide the potential for extended operational life well beyond the nominal 5-year mission duration.

2.4.1.4 Mission Architecture Overview

The mission begins with delivery of the rover on the manned lunar lander. An assumption has been made that the DMLRV, as was the case with the Apollo Lunar Roving Vehicle, would be carried as an auxiliary payload on the descent stage of a manned lander. In the case of the DMLRV, the full vehicle (Fig. 2.4.1-2) would be carried as two separate components. The manned 4-wheel rover would be self-contained and deployable by the astronauts as a fully functional single unit. The design of the 4-wheel portion of the rover is such that it could be used in the astronaut mobility application independent of the two-wheel trailer portion of the vehicle. Astronaut sorties would be limited by the duration of EVA suit life support systems, as well as the probable requirement for a "walk-back" capability.

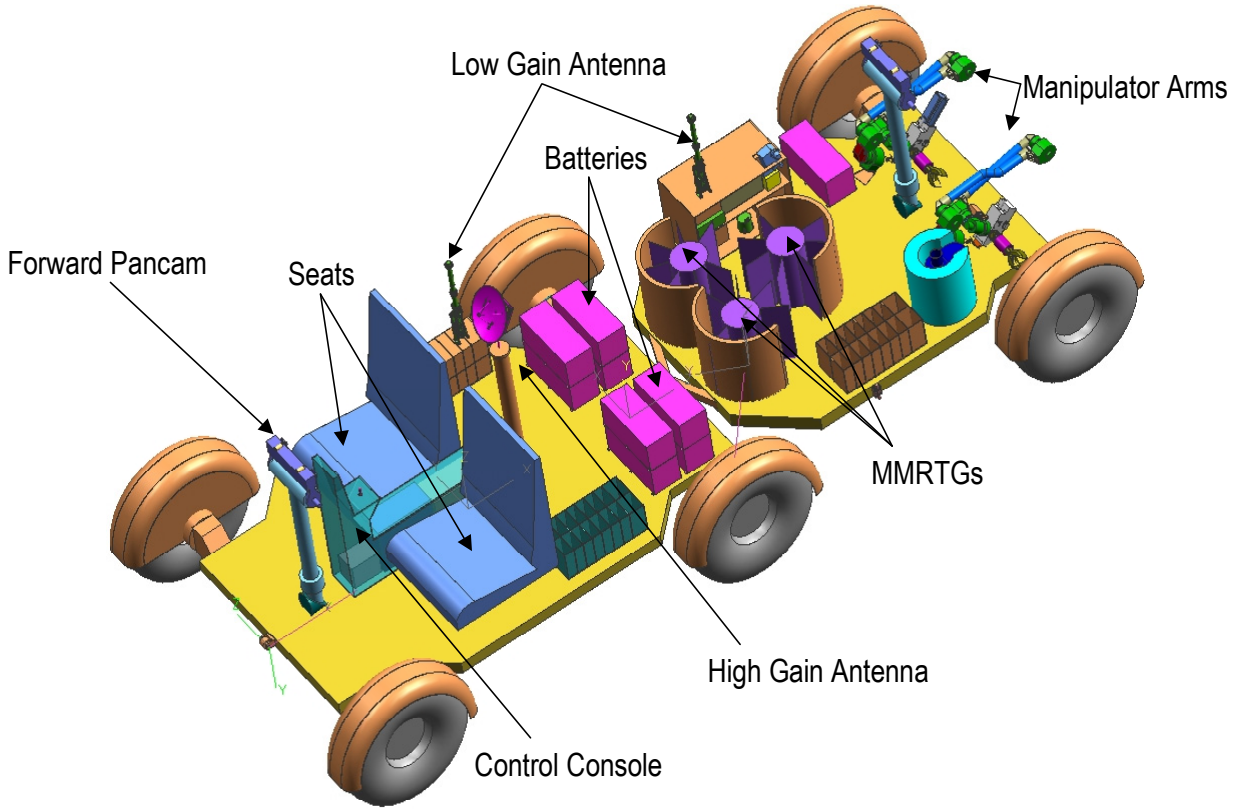

Figure 2.4.1-2. DMLRV Conceptual Design

Given this limitation in the duration of manned sorties (predicted to be no greater than ~8 hr), the 4-wheel rover would operate in the manned mode on battery power, with charging performed by the RPSs in-between sorties. The science trailer could be carried to provide continuous electrical power from the RPSs to be exploited by the astronaut crew for experiments carried out during sorties.

In order to support the teleoperation mode, a 2-wheeled trailer extension would be carried as a separate, second package on the lunar lander. Upon completion of the manned rover operations, the two-wheel module would be attached to the 4-wheel rover by the astronauts, creating a configuration optimized for teleoperated long-range exploration. The trailer design provides maximum flexibility for science experiments by standardizing payload interfaces. This allows for modular "plug-in" instrumentation that could be easily removed and replaced by astronauts during subsequent missions. Similarly, the trailer itself is a modular component to the overall rover and could be completely replaced with a new unit incorporating different science capabilities, or with a unit dedicated to infrastructure tasks (e.g. excavation and grading in support of site preparation activities). The RPSs located on the trailer enable long-range teleoperated exploration by providing day/night continuous operation with minimal "down" time required for battery charging. The continuous power supply from the RPSs provides a unique capability for operating science payloads in shadowed crater regions and during the extended lunar night period. The modular trailer design and RPS power supply are key to the versatility of the DMLRV concept, allowing a variety of potential tasks to be performed by a single infrastructure element.

The long range of the rover is intended to allow it to traverse to a subsequent landing site where it could be serviced, if necessary, and used by the next crew for human transportation. This subsequent expedition may bring additional experiment packages for incorporation into the DMLRV instrument suite for the next teleoperated exploration traverse.

Alternatively, once a promising site has been chosen for the location of a human base, a new two-wheeled module specifically designed for site preparation activities may be delivered by an astronaut crew. It is expected that preparation for a permanent human presence would require extensive regolith moving activities including grading, rock moving, and excavation to prepare for emplacement of a variety of base elements. The basic roving vehicle would provide the platform for a multipurpose site preparation infrastructure element, allowing for slow, but long-term regolith moving activities guided telerobotically from the Earth.

2.4.1.5 Power Source Trade Study

Alternatives to the RPS units as a power source for the rover were considered as part of this study. The DMLRV's design requirements include full time day/night capability with the ability to operate in permanently shadowed regions. In telerobotic mode, an all solar or solar/battery system would be inadequate for the DMLRV's mission needs, as exploration of permanently shadowed areas for water and other resources would be excluded or severely limited in duration. Such a layout would also limit operation to the 15-day monthly period of lunar day, unless a massive battery system was carried to allow for limited nighttime operations. The five year lifetime and extended range requirements of the rover would rule out an all battery powered configuration as the battery mass would be prohibitively large for the rover design. Since much of the rover's time would be spent in teleoperated mode, full-time operation in all light conditions increases the range and science gathering capabilities of the mission. The use of Standard RPSs would be the best option to achieve the mission objectives of long range capability with extended science operations available in permanently shadowed craters and during the long lunar night.

2.4.1.6 RPS Characteristics

The DMLRV would require three standard 110 We (BOM) RPSs to provide for its energy requirements (Fig. 2.4.1-3). This study considered the use of the MMRTG and SRG as the power system baseline, with the former detailed here, and the later summarized in Section 2.4.1.14. The MMRTG represents the most stressing scenario from a heat and radiation standpoint. In this design, the MMRTGs are mounted vertically on the DMLRV science trailer's deck as shown in Figure 2.4.1-3. Heat exchangers would be placed radially around the RPSs to limit the effects of the radiated heat on the crew and rover systems while collecting the excess heat emitted by the RPSs radiator fins for use in thermal control of rover systems.

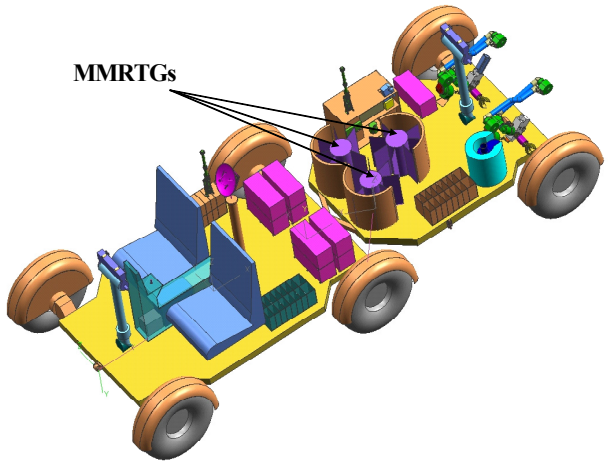

Figure 2.4.1-3. DMLRV MMRTG Layout

The three MMRTGs provide 330 We at BOM, falling to ~304 We at the end of the 5 year nominal mission, and down to ~279 We after an additional 5 year extended mission (Section 3 - Table 3-6). The DMLRV study used the standard MMRTG design; a more compact arrangement could be provided by removing the individual RPS fins and grouping the RPS units together in a single enclosure provided with a cooling loop that could transport waste heat to a remote radiator. For power dense missions such as regolith-moving applications, such an arrangement might be pursued to achieve the needed electrical generation capacity on the compact trailer unit. The enclosure may also provide advantages in dust protection over the finned configuration.

The lunar environment offers few major environmental challenges above those faced in near Earth interplanetary space. Temperatures on the lunar surface range from –190 to 110^{o}C, a somewhat wider temperature range than deep space, but expected to be within the capabilities of the RPS system. However, the upper temperature limit (110^{o}C) could reduce MMRTG efficiency. To mitigate this, a sunshade may be used to prevent the MMRTG from being exposed to direct sunlight. While the moon does in fact have a trace of an atmosphere, it is so thin that its effects are negligible. Dust accumulation on the rover heat sink fins and other radiator surfaces (as demonstrated on the Apollo missions) will likely require considerable attention in future design studies, but the vertical orientation of the MMRTGs in this configuration should mitigate this problem to some extent. The study has concluded that no issues appear to prevent the use of baseline MMRTGs on the lunar surface.

2.4.1.7 Science Instruments

The DMLRV is capable of supporting a wide assortment of scientific instruments depending on mission objectives. The continuous power available from the RPS widens the range of tools that could be accommodated in the rover's instrument suite. An array of potential instruments was studied (Table 2.4.1-1) to demonstrate the versatility of the rover and its science platform in assisting manned explorers and performing extensive telerobotic science gathering of its own in a geological survey mission.

Instruments on the rover could be located in a variety of areas (Fig. 2.4.1-4). The twin Pancam masts on the rover and trailer are mounting points for lights and imagers, providing a high-resolution 360° view of the surrounding terrain. An interchangeable science rack on the trailer (Fig. 2.4.1-5) provides standardized power and data interfaces, allowing astronauts to plug in and remove modular scientific instruments as needed, enabling the rover's instrument suite to be optimized for a particular sortie including the tools best suited for the task on hand. This also expands the rover's capabilities while operating tele-robotically as the instrument inventory could be reconfigured or augmented prior to the human crew's departure.

The twin robotic arms (Fig. 2.4.1-6) provide mounting points for tools and imagers that are best used close-up against the surface of the samples being analyzed. The robotic arms would also be equipped with end effectors capable of grasping rock and soil samples for delivery to deck-mounted science instruments or sample storage containers. The two arms could be used in conjunction with one another for holding samples with one manipulator and analyzing the sample with the other arm's instruments. Larger tools could be mounted directly to the rover's deck as proposed with the 2.5-m drill.

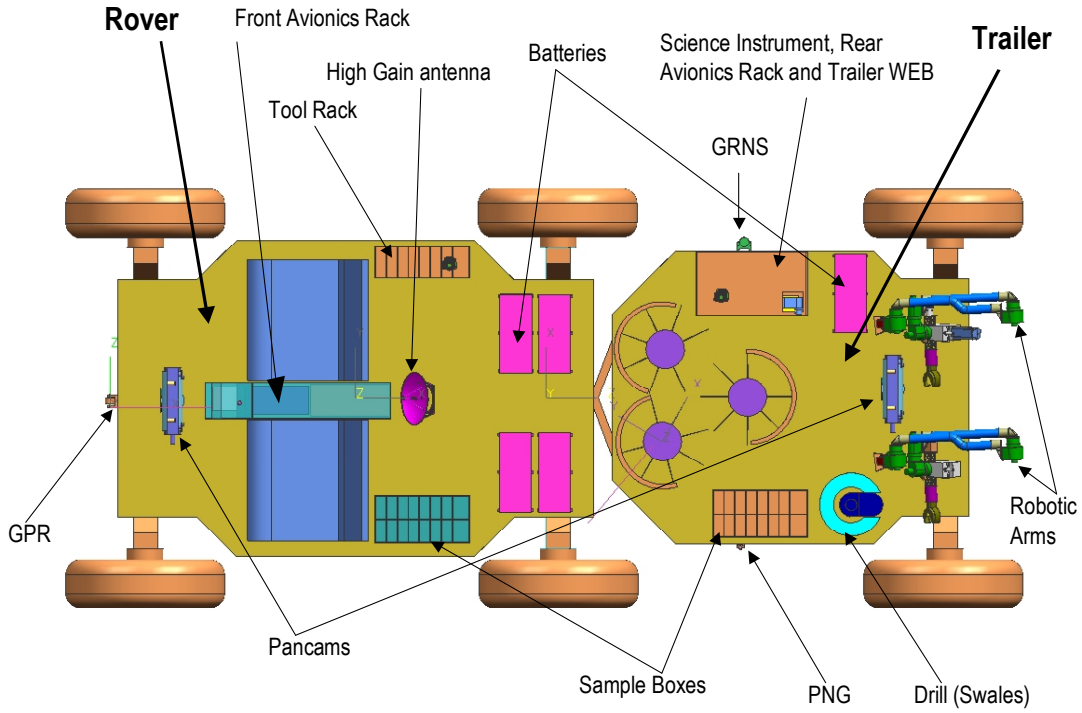

Figure 2.4.1-4. Instrument Accommodation of the DMLRV Rover

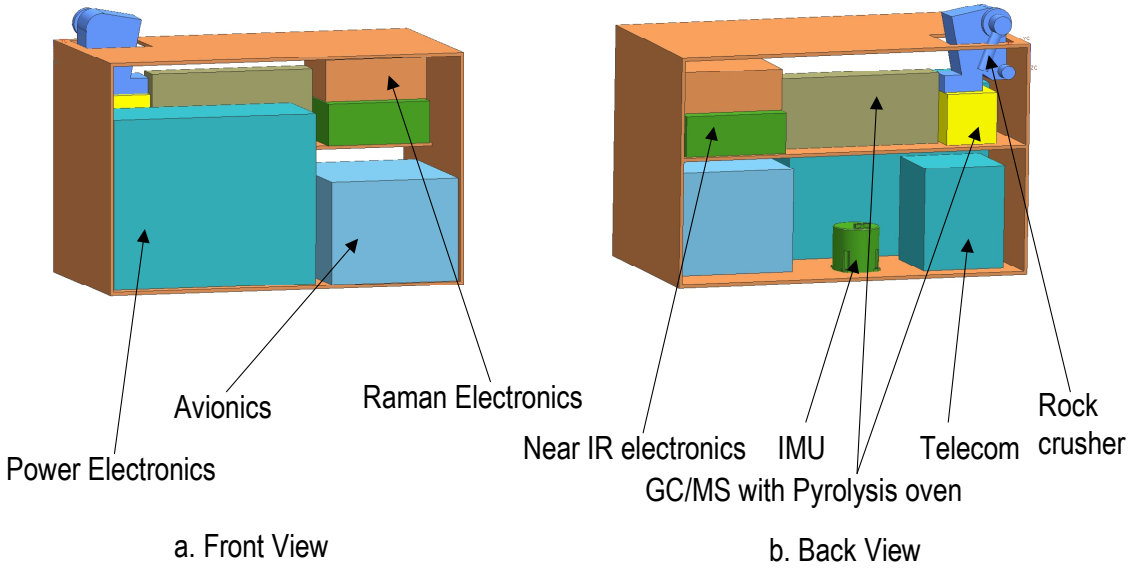

Figure 2.4.1-5. DMLRV Science Instrument / Rear Avionics Rack

Table 2.4.1-1. DMLRV Science Instrument Characteristics

Name	Purpose	Science Accomplished	Heritage
Pancam	Obtains panoramic images of surrounding terrain	• Provides a 360° stereoscopic view of the surrounding terrain to allow for accurate navigation and visual surveying of surface features	MER
Nav Lights	Nighttime Navigation	• Aids exploration at night and in permanently shadowed areas	None
Near-IR/VIS Hyperspectral Imaging Spectrometer	Pancam mounted unit determines mineral compositions of surface material using visual and infrared wavelength spectroscopy	• Search for water and other usable resources	MIDP AiMS instrument
GRNS	Detects surface and subsurface bulk concentrations of elements which make up usable resources	• Search for water and other usable resources • Aids in finding targets for drilling	NEAR, PIDDP
Engineering Cameras	Provide rapid frame rates for guidance of the manipulator arms and close in imaging of samples	• Aids telerobotic operation of arms in support of science instruments	Commercially based
CHAMP	Arm mounted color microscope used to examine the crystalline structure of rocks	• Geologic information on the formation of the rocks on the lunar surface • Search for usable resources	MIDP
Ultrasonic Corer	Arm mounted tool cuts small core samples for analysis with other instruments	• Geologic information on the formation of the rocks on the lunar surface • Search for water and other usable resources • Aids in preparing samples for further analysis	MIDP, ASTEP, ASTID
RAT	Arm mounted tool grinds off the surface layers of rocks to allow for analysis of their hardness and inner structure	• Geologic information on the formation of the rocks on the lunar surface • Aids in preparing samples for further analysis	MER
MRS	Arm mounted microbeam Raman spectroscope to identify minerals and their proportions and textures	• Geologic information on the formation of the rocks on the lunar surface • Search for water and other usable resources • Detection of organic compounds	PIDDP - Descoped from MER
GC/MS	Analyze mass spectra to determine isotopic ratios of evolved gas constituents inside samples.	• Geologic information on the formation of the rocks on the lunar surface • Search for water and other usable resources • Detection of organic compounds	Pathfinder/ MER
Pyrolysis Oven	Heats rock samples to release samples for analysis	• Geologic information on the formation of the rocks on the lunar surface • Search for water and other usable resources • Aids in preparing samples for further analysis	DRDF and ASTID
Rock Crusher	Pulverizes rock samples for pyrolysis oven	• Aids in preparing samples for further analysis	None
GPR	Images near to deep underground to find subsurface ice concentrations	• Search for water and other usable resources • Aids in finding targets for drilling	PIDDP

To navigate around the lunar surface and perform optical surveying, the DMLRV would carry two panoramic camera (Pancam) units similar to the Pancam unit used on MER (Fig. 2.4.1-7). These would provide stereoscopic vision to the rover allowing ranging to be determined to aid in producing maps and crossing terrain. The cameras also allow for multi-spectral imaging to increase the range of data that could be gathered through optical surveying. To accommodate the day/night capability of the rover, light-emitting diode (LED) lights would be located on the Pancam masts to provide navigation lighting under both modes of operation. Both the rover and its science trailer would have Pancam units allowing the rover to be operated effectively in either direction and expanding the field of view for the rover while surveying. The inclusion of a second unit increases the redundancy of the rover for long-term telerobotic operations.

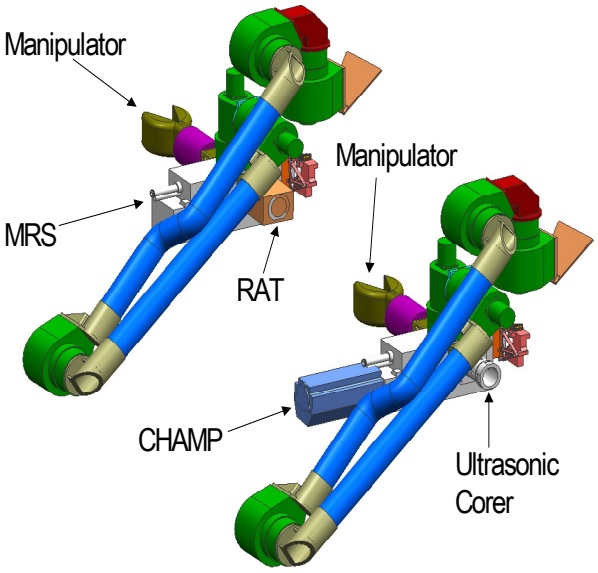

Figure 2.4.1-6. DMLRV Arm Instrument Layout

Near-IR/VIS Hyperspectral Imaging Spectrometers would be mounted on the Pancam masts to help determine the mineral compositions of surface materials. The spectrometers utilize rapid 2D imaging spectroscopy at hundreds of VIS and IR wavelengths to allow analysis of mineral mixtures. The instruments' ability to detect the spectral signature of water ice on the surface makes the tool a valuable asset in hunting down lunar resources.

A Gamma Ray/Neutron Spectrometer (GRNS) would allow the rover to determine the bulk concentrations of many rock-forming elements, including Hydrogen, Oxygen, and a host of others that may be important to enabling a sustained human presence. The tool could determine the local concentration of hydrogen-bearing materials in less than 5 minutes. The ability to determine subsurface elemental concentrations is essential for searching out locations where further investigation by drilling is desired. The GRNS is capable of penetrating 10-20 cm with gammas and 30-50 cm with neutrons. The addition of a 14 MeV pulsed neutron generator would allow for more sensitive measurements with lower backgrounds. In the baseline rover configuration the GRNS is located on the side of the science trailer (Fig. 2.4.1-4), although other locations are certainly possible.

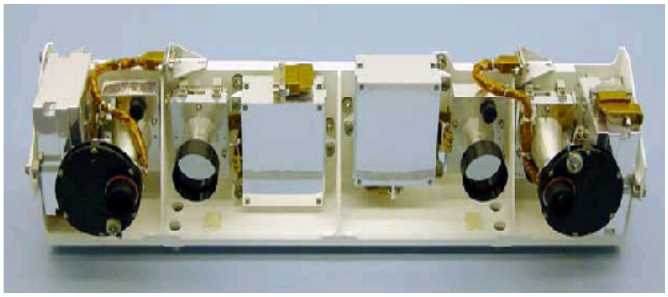

Figure 2.4.1-7. Pancamera Mast Head

To facilitate accurate guidance of the rover's two science trailer-mounted robotic arms, small engineering cameras capable of recording at frame rates up to 30 fps are located on each arm (Fig. 2.4.1-8). These cameras could be brought in close to provide detailed images of rocks, providing their own light with a ring of small LEDs around the camera lens.

For more detailed images, one of the arms would carry a Color Handlens Microscope (CHAMP). This tool (Fig. 2.4.1-9) could be brought up right against rocks to examine their crystalline structure without the need to first prepare the surface. The CHAMP is designed to accommodate variable resolution imaging.

Lightweight ultrasonic corers could be included to provide drilling with the accurate manipulation made possible by the robotic arms. These tools allow drilling through hard rock while producing only low axial loads and almost no torque on the mounting arm. A 1-cm diameter corer could collect 1 x 5 cm cores from most rocks, with the depth limited to 2.5 cm for the hardest volcanic rocks. The ultrasonic corer has a long lifetime, capable of cutting 300 cores before the core bit would need changing. Such maintenance could easily be performed by astronauts, extending the lifetime usefulness of the tool.

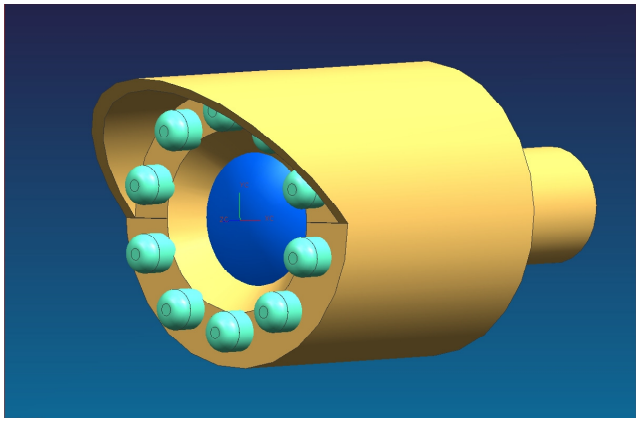

Figure 2.4.1-8. Engineering Camera with LEDs

To grind off the outer layer of rocks to allow better analysis and imaging, a Rock Abrasion Tool (RAT) could be mounted on one of the robotic arms. A RAT was carried by MER to grind off the rinds of weathered rocks on Mars. The RAT could measure the rocks hardness as it is penetrating into the rock, a useful measure in geological analysis.

Another potential arm-mounted instrument is a Microbeam Raman Spectroscope (MRS). This tool identifies many major, minor, and trace minerals, their relative proportions, cation ratios (e.g., Mg/Fe ratio) and can be oriented to resolve textural features (e.g., mineral clusters, veins). The MRS also provides definitive detection of water and some forms of carbon bearing materials. Being arm-mounted the MRS could be more accurately aimed than some of the other spectrometers on the rover. It provides relatively fast analysis times (integrating 50 Raman spectra per hour).

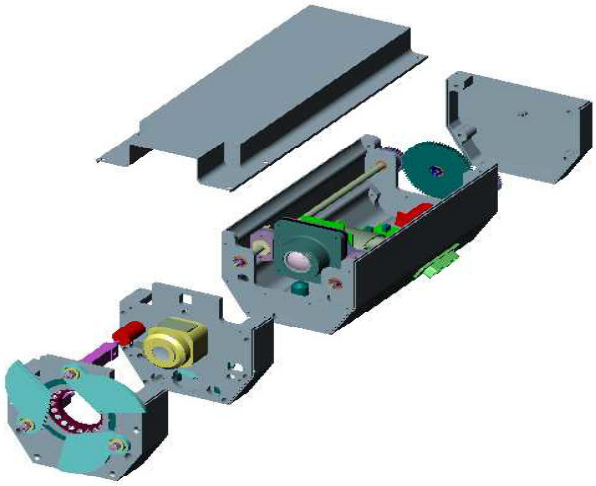

Figure 2.4.1-9. Exploded view of CHAMP

An onboard combined Gas Chromatographer/Mass Spectrometer (GC/MS) would provide mass spectra to determine isotopic ratios of evolved gas constituents from rock and soil samples delivered by arm. This could be used to identify the presence of organics left behind by comet impacts on the lunar surface in the past. The instrument could also be used to measure the trace atmospheric species resulting from reactions caused by surface impacts.

The addition of a pyrolysis oven (Fig. 2.4.1-10) allows for analysis of molecules released by rock samples when heated. Rock samples would be collected by the arms and introduced into the pyrolysis chamber and then heated to 1200K in a step-wise process. The piston design created by Ball Aerospace allows multiple samples to be heated in the oven increasing efficiency. The GC/MS would work in close conjunction with the oven to analyze the released gases.

A rock crusher would be used to prepare samples for analysis in the pyrolysis oven. This provides a homogenous sample that could be analyzed by several instruments simultaneously, providing comprehensive elemental, chemical, and mineralogical information on a sample. During the crushing process the core is divided into 2 bins: powder and rock chips. The powder sample is delivered to a sample carousel on a path to the analytical instruments. The rock chips (mm-scale) are deposited on a transparent slide and viewed from below by the Confocal Microscope (with a nested Raman spectroscope) and Context Imager.

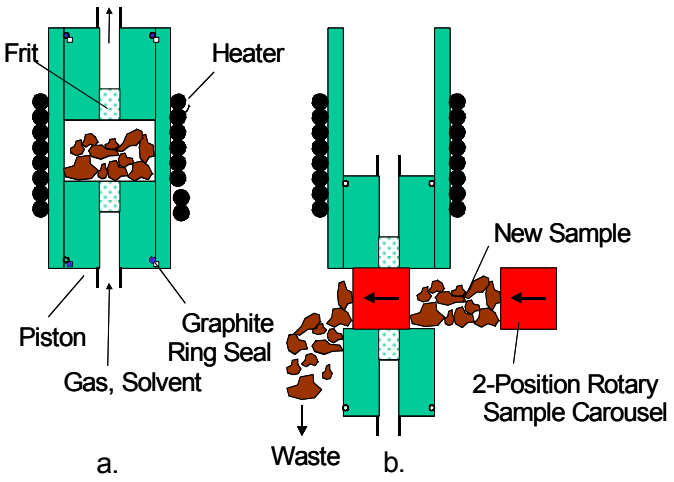

Figure 2.4.1-10. Ball Aerospace Pyrolysis Oven. (a) Sample in position for heating, and (b) Oven being loaded with a new sample.

Ground Penetrating Radar (GPR) would be employed to find interesting subsurface targets for further investigation (Fig. 2.4.1-11). The GPR could be used to search for subsurface ice concentrations and other resources that would be useful to lunar colonists. The baselined GPR would be capable of imaging layered or lenticular deposits to depths ranging up to 10-100 m with a nominal resolution of 0.5 m at an RF frequency of 150 MHz. Operating at higher power when stationary could allow for greater resolution. Two types of GPR have been considered; a long thin tape and a more conventional setup with twin metal antenna. The tape antenna provides a compact storage solution for when the GPR is not in use, but either setup could be accommodated.

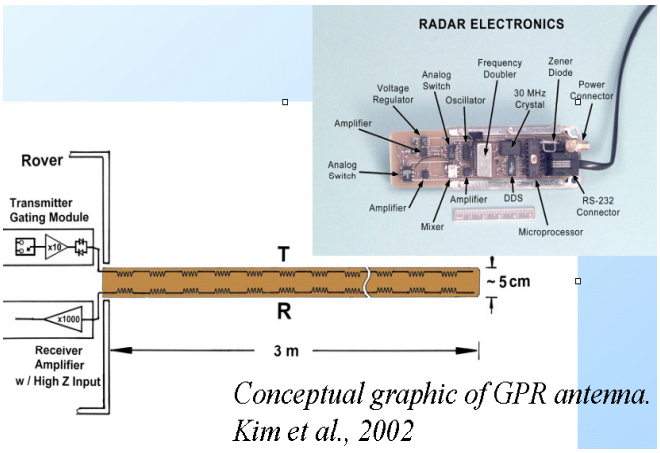

Figure 2.4.1-11. Tape Style GPR antenna

A compact 2.5-m drill designed by Swales could be carried onboard the science trailer deck for gathering subsurface samples from areas identified as promising by GPR and gamma/neutron spectroscopy. This tool allows for holes up to 2.5-m deep to be drilled into the lunar surface, although the depth may be reduced for harder rock. The drill uses 30-cm long drill segments to allow for full analysis of every 30 cm interval.

The drill head is relatively short-lived and may be dulled after 2-5 holes depending on rock type. This makes drill site selection an important process, using numerous instruments to determine the most promising sites prior to drilling.

The rover's wheels could provide a unique opportunity for real time in-situ resource detection by mounting contact sensors in the wheels themselves, capable of collecting data while the rover is traversing (Fig. 2.4.1-12). These sensors are designed to search for the presence of H, O, N, and C; the four elements deemed critical for in-situ resource utilization in planetary exploration. An impedance spectrometer and conductivity sensors would detect the presence of ice and water and help determine its salinity. A pH meter would detect the presence of acids and bases on the lunar surface, while the electrostatics sensor could recognize changes in mineral composition to identify geological boundary zones. The wheel-mounted sensors could be used while underway to help identify locations where further stationary analysis by the rover's instruments is warranted. This gives the rover a surveying capability that allows for science to be performed without the necessity to stop.

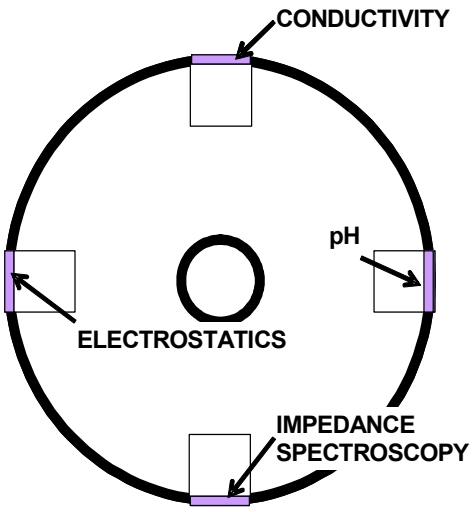

Figure 2.4.1-12. Wheel Contact Sensors

2.4.1.8 Data

The instrument suite is capable of collecting a wide array of information to be transmitted back to Earth in addition to the data needed ordinarily to operate the rover. The data rates for the baseline instruments are shown in Table 2.4.1-2. The rover's avionics are contained in two single string units; one on the rover and one on the science trailer. To handle data processing and control, each unit would employ a RAD 750-based computer, as well as electronics for the motors and actuators and 8 GB of flash memory. The avionics boxes on the rover and trailer are modular and fully interchangeable should repairs or replacements have to be made on the lunar surface.

Continuous two-way data flow is needed for effective and efficient teleoperation as well as Earth monitoring of manned excursions. To communicate while moving lowers the effective data rate by requiring either the use of a low gain omni directional antenna (LGA) or incorporation of relatively fast active pointing systems on a high gain antenna (HGA). The DMLRV baseline incorporates LGAs for communications while moving to avoid the added complexity of tracking mechanisms. A 0.3-m HGA would be used to transmit while stationary to raise the data rate for downlinked science data.

Table 2.4.1-2. Data Rate Estimates for the DMLRV Concept

Instrument	Data Rate/Data Volume
Pancam	50.4 Mbits/frame (raw). Need 12 frames for a full panorama
Near-IR/VIS Hyperspectral Imaging Spectrometer	162.2 Mbits/Vis to Near-IR spectra (raw)
GRNS	~100 kbits/spectra
Engineering Cam	1 µm pixels/s
CHAMP	9 Mbits/RGB image
MRS	17 kbits/spectra (raw)
GCMS	~10 kbits/mass spectra, ~200 kbits/evolved gas sample
Pyrolysis Oven	1 Gbits/sample (raw)
GPR	16 kbits/multi-frequency trace. 1 minute/trace.

2.4.1.9 Communications

The DMLRV would require a relatively high continuous data-rate to operate efficiently in a telerobotic mode on the lunar surface. The baseline telecom subsystem was designed to support a downlink transfer rate of 550 kbits/s over the LGAs while driving, with an increased capability of 10 Mbits/s through the HGA when the rover is stationary. To accomplish this, the rover transmits information in the X-band on both its 0.3-m HGA and omnidirectional LGAs directly to a 34-m DSN station on Earth. The relatively close proximity of the lunar surface to Earth stations allows for high data rates with only modest sized telecommunications equipment. The system could also make use of planned orbiting platforms to communicate back to Earth via relay link should the need arise due to a lack of direct contact.

The 0.3-m HGA is located on a mast on the forward portion of the main rover deck. It provides a high data rate transfer back to Earth for the science instruments and cameras. The HGA does not have the capability to track while the rover is traversing, although this capability likely could be added, at least for low speed traverses, with an attendant mass and complexity penalty.

For communication under driving conditions, the DMLRV would use omni-directional LGAs to achieve the necessary 550 kbits/s downlink transfer rate for the telerobotic operation. This would also be the primary communication mechanism under manned operation. The science trailer also carries an X-band LGA to provide versatility and redundancy to the telecom system.

X-band communication systems have a flight heritage shared with a number of past and current spacecraft. Like many systems on the DMLRV, the X-band telecom system shares elements with the telecom system used on MER. The use of established technology on the rover lowers the costs and challenges of development and implementation of the telecom subsystem for this mission.

2.4.1.10 Thermal

The cold temperatures experienced on the lunar surface would require the rover's actuators and electronics to be kept heated to maintain them within their operating ranges. Heat would be supplied by a combination of electric heaters and a loop heatpipe system, which takes excess heat from the RPS system and uses it to heat the vehicle electronics. Insulation would be provided to minimize thermal losses and reduce the power needed to warm the DMLRV's systems.

In addition to electricity, each MMRTG generates ~1890 Wt BOM of excess heat which must be rejected. The bulk of this RPS heat is rejected to the environment by the radiator fins attached to the body of the RPS. A portion of the waste heat from the RPSs would be used to provide heat to the warm electronics boxes on the rover and the science trailer.

Heat for the electronics would be supplied by a loop heatpipe system (Fig. 2.4.1-13), which brings a portion of the waste heat from the RPS units to the warm electronics boxes (WEB). Heat is exchanged with a working fluid, which is turned into a gas by the heat exchangers surrounding the MMRTGs, and then circulated around the rover to maintain reasonable operating temperatures in the electronic components. This eliminates having to heat the electronics with electric heaters, and makes use of what otherwise would be wasted energy. Due to the low amount of heat needed to keep the WEBs at operating temperatures, either the MMRTG or the SRG would be sufficient to support this thermal design. In addition to the electronics, the motors and actuators on board the rover would need to be heated to maintain their operating conditions. The DMLRV uses 22 actuators throughout its various systems. Boron-epoxy tube insulation would be used to reduce the heating requirements for these actuators to ~15 We. This highly effective insulation greatly would reduce the amount of power required for the electric heaters.

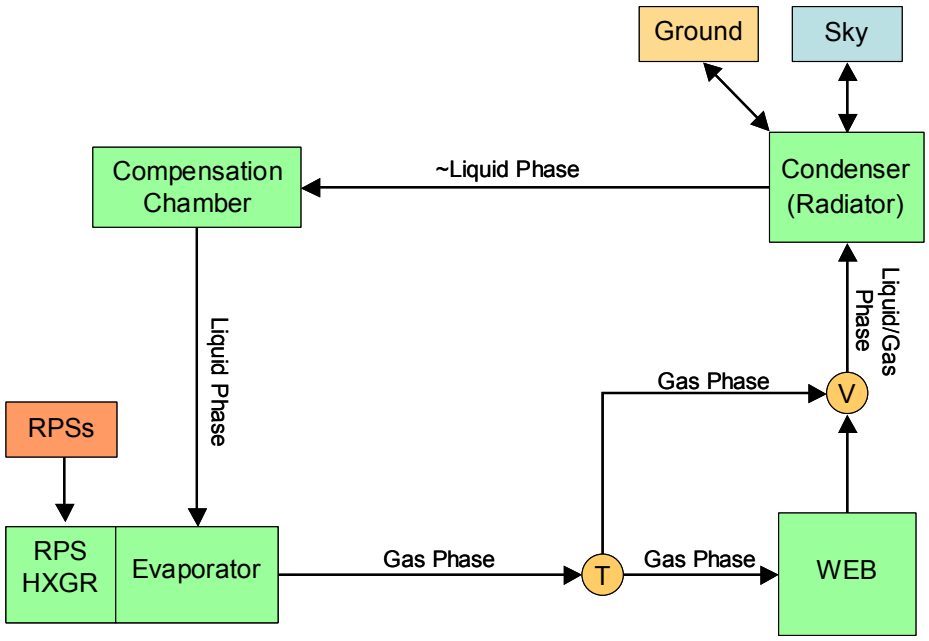

Figure 2.4.1-13. Loop Heatpipe Diagram of the DMLRV

2.4.1.11 Power

Three MMRTGs and rechargeable Li-Ion batteries would provide power to the rover's systems. The baseline design calls for the DMLRV to carry ten 25 A-hr Li-Ion batteries, with nine located on the rover and one on the science trailer. Estimated power loads are listed in Table 2.4.1-3.

For manned operation the batteries alone would provide the power to run the rover's systems, allowing the rover portion of the vehicle to operate independently of the science trailer for astronaut sorties. If needed, the rover batteries could be recharged by the RPSs on the science trailer between sorties.

Table 2.4.1-3. Power Level Estimates for the DMLRV Concept

Load Names	Power (We)	Margin	Power with Margin (We)
Rover Subsystems			
C&DH	27.3	30%	35.5
Power	3.9	30%	5.1
ACS	15	30%	19.5
Telecom	25-55	30%	32.5-71.5
Thermal	15	30%	19.5
Drive Motors (Teleoperation, 2 km/hr) Drive Motors (Manned Ops, 8 km/hr)	178.3 518.7	30%	231.8 674.3
Wheel Heaters	10	30%	13
Instruments			
Pancam Unit	6 operational, 1.5 standby	30%	7.8 operational, 1.95 standby
Navigation Lights	5	30%	6.5
Near-IR/VIS Hyperspacial Imaging Spectrometer	12	30%	15.6
GRNS	19	30%	24.7
Engineering Camera	0.5	30%	0.75
CHAMP	5	30%	6.5
Ultrasonic Corer	23	30%	29.9
RAT	8-11 depending on rock hardness	30%	10.4-14.3 depending on rock hardness
MRS	18	30%	23.4
GCMS	0.5 GC, 8 MS	30%	0.65 GC, 10.4 MS
Pyrolysis Oven	8	30%	10.4
GPR	5	30%	6.5
2.5-m Drill	15-35 depending on rock hardness	30%	19.5-45.5 depending on rock hardness
Wheel Contact Sensors	0.2/Sensor, 5 micro-controller	30%	0.26/Sensor, 6.5 micro-controller

When operated independently, the manned rover would have access to nine 25 A-hr batteries in the baseline design. The rover's range in this mode is largely limited by the power draw of the wheel actuators, which is impacted by the rover's mass and the velocity traveled. Table 2.4.1-4 shows the maximum range of the rover while traveling at 8 km/hr (average speed of Apollo LRV) with various payload masses. For reference, it is estimated that the payload mass of two astronauts in EVA suits would be about 400 kg.

In teleoperated mode, the baselined DMLRV would operate as a complete unit with Li-Ion batteries along with its full RPS compliment. The baseline design with 303.6 We (EOM) from three MMRTGs would be capable of over 30 hrs of continuous driving at 2 km/hr before needing to stop for an equivalent period to recharge its batteries. In an operational scenario, the rover would likely make frequent stops to perform science and data transmission operations and so would be unlikely to need to drive for such an extended period of time. During the stationary periods, power draw would be greatly reduced and the batteries would recharge, allowing the rover to operate essentially without interruption. The ability of the rover's wheel contact sensors and imagers to conduct science while the rover is traversing greatly increases the amount of ground the DMLRV could survey while traversing and improves the rover's ability to spot signs of local water and other promising targets. The contact sensors do require the rover to travel at $\leq$0.36 km/hr, so the rover would have to slow down from its nominal 2 km/hr cruising speed to utilize them to best effect. At these reduced velocities, the DMLRV's batteries would be in a continuous charging state, extending its driving duration indefinitely.

The DMLRV's RPSs alone provide ample electrical power to accommodate the ~280 We the entire strawman instrument suite would draw if operated simultaneously, meaning that power generation would not constrain the science instruments in normal operations. This available power leaves open for consideration the option of much more power intensive instruments in the science package.

Table 2.4.1-4. Rover Operating Duration and Range as Function of Payload Mass, driving at 8 km/hr

Payload Mass (kg)	Driving Duration (hr)	Total Driving Range (km)
800	5.1	40.8
750	5.3	42.6
700	5.6	44.6
650	5.9	46.8
600	6.2	49.2
550	6.5	51.8
500	6.8	54.6
450	7.2	57.8
400	7.7	61.2

2.4.1.12 Mass

The baseline DMLRV system has an estimated total mass of ~930 kg including a strawman instrument suite. The individual rover and trailer sections have masses of 445 kg and 485 kg, respectively. The mass breakdown by subsystem is shown in Table 2.4.1-5. The majority of the total mass is made up by the structure and power system. The DMLRV's versatile battery/MMRTG power system and sturdy frame for handling heavy loads make the system heavier then the Apollo LRV, but this new design offers significantly enhanced capabilities relative to the earlier rover.

To support lunar infrastructure development, a large payload capacity would be required to allow for hauling regolith or towing equipment into place. When operating in a science and exploration role, this capacity could translate into large science or supply loads. The DMLRV vehicle concept was designed to accommodate a maximum payload of 800 kg, of which 400 kg would be allotted to the two suited astronauts with the remainder being open for samples and equipment. In the teleoperated mode, the total science and sample mass could be increased to the entire 800 kg payload capacity. This would allow for considerable sample storage capability for the DMLRV's long teleoperated missions.

Table 2.4.1-5. Mass Estimates for the DMLRV Concept

Subsystem	Mass (kg)	Margin (%)	Mass with Margin (kg)	Notes
Rover Section	**342**	**30%**	**444.7**	
Structures/Mechanisms	125.8	30%	163.5	Projected from tubular frame concept
Human Operations	8	30%	10.4	Includes seats and instrument console
Mobility and Drive	43.2	30%	56.2	Wheels and Fenders
Thermal	16	30%	20.8	Heat pipes and radiators
Guidance and Navigation	2.5	30%	3.3	IMU, cameras
Avionics	16.8	30%	21.9	Two identical single string systems
Power	100.8	30%	131	Batteries and control electronics
Telecom	17.6	30%	22.9	Transmitters, 20 W TWTAs, antennas
Cables	7.5	30%	9.8	
Instruments	3.8	30%	4.9	Pancam, wheel contact sensors
Trailer Section	**373.3**	**30%**	**485.3**	
Structures/Mechanisms	87.6	30%	113.88	Estimated from rover mass
Mobility and Drive	21.6	30%	28.08	Wheels and fenders
Thermal	15	30%	19.5	Heat pipes, HXGRs, and radiators
Avionics	18.3	30%	23.8	Two identical single string systems
Power	155.7	30%	202.4	3 MMRTGs, battery, control electronics
Telecom	8.7	30%	11.3	Transmitters, 20 W TWTAs, antennas
Cables	7.5	30%	9.8	
Instruments	59	30%	76.6	Strawman instrument suite

2.4.1.13 Radiation

The rover and its crew would be exposed to two different radiation environments during their stays on the moon: the radiation field of the RPS, and the background radiation on the lunar surface. The lunar environment exposes the rover and crew to both galactic cosmic radiation (GCR) and the solar particle flux from the Sun. Interactions of GCR with the lunar regolith also generates neutrons, which would scatter back up to impact the systems. The long duration of the mission would expose the electronic systems of the rover to powerful Solar Particle Events (SPE). It is assumed that the astronauts would take cover in such an event; thus, the dose from SPEs is not taken into account for the astronaut dose rate while on the rover.

The three MMRTGs on the rover would represent a source of neutron and gamma radiation to the instruments and electronic components. The higher radiation field of the MMRTG (compared with the SRG) was used to represent the most stressing case for the doses to the crew and equipment. Table 2.4.1-6 shows the total 5-year mission dose received by the two electronics chassis and the Pancam units. These doses were based on rates calculated from analysis performed by JPL [37, 38] on the radiation field produced by MMRTGs. Rates for SPEs were calculated for an average year.

The results indicate that the maximum total dose to the rover electronics would be ~ 33 krads for the 5-year nominal mission duration, the majority of the dose being from SPEs, requiring a minimum of 66 krads hard parts or additional shielding to ensure safe operation. This level is easy to accommodate with existing hardened electronics and is not expected to pose a challenge to the mission.

Table 2.4.1-6. DMLRV Radiation Dose Estimates for Selected Subsystems

Source	Avionics Rack Front	Avionics Rack Rear	Pancam Head Front	Pancam Head Rear
Total Ionizing Dose over 5 yrs (rads(Si) behind 100 mils Al)				
MMRTG Total	**429.5**	**27971**	**191.4**	**666.6**
MMRTG Front Center	161.5	22885	69.0	196.4
MMRTG Rear Right	161.5	1008.8	69.0	196.4
MMRTG Rear Left	106.5	4077.5	53.3	273.9
Environment Total	**7530**	**7530**	**7530**	**7530**
GCR	36.5	36.5	36.5	36.5
SPE	7490	7490	7490	7490
Total Mission	**8121.2**	**23622.4**	**8728. 9**	**9929. 8**
Displacement Dose from Neutrons over 5 yrs (# 1MeV n/cm^2)				
MMRTG Total	**1.91E+10**	**1.36E+12**	**8.39E+09**	**2.99E+10**
MMRTG Front Center	7.20E+09	1.12E+12	3.03E+09	8.79E+09
MMRTG Rear Right	7.20E+09	4.66E+10	3.03E+09	8.79E+09
MMRTG Rear Left	4.71E+09	1.93E+11	2.33E+09	1.23E+10

Preliminary analysis of the radiation fields produced by the MMRTGs suggests that the dose levels would be low enough to allow safe operation of the rover with the science trailer attached for

manned operation (Table 2.4.1-7). This table also presents results from an assessment of the same design using four SRGs in place of the three MMRTGs. The hourly weighted dose rate to an unprotected human being from the Stirling powered trailer would be approximately 7.8 mrem/hr. This is only 23% of the background dose the astronauts would accrue from GCR while operating the rover. The dose rate from the gammas could be further reduced by the addition of shielding at the cost of added mass. These calculations do not take any shielding into account due to the astronaut's suits or scattering from the lunar regolith, both of which would affect the results.

Table 2.4.1-7. Estimated Radiation Dose to Crew While Using DMLRV Trailer

Operator Location	RPS Radiation		Background	Total Weighted Dose (mrem/hr)
	Gamma Dose (mrem/hr)	Neutron Dose (mrem/hr)	GCR Dose (mrem/hr)	
Estimated Total Crew Dose Rate (MMRTGs)				
Right or Left Seat	16.2	31.7	33.4	81.3
Estimated Total Crew Dose Rate (SRGs)				
Right or Left Seat	3.3	4.5	33.4	41.2

2.4.1.14 Alternate RPS Power System

While the previous mission analysis assumed an MMRTG-based power system, the MMRTG actually represents the more stressing example from a thermal and radiation perspective. In fact, the nature of the DMLRV's proposed mission and its operation may favor the SRG for this application. As the rover would be intended for manned operation, the lower dose accrued from the SRGs implies that they would be the preferred choice from a radiological point of view. The four SRGs (three primary and one spare) would incorporate a total of eight GPHS modules compared to the 24 modules carried on the three MMRTGs, resulting in a considerable reduction in the dose to the electronics and crew. In addition, their lower heat output makes radiated thermal energy less of a concern. The lower mass of the SRGs allows for the addition of the fourth (spare) unit with nearly the same total mass as three 3 MMRTGs while yielding an additional 110 We generating capacity to the 330 We baseline at BOM. This extra unit would enhance power system reliability and allow continuous operation while driving in telerobotic mode increasing the distance that could be covered during a teleoperated mission.

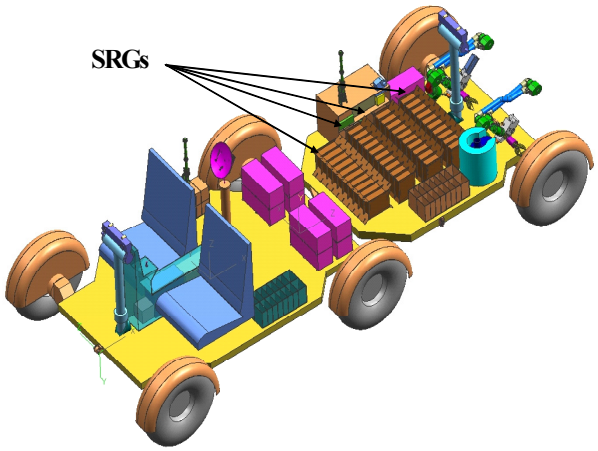

Figure 2.4.1-14. DMLRV Layout with SRGs

Should the preferred SRGs be used, they could be placed crosswise on the bed of the science trailer, as shown in Figure 2.4.1-14. This arrangement reduces open deck space on the science trailer (Fig. 2.4.1-15), but still provides ample room for science instruments on the outer portions of the trailer platform. Other potential arrangements of the SRGs could be accommodated, with configuration being made more flexible as a result of their lower thermal and radiation emissions. As mentioned, the DMLRV would carry a redundant fourth SRG (per current NASA and DOE guidelines [11]) increasing the elec-

trical power available to the rover. The four SRGs together would produce ~440 We at BOM, and would drop to ~419 We after 5 yrs at EOM, and down to ~398 We after 10 years of operation (Section 3 – Table 3-7). While the possibility of a unit failure may be higher with the SRGs, a single failure would result in a drop in electrical power down to the level of the baseline MMRTG mission, leaving the DMLRV still fully capable of completing its mission. The Stirling engine's vibrations must be considered in choosing and implementing an instrument suite, as very sensitive instruments (e.g., seismometers) may be affected by it. Detailed analyses need to be performed to assess this sensitivity and, if necessary, possible mitigation strategies.

Operating in conjunction with human explorers would provide periodic opportunities for maintenance and repairs on the rover and its power systems, allowing for replacement of a failed SRG should it become necessary.

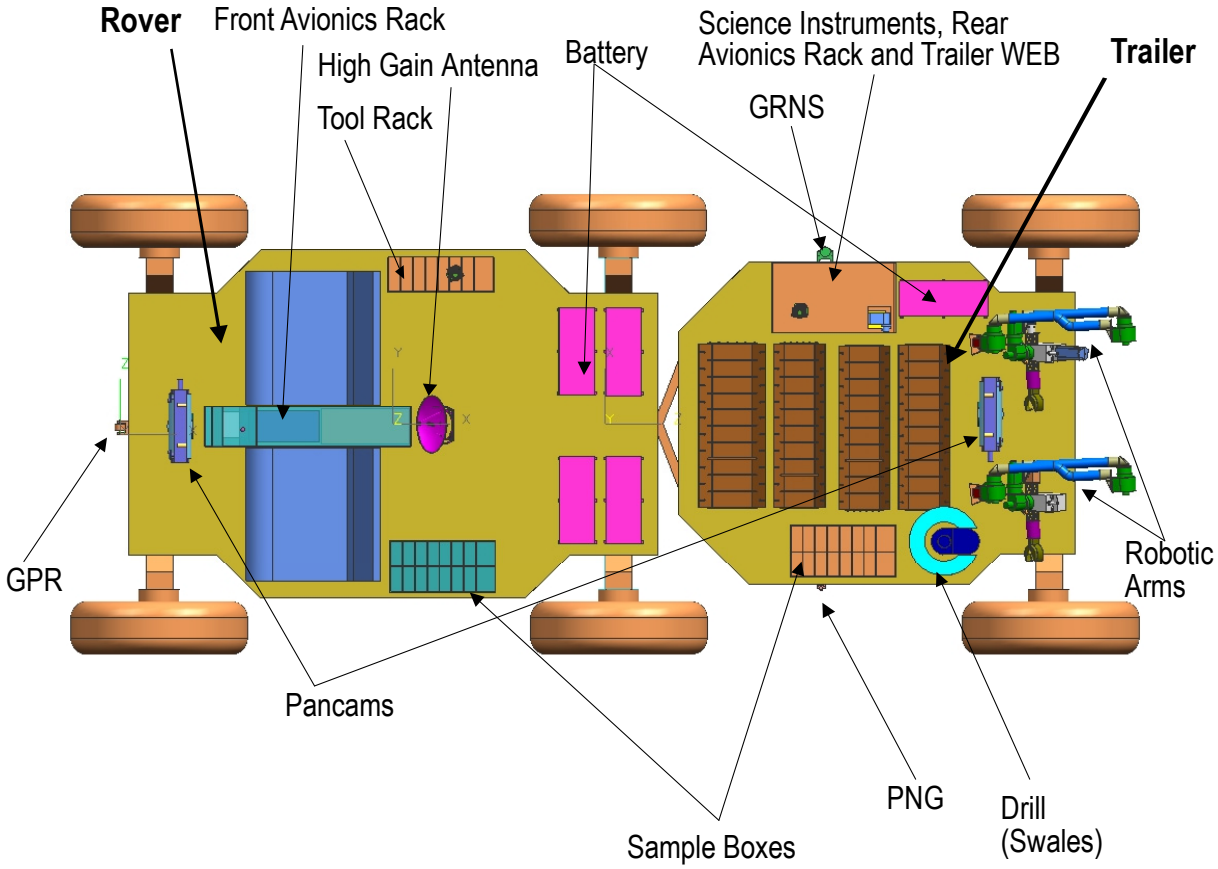

Figure 2.4.1-15. DMLRV Science Instrument Layout with SRGs

2.4.1.15 Additional RPS-Enabled Rover Mission Concepts

Technology from the DMLRV concept could be used on other rover missions. The concept developed for this study should be adaptable, with modifications, to the surface of Mars. The DMLRV could operate in a similar fashion supporting manned operations as an unpressurized surface rover, and performing telerobotic science and exploration in-between manned missions. The tailoring of the design to the low gravity environment of the Moon could limit the amount of architecture carried over onto a Mars mission. Mars presents additional challenges such as windborne dust and an atmosphere that could interact chemically with the rover's components. A manned Mars mission might have greater performance and system safety requirements than lunar missions, requiring a more robust frame and mobility system with greater mass due to increased component redundancy. Higher gravity and a more massive structure increases the power load on the wheel actuators, requiring greater battery capacity or more RPSs to provide baseload power. The low radiation levels encountered by the crew from the RPSs with the trailer attached could allow for the rover portion and science trailer to be operated as one unit to give the astronauts the safety provided by a continuous power and heat source and limit the mass of the battery system.

2.4.1.16 DMLRV Summary and Conclusions

The concept developed in this report is a new look at an old idea. The utility of an unpressurized roving vehicle for manned exploration was demonstrated in the Apollo program. The expansion of roving capabilities through the incorporation of a long-lived radioisotope power source enables a significant extension of the rover's capabilities when used in an unmanned, teleoperated mode. The ability to perform long range, long duration science and exploration, independent of solar illumination, has the potential to add a great deal to our understanding of the lunar geology over large areas. In further support of the Vision for Space Exploration, this concept can directly support the establishment of a lunar base through site exploration and characterization using a focused science instrument payload. Once the site is selected, the addition of regolith-moving equipment to the basic vehicle can provide the tools needed to prepare the site for human occupation.

It should be recognized that this study has only scratched the surface of the detailed design and the applications in which such a vehicle could be used. Further work remains to delve deeper into design areas such as long-range mobility and suspension components, telerobotic operations, thermal control, and dust mitigation and control. While detailed work is left to be done, it should be noted that none of these areas represent new technologies or new challenges, all have been addressed by past design teams, including both the US Apollo missions and the Soviet Lunakhod rovers.

A particular application that should also be investigated in more detail is the adaptation of the DMLRV to the site preparation role. One major driver for the development of such a vehicle may be the potential it holds for allowing long term regolith moving and excavation activities in support of the establishment of a permanent human presence on the lunar surface. The limits of this study allowed only a very cursory evaluation of the potential of the rover for such an application, but the design has been made as flexible as possible in expectation of a desire to more fully investigate this increasingly valuable option.

2.4.2 Titan Aerobot Concept

This section describes a conceptual Titan Aerobot mission that would have the goal of expanding our understanding of this scientifically important moon and building upon the knowledge gained from the Huygens probe of the Cassini-Huygens mission scheduled to enter Titan's atmosphere in 2005. This study is based on the results of an earlier mission study conducted in 2001 [39]. An RPS would be used to power the aerobot to permit long-duration and long-distance operations on Titan, and a small-RPS unit would be used to power an amphibious sonde used for exploring the surface and any liquid bodies.

2.4.2.1 Science Goals

The science goals for the Titan Aerobot mission are presented in Table 2.4.2-1. A fundamental goal of the mission would be to understand the chemistry of Titan's atmosphere (Fig. 2.4.2-1), solid surface, and any lakes or seas that might exist there. An understanding of the chemistry in these environments is necessary to determine whether biology has existed or is evolving at this time. The signatures of organic substances (e.g. tholins) have been identified with remote spectroscopy (and will be better understood when the Huygens Probe reaches Titan in early 2005). The characterization of these organic substances on Titan is another key goal of the mission. Investigations would also be performed to determine the composition of the solid surface of Titan and the nature of the geological and geophysical processes that would provide clues to Titan's evolution. Another goal is to understand the chemistry, dynamics and meteorology of Titan's atmosphere and its interaction with the surface. Finally, it would be a goal of the mission to take measurements in Titan's upper atmosphere with sufficient precision to characterize the atmosphere's interaction with Saturn's magnetosphere and the solar wind.

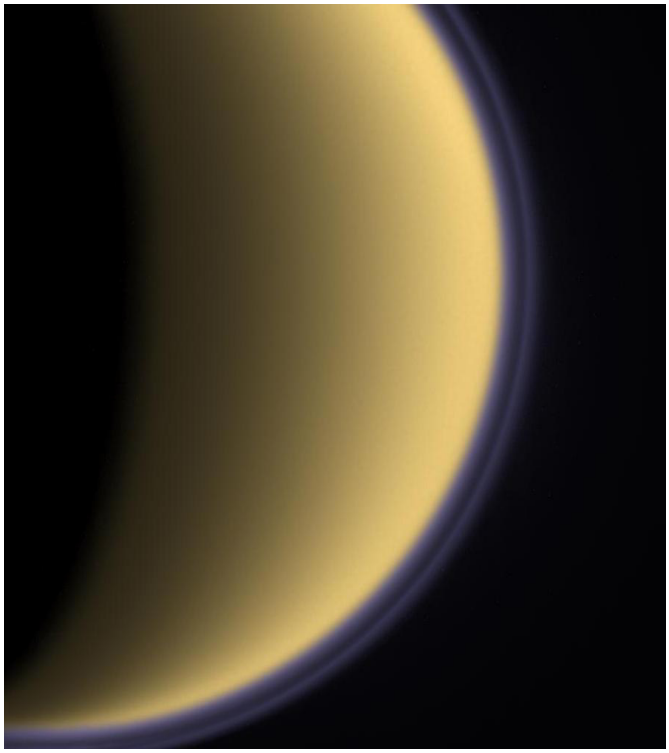

Figure 2.4.2-1. Image of Titan and Its Atmosphere Taken in 2004 by the Cassini Spacecraft, [NASA]

2.4.2.2 Mission Goals

The mission goals of the proposed Titan Aerobot mission would be to deliver a Titan Aerobot vehicle to the lower atmosphere of Titan and deploy three specialized data gathering landers to the surface and to the seas, to support the scientific instrumentation and deployment platforms to satisfy the science goals, and to design the mission elements with a minimum seven year mission duration (six year cruise phase and one year science mission.)

Table 2.4.2-1. Science Goals of the Titan Aerobot Mission Study

#	Science Objective
1	Identify and assess any pre-biotic and proto-biotic chemistry taking place at Titan.
2	Characterize the organics on the surface of Titan (distribution, composition, organic and chemical processes and context, energy sources).
3	Determine the composition of Titan's surface.
4	Characterize the geological and geophysical processes relating to the evolution of Titan.
5	Measure the atmospheric dynamics and meteorology, including seasonal variability, of Titan and their interaction with the surface.
6	Assess the atmospheric chemistry of Titan.
7	Determine how Titan formed and what the implications are for the formation of Saturn.
8	Investigate the nature of Titan's upper atmosphere and its interaction with the magnetosphere and solar wind.

2.4.2.3 Mission Architecture Overview

A key goal of the Titan Aerobot concept [39] would be deliver and deploy three lander vehicles (sondes), each with different features and capabilities. These vehicles would be deployed from an "aerobot" hovering over the surface of Titan. The aerobot is essentially a self-propelled blimp vehicle with the capability of ascending and descending through Titan's atmosphere, and translating via a propeller-based propulsion system.

The Aerobot concept would employ a direct-to-Earth communications link, with the blimp serving as the only data return link. The data from the sondes would be transferred to the Aerobot via a tether or UHF communications link, and stored on the blimp for eventual playback to Earth.

An illustration depicting the entry, descent, landing, and deployment of the Titan Aerobot is shown in Fig. 2.4.2-2. The direct entry is illustrated by the aeroshell – parachute sequence in the upper left in the figure. This would be followed by the deployment-inflation phase of the Aerobot. Once the Aerobot blimp is inflated, it would begin floating over the surface to generate a terrain map and search for possible sites to deploy the various sondes that are carried on the Aerobot. Once the sites were determined, detailed mapping would identify any surface hazards that must be avoided. This would be followed by the deployment of one or more sondes at the site.

There are three sonde concepts that would be carried aboard the Aerobot, with the expectation that Titan may have hydrocarbon seas and solid surface areas. The sonde concepts have been specialized for these different expected environments and would all be deployed by a tether to the surface from the Aerobot as shown in the right panel of Figure 2.4.2-2. The three types of sondes are illustrated in Figure 2.4.2-3. The simplest device, shown in figure 2.4.2-3a, is the passive sonde (PS) that would simply be lowered into a sea to acquire instrument data from beneath the surface of the sea while hanging from the tether. The tether would also provide power for the PS from the Aerobot's RPS system. It would have science instruments on-board to measure the chemistry and other characteristics of the sea. Because it would be connected to the Aerobot, the motion of the Aerobot would allow the PS to move through the sea for collection of data over an area along the path of the Aerobot.

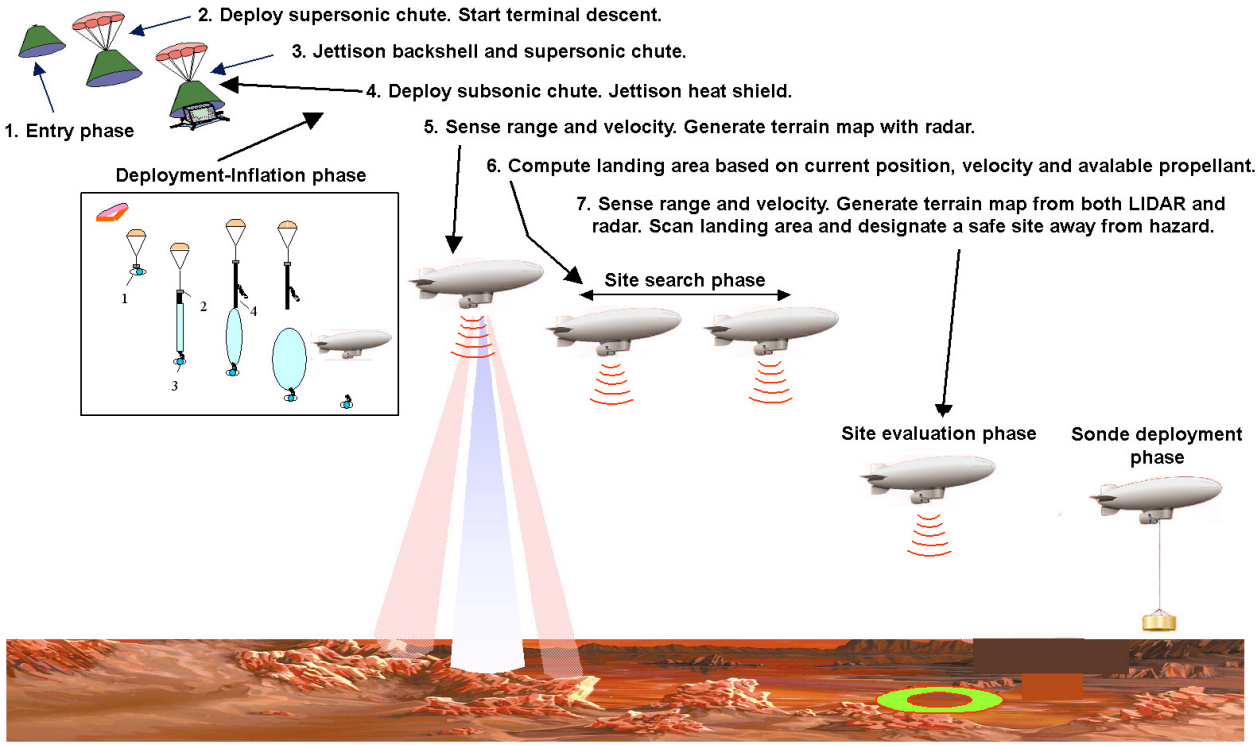

Figure 2.4.2-2. Titan Aerobot Approach and Deployment Profile

When the data collection was completed, the sonde would be retracted into the Aerobot. The thermal design of the PS relies on a phase change material for warmth (Section 2.4.2.9); as a result, the mission duration for any single deployment of the PS would be limited to ~10 hours in the expected 90K temperature of a Titan sea. The PS is reusable, and could be deployed elsewhere as desired. The second type of sonde depends on a high pressure gas gun device that is used to inject a single-use cylindrical "harpoon" coring device into a solid surface or a sea bottom surface, thereby acquiring a core sample of the material. The entire sonde system is tethered but only the core sample container (Fig. 2.4.2-3b) would be returned to the Aerobot by retracting the tether. A suite of sample processing tools and instruments would be located within the Aerobot to perform detailed chemistry and isotopic analysis on the core sample.

Whereas the first two sondes could be deployed and retracted into the Aerobot, the third sonde would be deployed by a tether and then released as an independent exploration vehicle, with its own power and telecommunications systems. The sonde would have a unique configuration as shown in Figure 2.4.2-3c, as it would be amphibious – capable of operating on land or in a sea. Its large upper cylinder would act as a buoyancy chamber for the sonde to allow it to float at the surface of a Titan sea. Operating in the floating mode (Fig. 2.4.2-4a), the amphibious sonde would travel through the sea using the wind pressure on the upper chamber as well as an electric motor driven propeller located at the center of the long submersed cylinder. The amphibious sonde would have two sets of crawling tracks to maximize its surface mobility (Fig. 2.4.2-4b) and is further discussed in Section 2.4.2.10.

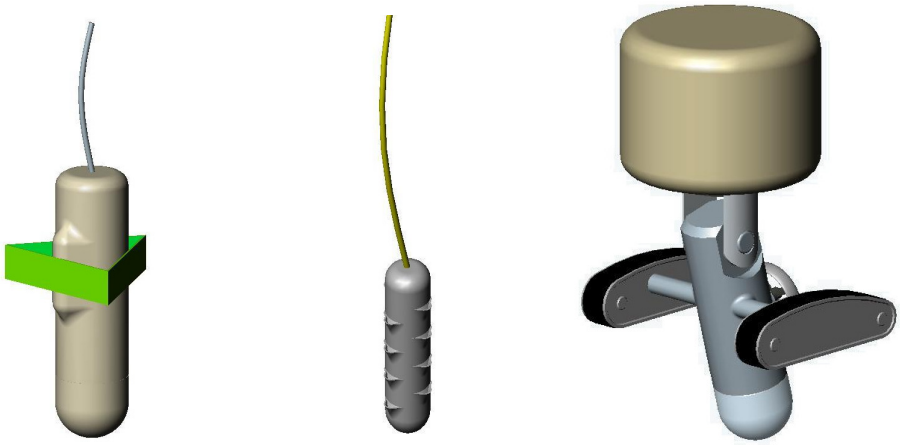

a. Passive self-orienting sonde with tether

b. Harpoon probe with tether

c. Fully amphibious sonde

Figure 2.4.2-3. Conceptual Titan Aerobot Sonde Vehicles (Drawn to Relative Scale).

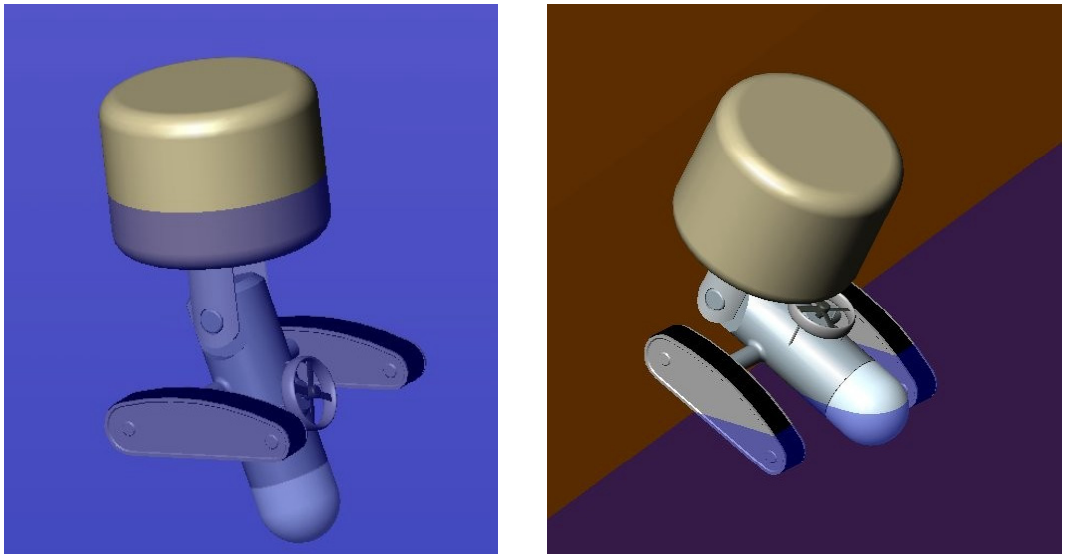

a. Floating

b. Crawling

Figure 2.4.2-4. Artist's Concept of Amphibious Sonde in Floating and Crawling Modes

The sonde packaging in the Aerobot gondola was not studied in detail [39], but notional packaging of the gondola and the RPS is illustrated in Figure 2.4.2-5. The figure shows the atmospheric entry configuration with the gondola and RPS mounted within the 3.25-m diameter heatshield (aeroshell). This is an early version of the packaging before the 1-m antenna was changed to a smaller patch antenna located on the gondola housing. The propeller and motor housings for the Aerobot are shown on each side of the gondola with the stowed propellers not shown. The notional ducting for the gondola's RPS power source, for cooling during launch, transit and entry, are also shown.

2.4.2.4 Power Source Trade Study

Different power sources were considered for the Titan Aerobot mission, including solar power, batteries, and radioisotope power systems. Solar power was deemed infeasible due to the low level insolation at Titan (distance ~9.5 AU), the low ambient temperatures, and the resultant prohibitive size and mass of solar arrays that would be required to power the Aerobot vehicle. Furthermore, a solar-powered Aerobot would have extreme restrictions in terms of where it could and could not operate in order to stay in sunlight. Batteries were also deemed impractical due to the long duration of the science mission (~1 year). An RPS power source was assessed as the best alternative due to its compact size, ability to provide excess heat to maintain operating temperatures of key subsystems and instruments, its long life (decades), and its ability to operate independent of the Sun. The MMRTG was considered as the baseline power source in this study, though the SRG could potentially be used instead. The extreme cold of Titan and its convective atmosphere could potentially require that the radiator fins of the MMRTG be shortened or removed to maintain operating temperatures during the science mission. During the 6-year cruise phase, the auxiliary cooling tubes in the MMRTG would be used by an external pumping and radiator system to prevent spacecraft overheating. The power output of the MMRTG is assumed to be 110 We (BOM), and the available power at the end of the 7-year mission would be approximately 97.9 We (Section 3 – Table 3-6).

A study was completed comparing the possible sources of power for the passive sonde that would be deployed by a tether from the aerobot into the sea. The issue was whether to supply power and heat to the sonde through the tether, or to include a GPHS based RPS source on the sonde itself. If an RPS was included in the PS configuration, some method would need to be devised for dissipating the heat from the RPS while it was stowed within the gondola. This complicated the gondola design with heat pipes and radiators that would be necessary. If this sonde were to be deployed and retracted repeatedly, this thermal management would be even more difficult. Another method of providing heat to the PS considered using a phase change material (a water jacket in this case) that would be heated by the MMRTG heat in the gondola and then would slowly freeze after the sonde was deployed. The heat of fusion from the phase change would be augmented by a small electric heater (~20 We) on the PS to extend its observational lifetime in the sea. Electrical power would be provided to the PS via a tether from the Aerobot. This technique would allow a passive sonde lifetime of ~10 hours in the 90K Titan sea before it became too cold and would be retracted for future deployment. Because of this latter flexibility, the phase change solution with supplemental electrical heaters was chosen as the baseline system.

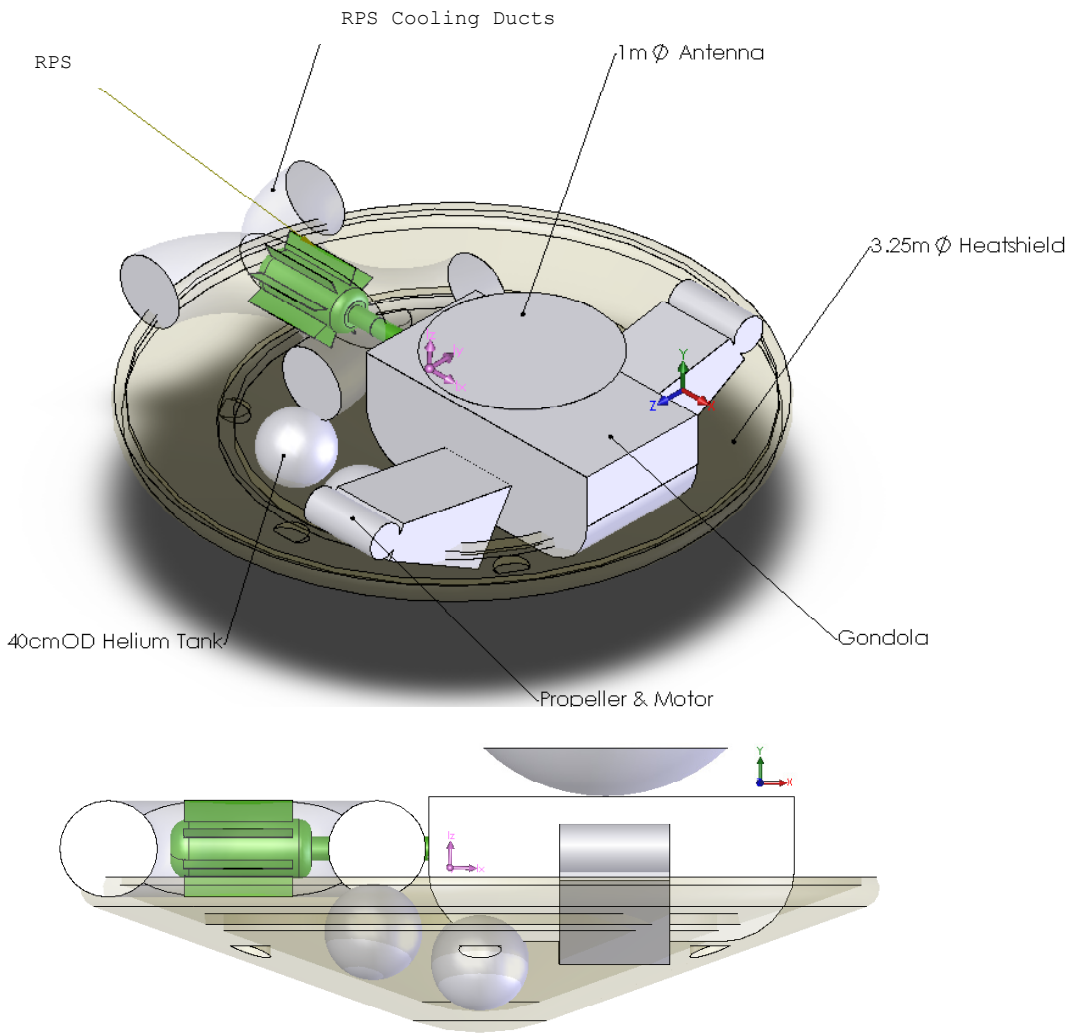

Figure 2.4.2-5. Titan Aerobot RPS Packaged in Aeroshell

2.4.2.5 Power System Characteristics

There would be two radioisotope power systems required for the aerobot mission. The first is a standard RPS that would be the fundamental source of power and heat for the gondola. The original mission study [39] assumed an MMRTG, and thus that configuration is assumed here. However, the SRG is potentially another viable option as discussed in Section 2.4.2.14. Figure 2.4.2-5 illustrates the gondola configuration with the MMRTG (in green) located to the side of the central structure. Cooling ducts would be included around the MMRTG to dissipate its heat during the cruise phase and Titan atmospheric entry. The second power source is a small-RPS unit [41] consisting of two single GPHS modules and is located on the aft end of the amphibious sonde to provide continuous power and heat for the vehicle. Cooling the small-RPS while the sonde is stowed in the gondola/aeroshell would require a heat pipe and external radiator design.

2.4.2.6 Science Instruments

The suite of science instruments that would be used on the Titan Aerobot vehicle and sondes is listed in Table 2.4.2-2. The measurement objectives of each instrument are given as well as the science goals they are intended to satisfy. The simplest of these instruments are the temperature and pressure sensors that would be used in the blimp to characterize the atmosphere at various locations. These instruments would also be used in the sondes to take measurements as the sondes descend into the sea. The instruments for measuring the bulk characteristics of the sea include the acoustic ranging instrument that would measure the density of the sea and the Light Emitting Diode (LED) photometer instrument that would measure the local turbidity of the sea around the submersible sondes. A Microscopic Near Field Imager (MNFI) would record the structural characteristics of the local environment and core samples taken by the sondes. Probably the most important instrument would be the Gas Chromatograph / Mass Spectrometer (GC/MS). It would perform gas/liquid/solid analysis of constituents, particularly examining the characteristics of tholins and the possible presence of chirality [39]. The instruments would perform a complete physical study of a subsurface liquid column in a shallow crater lake. The study would include temperature, pressure, opacity/particle suspension, and chemical constituents. After using the harpoon to extract a core sample from a shallow subsurface (<10 cm) depth from the solid icy conglomerate material bordering shallow lakes, a complete analysis of the core sample would be performed by the instrument set on the gondola. The sample analysis would include its physical characteristics, chemistry, presence of H_2O, and trace mineralogy [39].

Table 2.4.2-2. Titan Aerobot Science Instruments and Measurement Objectives

Instrument	Measurement Objective	Science Goal Addressed
Sonde Instruments		
Temperature Sensors	Atmospheric or Liquid Temp.	1,3,4,5,6,8
Pressure Sensors	Atmospheric pressure	5,6,8
Acoustic Ranging	Liquid Density	1,2,5
Light Emitting Diode (LED)	Liquid Turbidity	1,2,3,6
Microscopic Near Field Imager (MNFI)	Local Imaging	2,3,4,5,7
Gas Chromatograph/Mass Spectrometer (GC/MS)	Organic signatures/chirality	1,2,3,6,7
Aerobot Instruments		
GC/MS	Atmospheric analysis	1,5,6,8
Laser ablation/particle spectroscopy	Surface analysis	1,2,3,4,7
Acoustic Monitor	Sound	5
Science camera	Surface imaging	2,3,4,5,8
All-Sky Camera	Atmospheric imaging	5,6,8
Radar Sounder	Surface and subsurface imaging	2,3,4,5,7
Magnetometer	Local magnetic fields	3,4,7,8
Meteorology	Local atmospheric conditions	5,6,8

2.4.2.7 Data

Scientific data would be acquired differently from the many platforms in the Aerobot mission. The aerobot instruments would sample the atmosphere directly to determine atmospheric characteristics and chemistry. The data would be stored on board for transmission during direct-to-earth (DTE) communications intervals. The sondes would have different data acquisition modes. For example, a harpoon sonde would acquire a sample from the sea floor, and the sample would be retracted for analysis by the GC/MS or other instruments on the Aerobot gondola. The instrument data would then be returned to Earth. The passive sonde would contain its own analytical instruments and would return its data through the tether to the gondola for transmission to Earth. The amphibian would be deployed only once and then released from its tether. As it performed its journey, it would return its data through an RF link to the gondola for later return to Earth

2.4.2.8 Telecommunications

Two telecommunications systems are part of the Titan Aerobot design concept. The first is the direct-to-Earth (DTE) link from the Aerobot. The second is the Amphibious sonde link to the Aerobot. Fundamental to the DTE link is the latitude of the Aerobot [40]. Because the antennas would be located on the side of the Aerobot, it must be stationed at a latitude of greater than 80 degrees to provide the maximum telecommunications duration per contact with Earth. The DTE link is based on using the 70-m DSN stations and 35-cm patch antennas arranged around the blimp so that optimum direction to Earth could be selected depending on the orientation of the blimp at that time. The DTE link design uses a 22 W RF amplifier (65 We power required) at a worst case range of 1.65×10^9 km. Under these conditions, the maximum telemetry capability is estimated at 1 kbit/s for 8 hours/day, resulting in a total telemetry of about 29 Mbits/day.

The telecommunications links between the sondes and the Aerobot have different architectures. For the instrumented Passive sonde that is retractable on a tether, the telemetry from the instruments passes through the tether to the Aerobot C&DH memory for later return to Earth. The harpoon sonde does not return telemetry, because the tether simply delivers the harpoon sample to analysis instruments on the Blimp where the results of the analysis are relayed to Earth. The amphibian telecommunications link to the Aerobot would be via a UHF link from a patch antenna on the amphibian to a patch antenna on the Aerobot.

2.4.2.9 Thermal

The expected atmospheric temperature for the Aerobot operation is about 94K and the sea temperature is expected to be about 90K. The interior of the sondes and the gondola must be kept at a temperature of approximately 273K to maintain system operating temperatures. This temperature would be maintained using the excess MMRTG heat along with heat pipes to distribute the heat to all subsystems.

The sondes have a different environment than the Aerobot and must be temperature controlled. First, the harpoon sonde is expected to function mechanically without any heat input from the time the sample is acquired from the sea bottom until it is deposited in the Aerobot for analysis using the retractable tether. Secondly, the Passive sonde would have avionics and instruments that must be maintained at 273K using a heat source. The design concept for the PS is to use a water jacket in the sonde that is heated while the sonde is in the Aerobot prior to deployment into

the sea. Once the PS is in the sea, the water would begin to freeze and a small electrical current in the tether would provide 20 We of power for electric heaters in the sonde. The combination of the phase change of the water and the power through the tether would allow an operational life-time in the sea of about 10 hours which is sufficient for science data acquisition. Finally, thermal control of the amphibian sonde would be provided by the rejected heat from the onboard small-RPS. One issue with this design is to keep the amphibian cool enough during the interplanetary transit and when it is stowed in the Aerobot gondola prior to its deployment into the sea. The design of this cooling system remains to be done.

2.4.2.10 Mobility

Surface mobility for this mission would be provided using three methods: hovering and propulsion of the Aerobot, propeller propulsion of the Amphibious sonde in the sea, and crawling of the said sonde on the surface. The Aerobot would depend mainly on winds to allow it to move at speeds up to 10 cm/s but would also have electric motors driving propellers on its gondola that could provide speeds up to 2 m/s [40]. Thus, the placement of the harpoon and passive sondes would depend on this blimp mobility. The Amphibious sonde would have two types of mobility. While in the sea, a small propeller on the main body (see Fig. 2.4.2-4a) would provide a speed of at least 5 cm/s. When the amphibian would be operating on the surface using its crawler tracks (Fig. 2.4.2-4b), it would have a speed of a few cm/s. The operation would require about 39 We of power for the motors and about 20 We of power for avionics and power conditioning.

2.4.2.11 Power

Preliminary power estimates for the key deployable elements of the Titan Aerobot mission are summarized in Table 2.4.2-3. The most detailed estimates were performed for the Aerobot vehicle during an earlier study [40] and are presented herein. Power estimates of the Passive sonde (P-sonde) and the Active sonde are also presented in the table, but are less detailed than the Aerobot values.

The Aerobot would operate in one of four mutually–exclusive modes, including *Station Keeping*, *Science, P-Sonde Operation,* and *Telecom*. *Station Keeping* involves the Aerobot operating its propeller drive to maintain position over a designated target or to translate to a new position; the associated power draw is ~52 We. In the Science mode, the aerobot would employ its suite of remote-sensing and in-situ instruments as listed in Tables 2.4.2-2 and 2.4.2-3, while potentially operating its propeller drive (e.g., to maintain position while making measurements). The estimated power draw of the Science mode is 84 We. During deployment and operation of the Passive sonde (P-sonde), the Aerobot would enter the *P-Sonde Operations* mode where it would provide up to 56 We for P-sonde science instruments and electrical heating to supplement its phase-change thermal control system. The peak power draw on the Aerobot in this mode is estimated at 108.4 We, and would require the use of the supplementary battery system. At regular intervals, the Aerobot would enter Communications mode for direct-to-Earth communications of science and engineering data, and to receive new commands. This mode is the dominant power mode for the Aerobot vehicle, with a peak power draw of approximately 137 We. The MMRTG power output at the end of the mission (7 years) is estimated at 97.9 We (Section 3 – Table 3-6). Thus, to cover the peak loads incurred during the communications mode (as well as the *P-Sonde Operations* mode), a supplementary Li-Ion battery with ~560 W-hr capacity (assuming 30% depth of discharge) would be used to enable a four-hour telecom period. The battery would be recharged during lower-power modes, and could be fully charged (following a 4-hr telecom event) within 6 hours in the *Station-Keeping* mode using the MMRTG power source.

The Passive sonde (P-sonde) would operate in one of two modes, including *Standby* mode and *Science* mode. The *Standby* mode would be used during Sonde deployment from the aerobot, and would have an estimated power draw of 42 We, supplied by the Aerobot power system via a tether. Once the P-sonde had been properly positioned by the Aerobot, the sonde would enter the *Science* mode and begin making measurements with its suite of on-board instruments. The power draw of this mode is 56 We, and represents the stressing case for the Aerobot power system during P-sonde operations.

The Amphibious sonde (A-sonde) is a stand-alone, self-powered vehicle that is carried on the Aerobot and deployed to a target destination via a retractable cable. The A-sonde is a mobile vehicle designed to explore the surface of Titan any liquid bodies it may encounter. This sonde would use a conceptual small-RPS unit with 30 We (EOM) capacity, augmented by a secondary Li-Ion battery, to supply the extra peak power needed for some of its operations. The Amphibious sonde would operate in one of four modes, including *Standby*, *Science*, *Mobility* and *Communications*. *Standby* mode would be used during deployment of the A-sonde, during periods of inactivity, or when recharging the A-sonde's supplementary battery. The peak power draw during the *Standby* mode is 19.5 We, providing up to ~10 We of additional power for battery charging. The *Science* mode would be used during nominal science-gathering activities and assumes all instruments would be operating simultaneously. The power draw of this mode is 33.9 We. In practice, this mode could be divided into separate lower-power science sub-modes, which would permit continuous operations without using the supplementary battery system. When the A-sonde needed to move to a new location, it would enter *Mobility* mode to power its crawler tracks or propeller system. As expected, the mobility mode represents the stressing case from a power perspective, with an estimated power draw of ~59 We. A 100 W-hr Li-Ion secondary battery would be included in the A-sound to permit up to one hour of continuous mobility on a single battery charge (assuming 30% depth of discharge). Following the *Mobility* mode, the A-sonde would enter a lower-power mode to recharge its battery – a complete recharge could be accomplished in ~3 hours in the *Standby* mode. The fourth operating mode of the A-sonde is the *Telecom* mode, where it would uplink all its science and engineering data to the Aerobot for eventual relay to Earth. The A-sonde would also use this mode to receive new commands from the Aerobot, e.g., directions and distances to a newly designated target, etc. The power draw of this mode is estimated at 24.5 We.

In summary, the Aerobot mission concept would use two different RPS systems and secondary Li-Ion batteries to power its loads. The Aerobot would use one MMRTG and a 560 W-hr Li-Ion battery to power itself and the Passive sonde, and the Amphibious sonde would use a conceptual 30 We (EOM) small-RPS with 100 W-hr Li-Ion battery to provide independent power for its science and mobility systems.

Table 2.4.2-3. Power Estimates for the Titan Aerobot Concept (Includes 30% Margin)

Aerobot Modes	Power Modes, (W)				
	Mode 1, Station Keeping	Mode 2, Science	Mode 3, P-Sonde Operation	Mode 4, Telecom	Heritage
Aerobot	**52.4**	**84.2**	**108.4**	**136.9**	
Temperature Sensors	0.1	0.1	0.1	0.1	[40]
Pressure Sensors	0.3	0.3	0.3	0.3	New
Attitude Control	26.0	26.0	26.0	26.0	[40]
Command & Data	13.0	13.0	13.0	13.0	[39]
Power	13.0	13.0	13.0	13.0	[40]
Telecom				84.5	[39]
P-Sonde Power Draw via Tether			56.0		[40]
Instruments		31.9			
Laser ablation/particle spectroscope		6.5			[40]
Acoustic Moniter		0.3			[40]
Science camera		3.9			[40]
All-Sky Camera		1.3			[40]
Radar Sounder		6.5			[40]
Magnetometer		1.3			[40]
Meteorology		1.0			[40]
GC/MS		10.4			[40]
Sampling system		0.7			[40]
Passive Sonde Modes	**Mode 1, Standby**	**Mode 2, Science**			**Heritage**
Passive Sonde	**41.6**	**56.0**			
Command & Data	13.0	13.0			[40]
Power	2.6	2.6			New
Thermal Control	26.0	26.0			
Instruments		14.4			
Temperature Sensors		0.1			New
Acoustic Ranging		1.3			New
LED Light		1.3			New
MNFI		6.5			LR
GC/MS		5.2			[39]
Amphibious Sonde Modes	**Mode 1, Standby**	**Mode 2, Science**	**Mode 3, Mobility**	**Mode 4, Telecom**	**Heritage**
Amphibious Sonde	**19.5**	**33.9**	**58.5**	**24.5**	
Command & Data	13.0	13.0	13.0	13.0	[39]
Power Conditioning	6.5	6.5	6.5	6.5	New
Mobility (Propeller or Track)			39.0		New
Telecom				5.0	
Instruments		14.4			
Temperature Sensors		0.1			New
Acoustic Ranging		1.3			New
LED Light		1.3			New
MNFI		6.5			LR
GC/MS		5.2			[39]

2.4.2.12 Mass

The mass allocations for the aerobot and sondes are presented in Table 2.4.2-4. The Aerobot mass is conservatively estimated at ~530 kg including 30% margin. Estimates for the sondes are more preliminary, and the mass of the Amphibian sonde was estimated at about 33 kg as listed in the table. The other masses in this list are only preliminary estimates at this time.

The atmospheric entry system elements (aeroshell and parachute) were estimated at a total of 380 kg as listed. A hydrazine propulsion system that would be used during trajectory corrections prior to entry is estimated at 750 kg total. The interplanetary delivery system would be a Solar Electric Propulsion (SEP) system and its total mass including xenon propellant would be about 1535 kg total. The sum total of all of these systems (launch mass) is about 3250 kg. The launch vehicle of choice during the study would provide an initial launch energy (C_3) of about 12.9 km^2/s^2. The capability of this Atlas 551 vehicle at this energy would be about 5028 kg. Thus, a large (55%) mass margin exists in this preliminary estimate to account for excluded items and underestimates.

2.4.2.13 Radiation

One of the primary reasons for the VGA-SEP interplanetary trajectory would be to avoid Jupiter and its hazardous radiation environment on the trip to Saturn. Saturn does not have major radiation belts like Jupiter and would not expose the Titan Aerobot to significant cumulative radiation dose levels. The cosmic ray environment during interplanetary cruise would be the only natural radiation environment that would be encountered during this mission but it is not significant. A brief analysis was conducted during the Aerobot Blimp study [40] considering the natural as well as the radiation environment from the nuclear power sources. The results of the study suggested a maximum radiation design requirement of 50 krads (Si) behind 100 mils of Al with a radiation design margin of two for the avionics equipment.

2.4.2.14 Alternate RPS Power Architecture

Because of the large distance from the Sun to Saturn, the studies considered only nuclear power sources for operations at Titan. The power requirements (Section 2.4.2.11) of the Aerobot operations over extended durations at Titan require the standard RPS power system on the gondola. The decision to use the tethered deployment (and retraction) of the small passive sonde permitted the use of the Aerobot-based RPS power system to supply electrical power to the sonde heaters via the tether. The amphibian would be designed for extended autonomous operations and would not be retractable. Thus, it would require its own power source for power and heat – a small RPS. More efficient RPS power sources such as a Stirling Radioisotope Generator (SRG) would have less mass (34 kg) and use 25% of the plutonium fuel of the MMRTG on the Aerobot, making it an attractive alternate option from this perspective. In addition, the SRG would generate about 25% of the heat of an MMRTG, which would simplify the cooling design of the Aerobot during the cruise and entry phases. However, the electrical output of the current SRG design is relatively sensitive to its thermal operating environment (Section 3.2), and the convective atmosphere of Titan could significantly reduce the available output power of this RPS due to lowered Carnot efficiency and convective heat losses. Additional thermal and power system analyses would need to be performed to assess the overall feasibility of using the SRG for this mission concept.

Table 2.4.2-4. Mass Estimates for the Titan Aerobot Concept

Element	Mass (kg)	Mass w/ 30% Margin (kg)	Heritage
Aerobot	**407.8**	**530.1**	
Gondola	29.0	37.7	[39]
Thermal	51.0	66.3	[39]
Hull	23.0	29.9	[39]
Balloonet	10.0	13.0	[39]
Gaseous Hydrogen	23.0	29.9	[39]
Inflation System	138.0	179.4	[40]
Tether & Deployment	14.0	18.2	New
Instruments	14.8	19.2	[40]
Laser ablation/particle spectroscope	4.6	6.0	[40]
Acoustic Monitor	0.1	0.1	[40]
Science camera	2.6	3.4	[40]
All-Sky Camera	1.3	1.7	[40]
Radar Sounder	2.6	3.4	[40]
Magnetometer	0.1	0.1	[40]
Meteorology	0.9	1.2	[40]
GC/MS Sampling system	2.6	3.4	[40]
Power System (MMRTG, Batteries, etc.)	105	136.5	[41]
Amphibious Sonde	**25.4**	**33.0**	
A-Sonde System	22.8	29.6	
Instruments	2.6	3.4	
Temperature Sensors	0.1	0.1	[39]
Pressure Sensors	0.1	0.1	New
Acoustic Ranging	0.3	0.4	New
Light Emitting Diode (LED)	0.1	0.1	New
Microscopic Near Field Imager (MNFI)	0.5	0.7	LR
GC/MS	1.5	2.0	[39]
Passive Sonde	**10.0**	**13.0**	
P-Sonde System	7.4	9.6	New
Instruments	2.6	3.4	
Temperature Sensors	0.1	0.1	[40]
Pressure Sensors	0.1	0.1	New
Acoustic Ranging	0.3	0.4	New
Light Emitting Diode (LED)	0.1	0.1	New
Microscopic Near Field Imager (MNFI)	0.5	0.7	LR
GC/MS	1.5	2.0	[39]
Harpoon Probe	**7.7**	**10.0**	**New**
Aeroshell and Parachute	**292.3**	**380.0**	**[39]**
Hydrazine Propulsion Module	**576.9**	**750.0**	
Dry mass	423.1	550.0	[39]
Hydrazine propellant	153.8	200.0	[39]
SEP Propulsion Module	**1180.8**	**1535.0**	
Dry Mass	500.0	650.0	[39]
Xenon propellant	680.8	885.0	[39]
Launch Mass	**2500.9**	**3251.2**	
Atlas 551 Perf @ C_3 = 12.9 km^2/s^2	5028.0	5028.0	
Launch Mass Margin (%)	**101%**	**55%**	

2.4.2.15 Titan Aerobot Summary and Conclusions

The Titan Aerobot mission is a challenging concept that could be enabled by radioisotope power sources. The Aerobot system relies on a standard RPS system (the MMRTG was baselined) for all operations at Titan and would support multiple sondes with its electrical power and the excess. A key issue with using the MMRTG RPS is dissipating its waste heat during the interplanetary flight and during entry. The cooling ducts identified during an earlier Aerobot study [39] were an attempt to address this concern. In addition, the heat from the MMRTG was used to preheat a water jacket in the passive sonde so that it could thermally survive in the sea for 10 hours relying on the water's phase change heat of crystallization. The small-RPSs in the amphibian would enable it to have long life operation in the Titan sea and on land without dependence upon power from the Aerobot.

Although extensive element-by-element power analyses were not performed during the previous Aerobot studies [39, 40], preliminary analyses indicate that a feasible mission would be possible using standard RPS and Small RPS systems. This mission concept would provide an exciting exploratory mission to the surface and the seas of Titan with a rich scientific data return.

2.5 SATELLITE CONCEPTS

2.5.1 Saturn Ring Observer Mission Concept

This section describes a conceptual mission to the Saturn system, emphasizing extremely close-in observations of Saturn's extensive ring system. Such a mission could launch in the 2015-2020 time frame, with operations at Saturn commencing in approximately 2030. Standard RPSs would be used to generate all necessary electrical power during the 11-year mission.

2.5.1.1 Science Goals

The mechanisms of formation and evolution of planetary ring systems are poorly understood. These processes are of considerable scientific interest, as planetary ring systems are thought to share some characteristics with protoplanetary disks [42]. The key unknowns in analyses of protoplanetary disk evolution involve the collisional dynamics of the particles and its effects on the collective behavior of the rings, especially evolution. The goal of the Saturn Ring Observer (SRO) mission would be to obtain close-in observations of centimeter-scale ring particle interactions to better understand these processes.

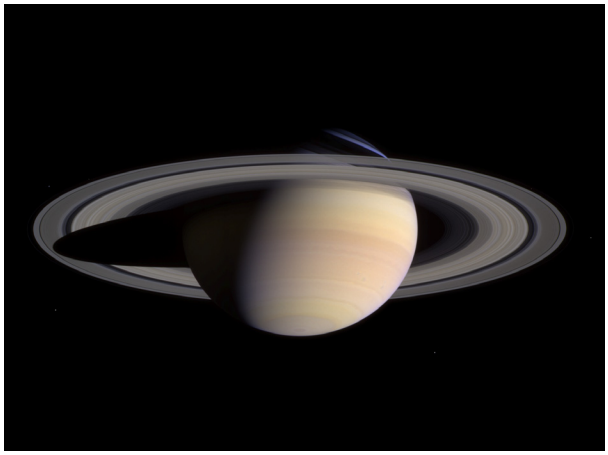

Figure 2.5.1-1. Saturn as Viewed from the Cassini Spacecraft During Approach [NASA]

The primary objective of the mission would be to observe and quantify ring particle properties at multiple key locations within the A and B rings. Individual ring particle properties to be investigated include particle sizes, particle shapes, rotation states, compositions, random velocity components, and surface textures. Two-particle investigations would focus on collision dynamics and collision frequency. Bulk and aggregate characteristics to be measured would include gross ring structure, particle density and surface mass density profiles (respectively, the number of particles and the total mass per unit area of ring surface), particle size distributions and spatial variation of size distribution at multiple ring locations, ring and ringlet thickness, layering and banding, wave characteristics, shepherding (e.g., by moons or moonlets) processes, and the neutral and ionized "ring atmosphere" environment. Lastly it would be important to characterize the electromagnetic environment near the rings and its relationship to ring structure and dynamics.

Secondary objectives of the mission would include observations of shepherding satellites (such as Pan, Prometheus, etc.), and the characterization of micrometeorite impact rates and dust particle populations in the near-ring environment.

2.5.1.2 Mission Goals

The goal of the Saturn Ring Observer mission would be to spend one year in close proximity to Saturn's A and B rings (Figs. 2.5.1-2 and 2.5.1-3), performing detailed observations and measurements of the rings and shepherding moons to achieve the science goals listed above. Co-orbiting operations very close to the ring plane (as little as 1 km separation) would provide a vantage point unprecedented in solar system exploration. Remote sensing and in-situ observations from that point, combined with the large focal-length optics of the SRO spacecraft, would yield a definitive data set that is relevant both to ring systems in general and protoplanetary disks, and would not be obtainable anywhere else in the solar system.

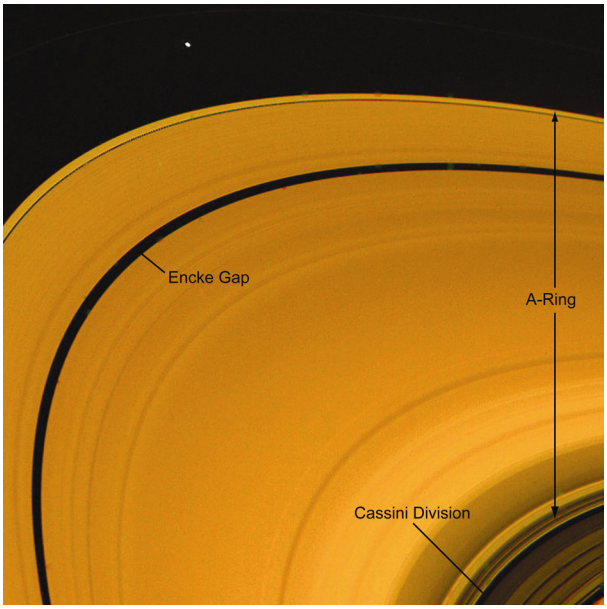

Figure 2.5.1-2. Detail of Saturn's A Ring [NASA]

2.5.1.3 Mission Architecture Overview and Assumptions

SRO would be a valuable follow-on mission to Cassini-Huygens and would utilize standard RPS technology to enable its 11-year mission duration. The technological cutoff date for this study was assumed to be 2011, with an early launch date of 2015.

The SRO spacecraft would be comprised of two stages, a Cruise stage and an Orbiter stage, along with a lifting body aeroshell (Fig. 2.5.1-4). To reach the Saturn system, the SRO would use a Venus, Earth, Earth, Jupiter gravity assist (VEEJGA) to minimize fuel usage and associated mass. To enter Saturn orbit, the trajectory of the SRO would be designed to penetrate the upper atmosphere of Saturn (~61,000 km) whereupon the spacecraft would aerocapture into an elliptical orbit (Fig. 2.5.1-5). The aeroshell would be jettisoned following aerocapture. Subsequently, the Cruise stage would perform a large propulsive maneuver to circularize the spacecraft orbit within Saturn's B-Ring, slightly inclined to the ring plane. Following circularization, the Cruise stage would be jettisoned and the self-contained Orbiter stage would commence the year-long science mission, performing periodic propulsive maneuvers to maintain the desired proximity to the ring plane and to move the Orbiter radially across the rings for multi-location observations and measurements (Fig. 2.5.1-6).

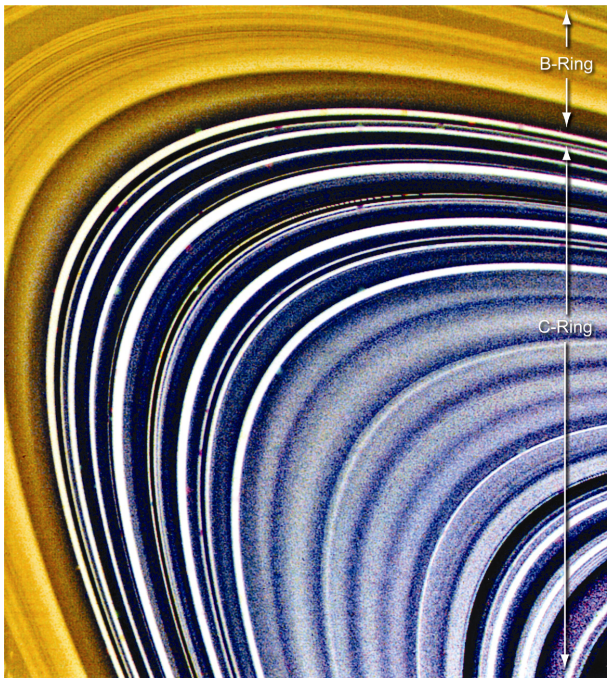

Figure 2.5.1-3. Detail of Saturn's B and C Rings [NASA]

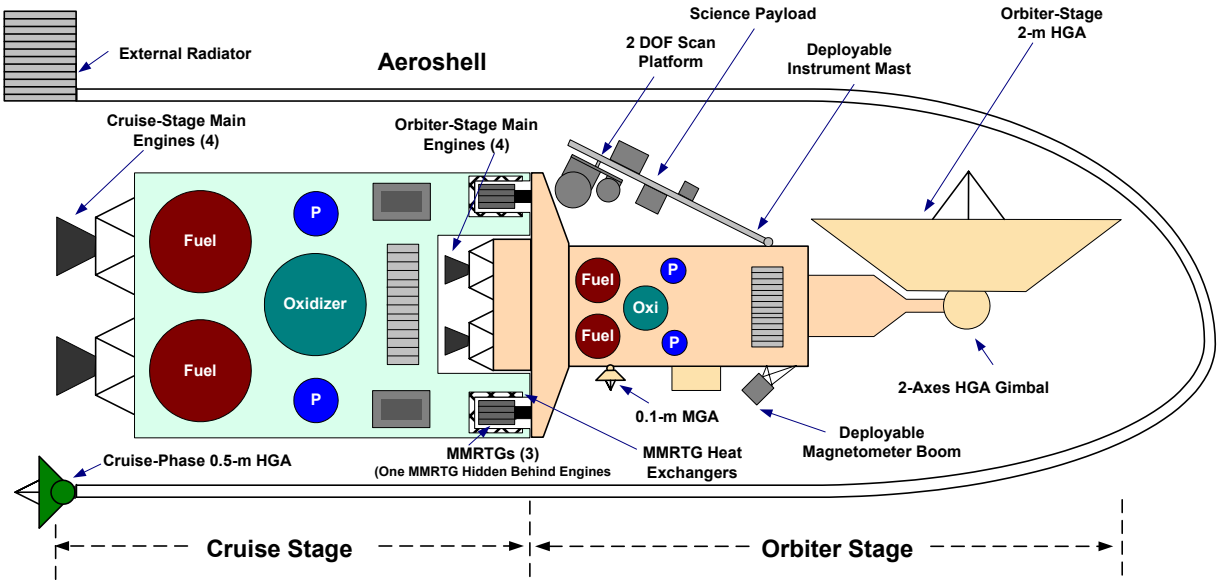

Figure 2.5.1-4. Conceptual Illustration of the SRO Spacecraft and Aeroshell

The Cruise stage portion of the SRO spacecraft would consist primarily of a large rocket propulsion system with antennas for communication with Earth. It would require a sizable propulsion system sufficient to perform the 3400 m/s orbit circularization burn that follows the aerocapture maneuver. The Cruise stage would interface directly with the Orbiter stage that supplies all necessary electrical and thermal power via three MMRTG RPSs. Following orbit circularization, the Cruise stage would be separated from the Orbiter, having fulfilled its mission.

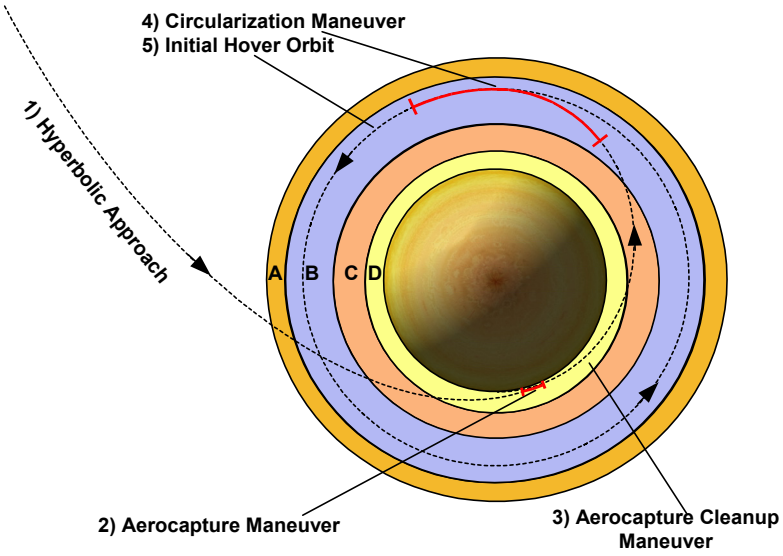

Figure 2.5.1-5. Aerocapture Delivery of SRO to Hover Orbit [43]

The Orbiter would be a self-contained spacecraft that includes the scientific instrumentation, avionics, power systems, communications electronics and thermal control systems. The Orbiter would possess a high gain and medium gain antenna (HGA and MGA) for communications with Earth, and a propulsion system for trajectory correction maneuvers (TCMs) and attitude control. The Orbiter would be designed to "hop" above the rings using bipropellant engines to maintain a nominal distance of 1 to 1.4 km above the centerline of the ring plane (Fig. 2.5.1-7). The Orbiter would nominally carry enough fuel for 1 year's worth of "hopping". Once in orbit, the Orbiter would initiate detailed observations of the Saturn ring system, beginning with the B ring at 110,000 km, and finishing with the A ring at 128,000 km (Table 2.5.1-1 and Fig. 2.5.1-6) at the end of one year.

The Cruise and Orbiter stages would initially be housed within a protective aeroshell that enables aerocapture. The use of the ablative aeroshell provides a much larger delivered payload mass fraction into orbit at Saturn. As the aeroshell penetrates the atmosphere, the aerodynamic drag rapidly reduces the velocity of the spacecraft to 28 km/s, resulting in the SRO entering an elliptical orbit with a periapse of ~61,000 km and an apoapse of 110,000 km.

Following aerocapture, the SRO spacecraft (Cruise and Orbiter stages) would be extracted from the aeroshell. Approximately two hours later, the Cruise stage would begin a two-hour long propulsive maneuver using its four main engines to perform a 2900 m/s burn to circularize the orbit to the desired 110,000 km altitude.

Once the SRO orbit had been circularized, the Cruise stage would be jettisoned from the Orbiter stage. The Orbiter would then rely solely upon its own systems to continue the mission.

The Orbiter's orbit plane would be very slightly inclined (few degrees) with respect to the ring plane. To prevent ring plane crossings and potential collisions with ring particles, the Orbiter would fire its main engines prior to each nodal crossing such that the spacecraft altitude is nominally maintained between 1 and 1.4 km above the ring plane. The altitude profile of the Orbiter is notionally shown in Figure 2.5.1-7, with the spacecraft appearing to "hop" above the ring plane every 2.5 to 3.25 hours depending on radial position. Four hops would be performed each orbital revolution, with each hop changing the longitude of the ascending node by 90 degrees.

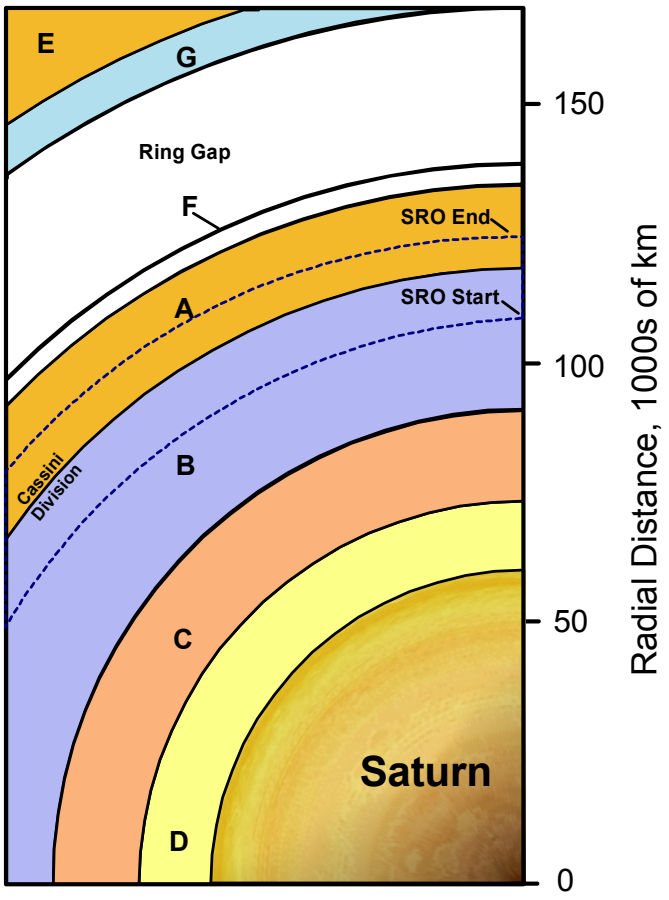

Figure 2.5.1-6. Saturn's Ring Structure and SRO Operating Range [43]

The Orbiter would co-orbit with the ring particles at each location, allowing long-term observation and tracking of particle interactions and dynamics. The Orbiter would stay at each selected radial position for an average of one week in order to perform detailed science measurements. At the end of the week, the Orbiter would ignite its main engines to perform a quasi-Hohmann transfer to the next target location (increasing its distance from Saturn each time). A total of ~50 radial translations would be performed over the course of the mission, providing a variety of different locations at which to take measurements. The translation time between radial locations would be between 5 and 6 hours depending on the radial position.

The baseline SRO spacecraft would be a large vehicle, requiring a next generation heavy launch vehicle (LV) to perform the mission. Detailed trades were also performed to assess the minimal science payload and mission duration that could be supported by an existing LV (Section 2.5.2); however, it was concluded that a larger LV must be used to launch any scientifically justifiable variant of the SRO spacecraft were a single LV to be used. It is conceivable that the SRO could be launched in multiple sections using existing LVs and then assembled in Earth orbit; however, this option was not explored herein. Instead, this study assumes that a larger boost vehicle would be available in the 2015 timeframe to support the SRO mission, a reasonable assumption considering the identified need for heavier boosters for manned missions to the Moon and Mars, and for the proposed Jupiter Icy Moons Orbiter (JIMO) spacecraft. The SRO launch vehicle is assumed to have a lift capability of ~28,000 kg to a C_3 of 15 km^2/s^2, equivalent to those currently being considered using EELV-derived concepts [46].

Table 2.5.1-1. Saturn Ring Plane Characteristics [44, 45]

Ring	Inner Radius (km)*	Outer Radius (km)	Thickness (km)
D	68,000	76,500	Unknown
C	74,500	92,000	Unknown
Maxwell Gap	87,500	87,770	
B	92,000	117,500	0.1 to 1
Cassini Division	117,500	122,200	Unknown
A	122,200	136,800	0.1 to 1
Encke Gap	133,570	133,895	
Keeler Gap	136,530	136,565	
F	140,210	140,240 to 140,710	30 to 500
G	165,800	173,800	100 to 1,000
E	180,000	480,000	1,000 to 30,000
* Distance measured from the planet center to the start of the ring.			

The SRO would be a 3-axis stabilized spacecraft using reaction wheels for fine pointing and small thrusters for reaction wheel desaturation. Attitude determination would be performed by an Inertial Measurement Unit (IMU) and star trackers during the cruise phase, and exclusively by star trackers while in orbit about Saturn. Coarse analog sun sensors would be used for contingency operations.

The SRO Orbiter would use an advanced autonomous collision avoidance system to identify potentially threatening particles that may be on a collision course with the spacecraft and to perform the necessary collision avoidance maneuvers. The velocities of ring particles in the direction out of the ring plane are expected to be slow enough (<15 cm/s) to provide sufficient time for the Orbiter to identify them using its LIDAR, process the data, generate a collision avoidance trajectory, and perform the necessary burn. These burns would generally be perpendicular to the ring plane, effectively initiating a ring-hop ahead of its nominally sequenced time. The size of the ring particles in the A and B rings (where the SRO would operate) are expected to be in the range of 1-cm to 1-m in diameter.

The SRO Orbiter would require fine attitude knowledge for pointing its narrow angle camera (NAC) and precise attitude control to prevent image smear. The proposed SRO Orbiter would have pointing knowledge of 45 arcsec and be controlled to 90 arcsec. Pointing stability would be controlled to within 0.3 arcsec/sec per axis to meet the camera stability requirements. This corresponds to sub-pixel stability over the nominal NAC exposure duration.

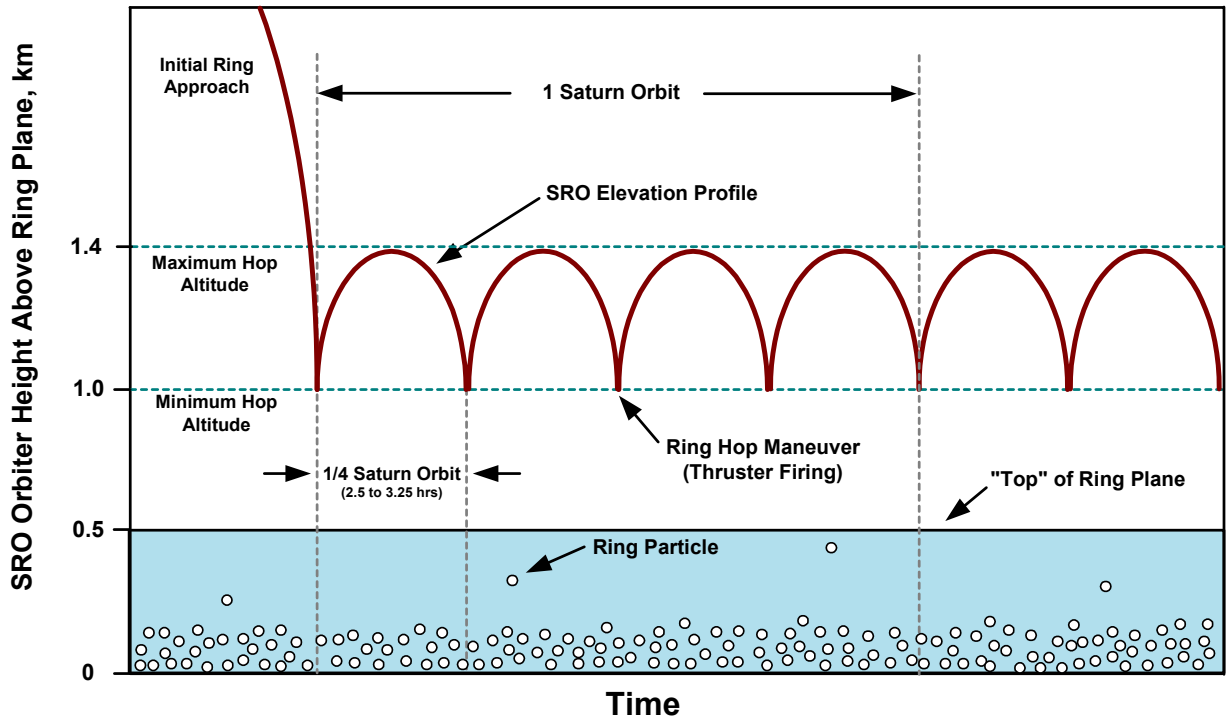

Figure 2.5.1-7. SRO Orbiter Elevation Profile Above Ring Plane as a Function of Time

Due to the lengthy mission duration and potentially hazardous operating location, the SRO spacecraft would include full functional redundancy for all mission critical components, excluding instrumentation.

2.5.1.4 Power Source Trade Study

Multiple power system options were considered for the SRO mission study, including solar power and radioisotope power systems. Key factors considered in the power system trade study were the power system's mass, physical size, tolerance to the space environment, and overall feasibility. In the final analysis, RPSs were considered the only viable technology for this class of mission for the following reasons. Saturn is ~9.5 AU distant from the Sun, resulting in the Orbiter receiving only about $1/90^{th}$ of the insolation at Earth's orbit. This corresponds to ~15 W/m^2. Assuming that a new generation of Low-Intensity Low-Temperature (LILT) tolerant solar arrays could be developed and qualified in time for this mission, and using reasonable assumptions for specific mass and volume of the arrays, the total amount of SA area required to power the Orbiter spacecraft would be on the order of 150 m^2 (Table 2.5.1-2). This corresponds to a SA mass of ~370 kg. Adding batteries for operations during eclipse increases the SA system mass to nearly 390 kg, and does not include the additional required systems such as gimbals, cabling and power converters that increase the mass further. These Orbiter SAs would need to be folded within the aeroshell during the cruise phase, and thus would be inoperable during the first 10 years of the mission. Thus, a second solar array system would be required that could be externally mounted to the aeroshell and ejected prior to aerocapture at Saturn, further increasing the

spacecraft mass. Since the power draw during the cruise phase is only marginally lower than during the Science phase, this second SA system would have a mass greater than 300 kg, resulting in an overall power system of ~690 kg (w/o margin). Solar cells are sensitive to radiation exposure, which could significantly decrease their efficiency over the mission lifetime [47]. This reduction in efficiency would require an even larger array that could further increase the SA mass. In comparison, the mass of an RPS system using three MMRTGs and batteries is estimated at ~143 kg without margin (Section 2.5.1.12), which is roughly 20% of the solar array option. Considering that any mass added to the spacecraft has a multiplicative effect on the amount of propellant that must be carried and the size of the aeroshell, it becomes clear that RPS is the only practical option for this mission.

Table 2.5.1-2. Solar Array Power System Design Parameters

Parameter	Value
Total Power Electrical Reqt for SRO Mission (W)	280
Total Received Solar Energy per m^2 at Saturn	15.15
Required Solar Array Area of Orbiter Stage (m^2)	149
Reqd Solar Array mass of Orbiter Stage (kg)	372.1
Reqd Battery Mass to Run Through Shadow (kg)	17.0
Total Mass of Orbiter Stage SA Power System (kg)	389
Total Mass of Cruise Stage SA Power System (kg)	300
Total Mass of SA Power System w/o Margin (kg)	**689**

From a size perspective, the large solar arrays required for the Orbiter would induce additional complexities and require additional SA support structure to handle the propulsive maneuvers associated with ring hopping and translations. Larger reaction wheels would be required to maintain spacecraft pointing requirements, increasing the Orbiter mass even further. Induced oscillations of the arrays following Orbiter propulsive maneuvers could affect spacecraft pointing and stability performance, thus reducing the ability of the SA-powered Orbiter to meet its science requirements. The large size and relative fragility of the SRO solar arrays would also be sensitive to ring particle bombardment, potentially imposing significant constraints on how close the spacecraft could operate to the ring plane. Lastly, the deployment of large arrays on the Cruise or Orbiter stages would introduce additional risk in that failure to fully deploy or properly track the sun could potentially doom the mission. On the other hand, the relatively small size of the RPS system would reduce the size of the reaction control system, would be less susceptible to propulsion-induced oscillations, and would not require any complex mechanical deployment.

In conclusion, the SRO spacecraft would require nearly 300 We of power at Saturn to operate its science instruments, drive its propulsion system, and transmit its science data back to Earth. This power system would need to operate for 11 years or more at distances up to 1.6 billion kilometers from the Sun. While many power system technologies were considered for the SRO mission, radioisotope power systems were considered the only feasible power system for this application.

2.5.1.5 RPS Characteristics

Three MMRTGs are assumed in the mission study to provide all necessary electrical power for the SRO spacecraft. This corresponds to a total of approximately 330 We at BOM, and ~ 275 We after 11 years from BOM (Section 3 – Table 3-6). SRGs could potentially meet the mission requirements just as effectively, as discussed in Section 2.5.1.14. The RPS system would reside on the SRO Orbiter stage, and power both the Orbiter and Cruise stages during the mission. The ~5230 Wt (EOM) of residual waste heat would be used to maintain operational and survival temperatures of the Cruise and Orbiter stages using radiatively coupled heat pipes.

2.5.1.6 Science Instruments

The baseline payload chosen for this study consists of instruments for characterizing the intrinsic properties (composition, geometry, density, etc.) and dynamics of a population of particles a couple of centimeters and larger in size in a quasi-inertial and electromagnetically active environment. It is understood that the actual instrument complement for the mission would be selected by a team composed of Project and NASA personnel, based upon the recommendations of a science definition team drawn from the planetary and origins science communities. However, the selected payload (Table 2.5.1-3) in this baseline configuration gives the study team a representative set of requirements, including but not limited to such aspects as mass, power, pointing and stability, positioning, etc., that demand a realistic platform and thus provides a higher-fidelity study result. There are three general classes of instruments in this payload: those that measure ring particle geometry and dynamics, those that measure composition, and those that measure the electromagnetic environment.

The geometry and dynamics class includes wide-angle and narrow-angle imaging, and LIDAR. A Narrow-Angle Camera (NAC) provides geometry and 2-D dynamics (components perpendicular to the camera pointing vector) of individual particles larger than ~2 cm, with the LIDAR providing particle locations and velocities in the third dimension. The LIDAR also serves the engineering function of measuring the distance from the spacecraft to the ring plane, data that is vital for controlling the thrusters that maintain the standoff distance. Both the NAC and the LIDAR observe a limited area of the rings, and are pointed such that they view the co-orbiting zone directly "beneath" the spacecraft with a field of view (FOV) of 1.2^{o}. A Wide-Angle Camera (WAC) observes a much larger area of the rings with an FOV of 120^{o}, providing context to the NAC images and observing bulk and aggregate structure and behavior.

Two instruments in the composition-measuring class cover both remote sensing and in-situ measurement techniques. A Visual and Infrared Spectrometer (VISIR) measures reflection spectra from the ring particles, providing information about composition, especially for non-volatile components. An Ion and Neutral Mass Spectrometer (INMS) directly measures the composition of the "ring atmosphere", the cloud of molecules and atoms volatilized and sputtered from the ring particles by a variety of processes.

Magnetic and electric fields would be measured by separate magnetometer and electric field antenna. Standard techniques for measuring electric fields in space are not appropriate here, since the fields of primary interest might not oscillate at radio or even audio frequencies, but rather are slowly-varying, almost DC fields. Some phenomena, such as meteoroid impacts on ring particles, can generate waves or other rapidly-varying fields, so the instrument would be able to measure those as well.

Lastly, a dust detector would be included in the baseline instrument suite to measure the micrometeoroid flux near the rings. This instrument would permit the determination of the rates and energies of micrometeoroid impacts on the ring particles.

Table 2.5.1-3. Science Payload and Instrument Descriptions for the Proposed SRO Mission

Instrument	Purpose	Science Objectives Addressed
1. Narrow Angle Camera	Obtains images of individual ring particles and other objects at a resolution of 0.5 cm/pixel	Collision dynamics Behavior of particle agglomerations Particle geometry Particle and mass density profiles (ring radial structure) Particle size distributions Particle random velocity components Ring vertical structure Shepherding moon observations
2. Wide Angle Camera	Obtains larger-scale images of larger ring particles, moons, and rings as aggregates of particles	Particle geometry (large particles) Particle and mass density profiles (ring radial structure) Particle size distributions Ring vertical structure Shepherding moon observations Particle random velocity components Behavior of particle agglomerations Context for NAC images
3. Visible and Infrared Spectrometer (VISIR)	Obtains high-resolution aggregate spectra of ring particles at visible and IR wavelengths	Particle elemental and mineralogical composition Ring structure (variation of composition with location) Composition of moons
4. Ion and Neutral Mass Spectrometer (INMS)	Obtains mass spectra of neutral and ionized species near the rings	Particle elemental and mineralogical composition Composition and structure of the “ring atmosphere”.
5. Magnetometer	Measures magnetic field strength and direction near the rings	Measures the static and quasi-static magnetic environment of the rings to investigate possible connections between ring structures and magnetic phenomena.
6. E-Field Meter/Plasma Wave Spectrometer	Measures electric field strength and direction near the rings, and plasma waves	Measures the static and quasi-static electric field environment of the rings to investigate possible connections between ring structures and electric fields.
7. LIDAR	Measures out-of-plane components of ring particle position and velocity	Provides the 3rd dimension of position and velocity needed for dynamics analyses. Also serves the engineering function of determining distance to the ring plane, for controlling thruster burns.
8. Dust Detector	Measures the micrometeoroid flux near the rings	Determine rates and energies of micrometeoroid impacts on ring particles.

2.5.1.7 Data

The SRO mission would be divided into separate cruise and science phases. During the cruise phase, data would be limited to health and status information of key subsystems, and the resultant data volume would be relatively small and easily manageable by the SRO’s communication system. During the science phase, however, the data volume would be significant, as the eight scientific instruments would be operated in parallel. The data volume obtained during the science phase is estimated at 1380 Mbits/day (24 hours), indicated in Table 2.5.1-4, and represents the stressing case in terms of sizing the transmitters and antennas for the SRO mission.

SRO science instruments would use individual measurement sampling rates based on the phenomena being observed and its rate of change. The sampling rates would range from just two measurements per hour for wide-angle camera images, up to 3600 measurements per hour (1 Hz) for the electric field/plasma wave instrument and magnetometer during entry and exit of the Orbiter from Saturn’s shadow. The key data volume drivers would be the narrow angle camera and

LIDAR, each employing a 4096x4096x8 bit CCD with high performance compression. These two systems would operate in unison to generate detailed spatial and temporal maps of the ring particles that are used to fulfill the science requirements and for collision avoidance. These systems would operate at a rate of six frames per hour, each yielding 3.95 Mbits/frame or ~570 Mbits/day. The data produced by these two instruments would account for 83% of the total data volume.

The wide angle camera would use the same resolution CCD and compression system as the NAC and LIDAR, but would require less frequent imaging (2 frames/hour) due to the larger field of view. The resultant data volume of the WAC would be 187 Mbits/day or 13.5% of the total. The remaining 3.5% of the data volume would be consumed by engineering data and the six remaining instruments, comprised of the VISIR, Electric Field/Plasma Probe, Magnetometer, INMS, Dust Detector, and VISIR.

Each year, communications with the spacecraft would be temporarily interrupted as Saturn and Earth approach opposing sides of the Sun, lasting for up to one week, as happened with Cassini in July 2004. To compensate for this event, the SRO data storage system would be designed to store a minimum of two week's worth of science and engineering data at their full data rate, corresponding to 19 Gbits. Once communication was reestablished, the SRO could temporarily expand its nominal 8 hours telecom window until all the stored data was downloaded to Earth.

Table 2.5.1-4. Data Rate Estimates for Conceptual SRO Instrumentation Suite

Instrument	Data Rate (kbits per measurement)	Measuremt Frequency (# / Hr)	Number of Measurements per day	Accumulated Data Volume per Day (kbits)	Accumulated Data Volume per Day (Mbits)
VISIR	25	10	240	6000	6
Wide Angle Camera	3950	2	48	189600	190
Narrow Angle Camera	3950	6	144	568800	569
Electric Field / Plasma Probe	0.200	3600	86400	17280	17
Magnetometer	0.200	3600	86400	17280	17
INMS	50	5	120	6000	6
Dust Detector	0.018	3600	86400	1555	2
LIDAR	3950	6	144	568800	569
Engineering Data	0.1	3600	86400	8640	9
		Total Accumulated Data Volume / Day (Mbits)			1384
		Required Uplink Rate (kbit/s)			**48.1**
		Design Uplink Data Rate (kbits/s)			**80.0**
		Margin in Data Rate			66%
		Maximum Uplink Data Volume / Day (Mbits)			2304
		Req'd Data Storage Volume (Mbit)			**19375**
		Design Data Storage Volume (Mbits)			**32000**
		Margin in Data Storage Volume			65%

2.5.1.8 Communications

The SRO communications system design would consist of individual Cruise and Orbiter-stage subsystems. The Cruise stage communications subsystem would be utilized during launch, cruise, aerocapture and orbit circularization phases of the mission to receive commands from Earth, and transmit back engineering data prior to the beginning of the science mission. The Orbiter-stage communications subsystem would be utilized during the science mission for data download and commanding. The Orbiter stage would house all communications electronics for the entire spacecraft (Cruise and Orbiter stages) as illustrated in Figure 2.5.1-8. The use of a common set of transmitters, receivers, and other key electronics would minimize the number of systems duplicated between the two stages, potentially saving mass and complexity. The Cruise stage would include a dedicated high gain antenna (HGA) and two low gain antennas (LGAs). The Orbiter stage would be comprised of HGA and MGA antennas and the communications electronics. The electronics would use fully redundant amplifiers and circuitry, and functional redundancy exists for the antennas to increase operational reliability. Following orbit circularization about Saturn, just prior to separation between the Orbiter and Cruise stages, RF communications would be rerouted from the cruise stage antennas to the Orbiter stage antennas via the

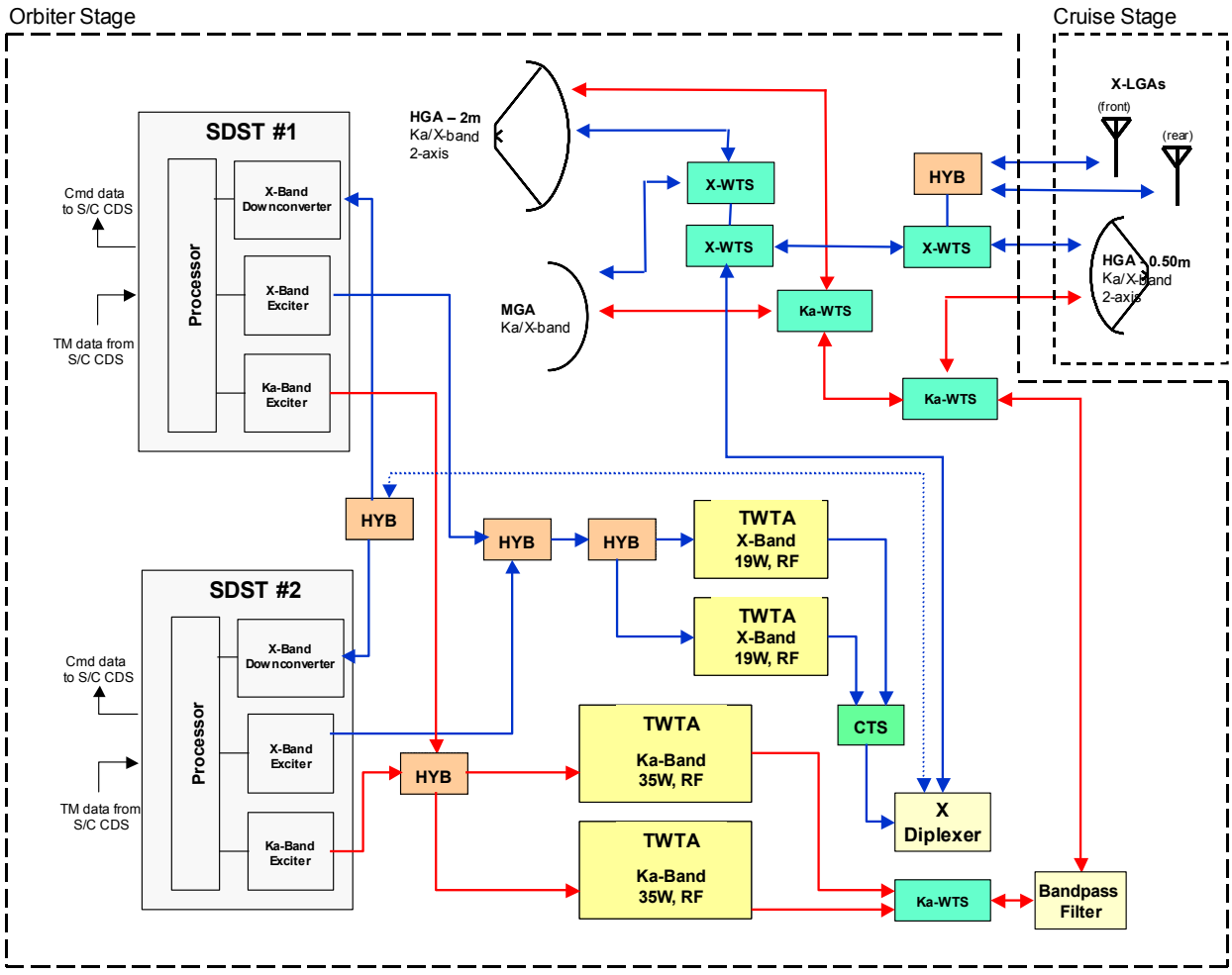

Figure 2.5.1-8. SRO Communications System for Cruise and Orbiter Stages

Orbiter's waveguide transfer switches (WTSs) as shown in the figure. Following separation, the Cruise stage would be discarded (soon become another ring particle) and all subsequent communications with Earth would be via the Orbiter's communications system. This study assumes that the Deep Space Networks (DSN's) 34-m dish would nominally be used to receive all science and engineering data from the spacecraft and used for command uplinks. Were the DSN 70-m antennas used in place of the 34-m antennas, the data rates specified herein could potentially be increased by a factor of four. However, baselining the 34-m DSN antennas ensures a conservative SRO communications architecture.

During the cruise phase, communications with the spacecraft would be via the Cruise stage's gimbaled 0.5-m Ka/X-band HGA. The HGA would nominally transmit at X-band with a minimum download data rate of ~170 bits/s (assessed at 10.5 AU) for engineering data sent to Earth (Table 2.5.1-5). The Cruise Stage has the capability to use the higher-power Ka-band transmitter (designed primarily for the Science Phase) were high-bandwidth communications necessary with Earth. Using the Ka-band option with the 0.5-m HGA would yield a download data rate of ~5 kbits/s at Saturn. The Cruise stage HGA is mounted external to the aeroshell, and would be jettisoned prior to aerocapture to prevent non-uniform drag as the SRO decelerates within Saturn's atmosphere. Two X-band LGAs are included for contingency purposes (e.g., recovery of a spinning spacecraft), and would be used to provide a carrier signal for spacecraft tracking during the orbit circularization burn. Once the spacecraft's orbit had been circularized, the Orbiter stage would be separated from the Cruise stage (the aeroshell having already been jettisoned following the aerocapture maneuver) and subsequent communications would be through the Orbiter's antenna system.

The Orbiter would possess a gimbaled 2-meter Ka/X-band HGA and a fixed Ka/X-band MGA. The HGA is the primary Orbiter antenna and would nominally be used for downloading science and engineering data in Ka-band during the science mission. The maximum HGA downlink date rate is estimated at 80 kbits/s, providing significant margin over the required data rate specified previously.

Table 2.5.1-5. Maximum Download Data Rates from the SRO Spacecraft to the DSN

SRO Stage and Antenna Type	Ka-band Data Rate 35 W (RF) at 10.5 AU	X-Band Data Rate 19 W (RF) at 10.5 AU	Description
Cruise Stage			
HGA (0.5-m) Ka/X-Band	5 kbits/s	167 bits/s	HGA is primary antenna for transmitting engineering data to Earth and receiving commands (both in X-band) during Cruise phase. Assumes 34-m DSN antenna. Ka-band also available as needed.
LGA X-Band Only	N/A	< 1 bit/s	X-band LGAs Used for near-Earth contingency purposes and spacecraft tracking during orbit circularization burn.
Orbiter Stage			
HGA (2-m) Ka/X-band	80 kbits/s	2.7 kbits/s	HGA is primary antenna for transmitting science and engineering data to Earth (Ka-band), and receiving commands (X-band).
MGA (0.1-m) Ka/X-band	200 bits/s	6.7 bits/s	MGA is backup to 2-m HGA and would be used for contingency purposes.

For purposes of redundancy and contingency, the HGA could be operated in X-band at a lower data rate mode, corresponding to a maximum data rate of 2.7 kbits/s. Command uplink would nominally be performed via the Orbiter's HGA in X-band, and be backed up by the MGA.

The SRO Orbiter would have a baseline communications window of 8 hours per day, spread throughout the 24-hour interval (i.e., not contiguous), which would be necessary to satisfy the required science measurement schedule. This communications window corresponds to a total data volume capability of 2.3 Gbits per day, offering significant margin relative to the ~1.4 Gbits of science data baselined per day (Section 2.5.1.7). This window could be expanded were additional science data requested (especially high-rate imaging) or following a solar conjunction. During this later event, the longer communications window would be needed to download the week (or more) of buffered science data back to Earth.

2.5.1.9 Thermal

The SRO design would use a combination of passive and active thermal control systems to maintain operating and survival temperatures during the mission. During the cruise phase, the Orbiter would be stored within a protective aeroshell (Fig. 2.5.1-4), which would thermally insulate the Orbiter stage by preventing the spacecraft from directly radiating to the cold of deep space (T_{amb}~4K). Supplemental electric heaters would be used on the Orbiter to regulate the temperature of the instruments, sensitive subsystems, and the fuel, oxidizer and pressurant. The Cruise stage, also located within the aeroshell during the cruise phase, would maintain system temperatures via a loop heat pipe system radiatively coupled to the RPSs on the Orbiter. The three MMRTG RPSs would jointly produce a total of ~5670 Wt (BOM) of excess heat that would be absorbed by the heat exchanger and circulated through the Cruise stage, primarily to warm the fuel, oxidizer and pressurant tanks (Fig. 2.5.1-9). The RPS heat would then be rejected to deep space by radiators mounted externally to the aeroshell. The radiators would use thermal control louvers or polychromatic surfaces to actively control the heat rejection rate, and would be jettisoned just prior to the aerocapture maneuver to prevent them from being uncontrollably burned off during aerocapture (possibly affecting spacecraft attitude control) and to prevent heat flow into the Cruise and Orbiter stages. Flow control valves would be used to redirect the working fluid as needed through the cruise stage and between the aeroshell radiators (used prior to aerocapture) and the cruise stage radiators (used following aeroshell jettison).

During the ~15 minute aerocapture event, the aeroshell would protect the Cruise and Orbiter stages from the intense external heat generated during their hellish deceleration through Saturn's upper atmosphere via a combination of ablation of the aeroshell material (using a carbon-based material) and radiative heat exchange - the aeroshell would be designed to emulate a black body to maximize radiative heat loss. The heat generated by the MMRTGs during aerocapture would either be stored in the thermal mass of the system until aeroshell separation, or if determined to be too great (via detailed analysis), could be managed using a phase change material such as water that would be vented out the rear of the spacecraft.

Upon completing the aerocapture maneuver, the clamshell-designed aeroshell would separate, freeing the Cruise and Orbiter-stage spacecraft. The Cruise stage flow control valves would then be reconfigured to reject the MMRTG heat via body-mounted radiators during the course of the subsequent circularization burn. The Orbiter stage would stay warm using blankets of multilayer insulation (MLI) augmented with electrical heaters.

Following the circularization burn, the spent Cruise stage would be jettisoned, exposing the Orbiter-stage MMRTGs to the ambient background temperature where their integrated fins would

passively maintain their operating temperatures. The Orbiter itself would continue to rely upon a combination of MLI blankets, self-heating of powered instrumentation and subsystems, supplemental electric heaters, and polychromatic radiators or thermal control louvers to regulate the temperatures of the instruments, propulsion system, and other thermally sensitive subsystems.

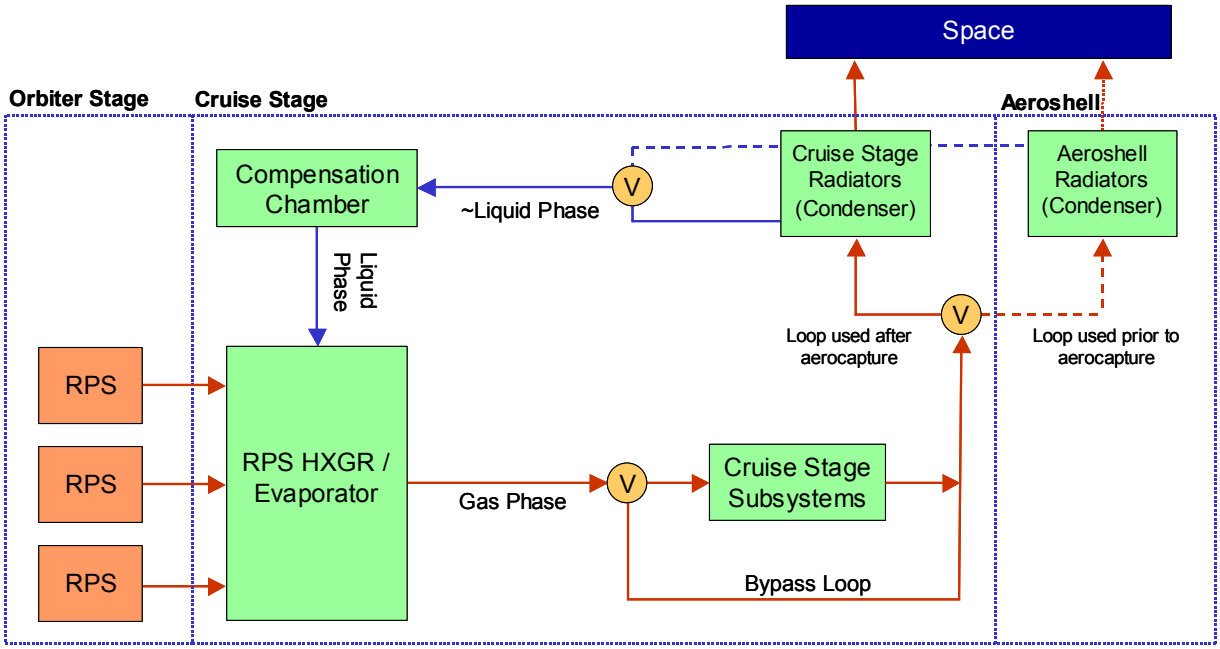

Figure 2.5.1-9. Block Diagram of the SRO Thermal Control Loop

2.5.1.10 Propulsion

The SRO's carrier stage would be tasked with performing the deep-space trajectory correction maneuvers (TCMs) required to prepare for and correct from the gravity-assist flybys of Venus, Earth (twice) and Jupiter (Fig. 2.5.1-10), and to perform the orbit circularization and cleanup burns following aerocapture around Saturn (Fig. 2.5.1-5). This stage would consist of separate high- and low-thrust systems, with the high thrust system comprised of four gimbaled 890 N (I_{sp} of 325 s) bipropellant main engines using nitrogen tetroxide (NTO) and hydrazine (N_2H_4). The low-thrust system would be comprised of twelve 0.7 N monoprop thrusters (N_2H_4) and used to perform attitude control. The delta V requirement of the carrier stage is estimated as 3650 m/s, with 3400 m/s allocated to circularization and subsequent cleanup maneuvers. The total mass of the cruise-stage propellant (fuel, oxidizer and pressurant) would be ~10470 kg (Table 2.5.1-8). The duration of the circularization burn is estimated at ~2 hours.

The Orbiter propulsion system includes separate high, medium and low thruster systems, with the high-thrust system comprised of four 45 N bipropellant (NTO/ N_2H_4) main engines with an Isp of 326 s. These engines would be used to perform the ring hops above the ring plane with minimum and maximum heights of 1 and 1.4 km, respectively.

The nominal mission profile would include 4 ring hops per orbit, corresponding to one hop every 2.5 to 3.25 hours (depending on radial distance from Saturn). The duration of each ring hop burn is approximately 2 seconds, and would impart an average delta V of approximately 0.3 m/s per hop. Additional hops could be employed were the collision avoidance system to detect the Or-

biter approaching a thicker section of the ring plane (e.g., spokes or waves) or if incoming particles were detected on a collision course with the spacecraft.

The high-thrust system would also be used to incrementally translate the spacecraft from the initial 110,000 km circular orbit to the final 128,000 km orbit. Ring translations would occur an average of once a week, permitting sufficient time for detailed static and dynamic fields and particles measurements at each radial location. This corresponds to approximately 52 translations over the course of the science mission, with each translation covering a radial distance of ~350 km. Each translation would use a Hohmann transfer, requiring a delta V of ~30 m/s and a burn duration of ~4 minutes.

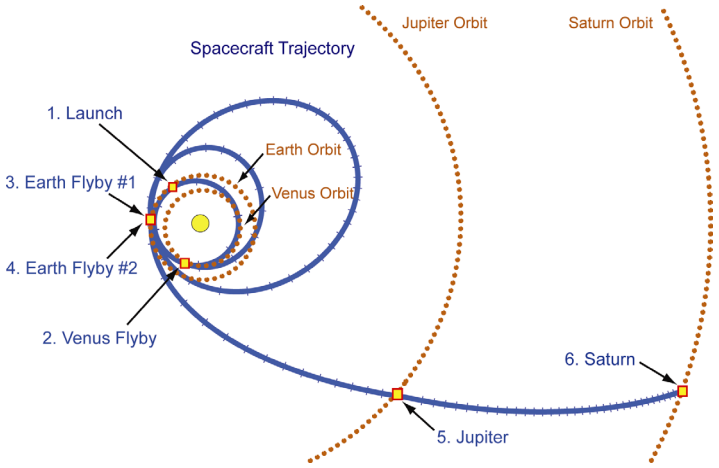

Figure 2.5.1-10. VEEJGA Trajectory of the SRO Spacecraft. The line segment between adjacent tick marks corresponds to one month of flight time.

The Orbiter's intermediate-thrust system incorporates four 4.5 N monoprop (N_2H_4) thrusters that are used for roll control during primary engine burn, desaturation of the reaction wheels, to perform small TCMs, and for coarse attitude control. The Orbiter maintains fine attitude control (e.g., for pointing of instruments, etc.) using its low-thrust propulsion system comprised of twelve 0.7 N monoprop (N_2H_4) thrusters. The total delta V requirement of the Orbiter stage would be ~2280 m/s, with ring translations requiring ~1510 m/s (66% of total) and ring hops requiring ~770 m/s (34% of total) as indicated in Table 2.5.1-6.

It is observed that the large delta V required for moving radially across the ring plane from 110,000 km to 128,000 km dominates the propellant requirements of the Orbiter, and constrains the area of exploration even for a mission assuming a JIMO-class launch vehicle. A trade study

Table 2.5.1-6. Delta V Estimates for the SRO Cruise and Orbiter Stages

Activity	Delta V (m/s)	Description
Cruise Stage	**3650**	
Cruise Phase in Deep Space	250	Trajectory correction maneuvers and attitude control over 10 year cruise phase.
Periapse Raise	2900	Used to insert SRO into a circular 110,000 km orbit around Saturn following aerocapture.
Circularization Burn	500	Delta V required for orbital insertion cleanup maneuvers following circularization burn.
Orbiter Stage	**2275**	
Ring Hops	768	Average of 4 ring hops per orbit for 1 year. Corresponds to a mean delta V of ~0.3 m/s per hop.
Ring Translations	1507	Average of 1 ring translation of 3 km every week. Corresponds to a mean delta V of ~30 m/s per translation.
Total Delta V	**5925**	

was performed to assess the effect of reducing the total translation distance and mission duration upon the required amount of delta V and spacecraft mass. The results of this study are presented in Section 2.5.2.

2.5.1.11 Power

The SRO spacecraft would employ three MMRTGs and secondary batteries to supply all electrical power during the mission. The electrical output of the three MMRTGs is ~330 We at BOM, corresponding to ~275 We at EOM (11 years after SRO launch). The power system (RPSs, batteries, and power distribution subsystem) would be located on the Orbiter stage; the Cruise stage would rely on the Orbiter stage to supply all its power needs for propulsion, etc. The SRO has six mutually exclusive operating modes (Fig. 2.5.1-11, Table 2.5.1-7) corresponding to key sequences and activities during the mission. The modes are designed to prevent the power demand from exceeding that available from the Orbiter power system.

The power modes of the SRO spacecraft are divided into three distinct cruise-phase modes and three science-phase modes. The three cruise-phase modes are *Launch*, *Cruise* and *Aerocapture & Circularize*. The three science-phase modes are *TCM (Hops and Translations)*, *Science* and *Science and Telecommunications*.

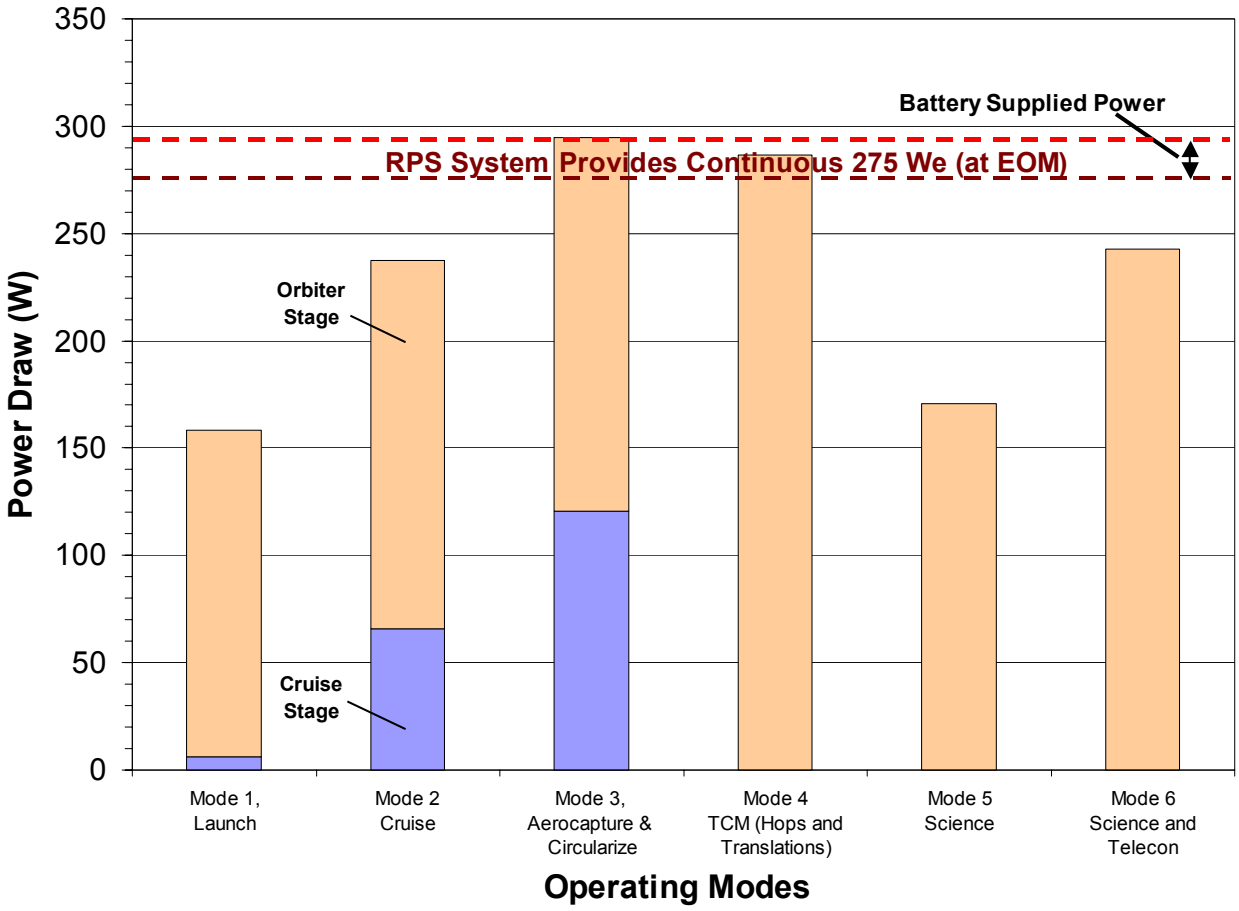

Figure 2.5.1-11. Operating Modes and Power Level Estimates for the SRO Spacecraft

Table 2.5.1-7. Power Level Estimates for the SRO Spacecraft (Including 30% Margin)

Subsystem	Power Modes, (We)					
	Cruise Phase Modes			Science Phase Modes		
	Mode 1, Launch	Mode 2 Cruise	Mode 3, Aerobrake & Circularize	Mode 4 TCM (Hops and Trans.)	Mode 5 Science	Mode 6 Science and Telecon
Orbiter Stage	**152.1**	**172.1**	**172.1**	**286.8**	**170.8**	**242.8**
Instruments	**21.3**	**21.3**	**21.3**	**85.0**	**85.0**	**85.0**
VISIR	2.5	2.5	2.5	10.0	10.0	10.0
Wide Angle Camera	2.5	2.5	2.5	10.0	10.0	10.0
Narrow Angle Camera	2.5	2.5	2.5	10.0	10.0	10.0
Electric Field / Plasma Probe	2.5	2.5	2.5	10.0	10.0	10.0
Magnetometer	0.3	0.3	0.3	1.0	1.0	1.0
Ionized Neutral Mass Spectrometer (INMS)	2.0	2.0	2.0	8.0	8.0	8.0
Dust Detector	1.5	1.5	1.5	6.0	6.0	6.0
LIDAR	7.5	7.5	7.5	30.0	30.0	30.0
ACS	**31**	**51**	**51**	**24**	**24**	**24**
Star Trackers	4	4	4	4	4	4
IMU	27	27	27			
Reaction Wheels		20	20	20	20	20
C&DH	**20**	**20**	**20**	**20**	**20**	**20**
Processor	20	20	20	20	20	20
Power	**20.2**	**20.2**	**20.2**	**20.2**	**20.2**	**20.2**
Battery						
MMRTGs						
Power Conditioning	20.2	20.2	20.2	20.2	20.2	20.2
Thermal	**19.3**	**19.3**	**19.3**	**19.3**	**19.3**	**19.3**
Heaters	4.3	4.3	4.3	4.3	4.3	4.3
Propulsion Tank Heaters	10	10	10	10	10	10
Propulsion Line Heaters	5	5	5	5	5	5
Telecom	**38**	**38**	**40**	**0**	**0**	**72**
X-band TWTA , RF=19W	38	38	38			
Ka-band TWTA, RF=35W						70
Antenna Articulation Mechanism (2-axis)						2
Propulsion	**2.31**	**2.31**	**2.31**	**118.31**	**2.31**	**2.31**
HP Transducer	0.66	0.66	0.66	0.66	0.66	0.66
LP Transducer	1.65	1.65	1.65	1.65	1.65	1.65
DM Monoprop Thrusters 1 (4.5 N)				20		
DM Monoprop Thrusters 2 (0.7 N)				36		
Biprop Main Engine (45 N)				60		
Cruise Stage	**6**	**65.6**	**120.6**			
C&DH	**6**	**6**	**6**			
Data Processor	6	6	6			
Propulsion	**0**	**36**	**95**			
DM Monoprop Thrusters (0.7 N, Isp=210s)		36				
Biprop Main Engine (890 N, Isp=325s)			95			
Telecomm	**0**	**2**	**0**			
Antenna (0.5m 2-axis, parabolic)		2				
Antenna Articulation Mechanism (2-axis)		2				
Thermal	0	19.6	19.6			
Heaters		6.5	6.5			
Prop Tank Heaters		6.5	6.5			
Prop Line Heaters		6.5	6.5			
SRO Spacecraft (Cruise and Orbiter Stages)	**158.1**	**237.7**	**292.7**	**286.8**	**170.8**	**242.8**

The maximum power draw during the cruise phase modes is estimated at 293 We, driven primarily by the Cruise stage propulsion system used during the orbit circularization maneuver. The peak power draw of this mode exceeds the available RPS power, and thus redundant 400 W-hr batteries would be used to carry the peak energy demand of the ~2 hour circularization burn and subsequent clean-up activities. Batteries are the preferred solution rather than additional RPSs, as the circularization burn is a one-time occurrence and adding batteries is lighter (8 kg) than adding an additional MMRTG (45 kg).

During the three science phase modes (*TCM*, *Science,* and *Science and Telecom*), the dominant power mode is *TCM*, with a power draw of ~287 We. This is driven by the operation of the propulsion system valves and the need to keep all instruments fully powered during the science mission in order to maintain their operating temperatures and keep them in a hot-standby configuration (i.e., to prevent having to endure potentially lengthy startup times). Secondary batteries are used to cover the peak power demand during the *TCM* mode as it exceeds the steady state power output of the RPSs.

In summary, the SRO power system would be located on the Orbiter stage and be comprised of three MMRTGs and secondary batteries to handle all power demands during the mission. A moderately sized Li-Ion battery would be used to cover the peak power draw of the *Aerobrake and Circularize* mode and the *TCM* mode, above and beyond what the three MMRTGs generate.

2.5.1.12 Mass

The total wet mass of the SRO spacecraft, inclusive of the Cruise and Orbiter stages and aeroshell, is estimated at ~18,700 kg including 30% margin (Table 2.5.1-8). The bulk of the SRO spacecraft is comprised of propellant for the orbiter and cruise stages (11,500 kg, 61% of the total spacecraft mass) and the aeroshell used for aerocapture (4650 kg, 25%). Together, the propellant and aeroshell comprise 86% of the total launch mass.

The SRO instrument mass would be ~130 kg, corresponding to less than 1% of the total launch mass. The instrument mass is dominated by the large aperture NAC (65 kg) that is needed to obtain the requisite 0.5 cm/pixel resolution images. The total mass of the Orbiter stage is ~1840 kg (wet) and is comprised of an 860 kg (dry) spacecraft and nearly 1,000 kg of propellant and pressurant used for performing ring hops and translations during the science mission.

The mass of the Cruise stage is estimated as ~12,200 kg (wet), and comprised of a ~1750 kg (dry) spacecraft, and ~10,500 kg of propellant and pressurant. The bulk of this propellant is used to correct and circularize the SRO orbit following aerocapture (delta V of 3400 m/s), with the remaining amount (delta V of 250 m/s) used for TCMs during the VEEJGA flybys and during Saturn approach. The aeroshell mass is estimated at approximately 4650 kg [48]. Though the mass of the aeroshell appears relatively high, it is lower than other credible near-term orbit insertion alternatives including the use of chemical rockets engines.

Ion thruster were initially considered for the SRO concept in order to reduce the propellant mass; however, preliminary analyses indicated that the additional power required to drive the ion thrusters would itself be mass prohibitive. That is, a multi-kW solar electric propulsion (SEP) system would be required during the cruise phase, and a $\geq$800 We radioisotope electric propulsion system (REP) needed during the science mission to hover above the ring plane. As a key mission goal was to minimize mass, lighter chemical rockets were baselined for this concept.

Table 2.5.1-8. Mass Estimates for the SRO Orbiter, Cruise Stage and Aeroshell

Subsystem	Mass, (kg)		
	All Units w/o Margin	Margin, %	All Units w/ Margin
Orbiter Stage (Dry)	**658**		**862**
Orbiter Stage (Wet)	**1614**		**1843**
Instruments	99	30%	129
VISIR	12	30%	16
Wide Angle Camera	2	30%	3
Narrow Angle Camera	50	30%	65
Electric Field / Plasma Probe	2	30%	3
Magnetometer	2	30%	3
Ionized Neutral Mass Spectrometer (INMS)	6	30%	8
Dust Detector	5	30%	7
LIDAR	20	30%	26
ACS	21	10%	23
C&DH	10	30%	13
Structures and Mechanisms	240	30%	312
Power	142	30%	184
Battery Li-Ion	8	30%	10
MMRTGs	135	30%	176
Power Conditioning	14	30%	18
Thermal	21	29%	27
Telecom	25	20%	30
Propulsion	87	23%	107
Propellant and Pressurant	956	3%	981
SRO Orbiter System Contingency	18	0%	18
Cruise Stage (Dry)	**1363**		**1757**
Cruise Stage (Wet)	**11594**		**12227**
C&DH	2	30%	3
Structures and Mechanisms	834	30%	1084
Thermal	51	29%	66
Telecomm	3	19%	4
Propulsion	307	26%	389
Propellant and Pressurant	10231	2%	10470
Cabling	53	30%	68
S/C Adapter	101	30%	131
Cruise Stage System Contingency	12	0%	12
Aeroshell	**4648**		**4648**
Total Launch Mass (Dry)	**6670**		**7266**
Total Launch Mass (Wet)	**17856**		**18718**

2.5.1.13 Radiation

The SRO spacecraft would be exposed to both external and internal sources of radiation during the course of its mission. While shielding would be required to protect delicate spacecraft electronics and key subsystems, the total radiation dose is expected to be relatively mild compared with other successful planetary missions (e.g., Galileo), and in line with that experienced by the Cassini spacecraft. External sources of radiation include solar wind, belts of charged particles trapped in planetary magnetic fields, galactic cosmic rays, and high-energy particles generated by solar events [49]. The total external radiation dose received by sensitive subsystems and instruments would not be expected to exceed ~20 krads (Si) behind 100 mils of aluminum shielding [49]. Radiation would also be produced by the plutonium within the three MMRTGs, consisting primarily of alphas from the decay of Pu and gammas and neutrons from spontaneous fission reactions of the impurities within the PuO_2 fuel. Alpha particles are also generated, but are trapped within the MMRTGs and thus are not an issue. The maximum internal radiation dose received by the instruments and sensitive subsystems is estimated at 30 krads [50] over the mission lifetime. The total radiation dose due both to external and internal sources is thus estimated at ~50 krads (Si). Employing a radiation safety factor of 2, the SRO spacecraft would use subsystem components rated for a minimum of 100 krads, well within the capability of existing technology (Galileo spacecraft components were rated significantly higher than the SRO mission). The fact that the Cassini spacecraft is operating flawlessly in orbit about Saturn illustrates that radiation shielding is not a significant driver for this mission.

2.5.1.14 Alternate RPS Power System

The SRO design concept described herein assumes the use of MMRTGs, but SRGs are another potentially attractive option assuming that the SRG-induced vibration and EMI environments do not interfere with operation of the narrow angle camera and plasma wave experiment. NASA/DOE guidelines [11] currently recommend that additional redundant SRGs be used to ensure power system reliability; thus, a Stirling-based power system would require four SRGs versus three MMRTGs. Fortunately, the lighter unit mass of the SRG (34 kg) means that the overall RPS power system would have approximately the same mass (four SRGs weigh approximately the same as three MMRTGs). Though a detailed thermal analysis was not performed for this mission concept, it is expected that the lower heat generation rate of the SRG would be preferred during the aerocapture maneuver where the excess thermal power would need to be stored for 15 or more minutes until aeroshell separation. Furthermore, the SRG would have the added benefit of lower plutonium usage (25% that of the MMRTG), which is particularly relevant as the United States does not currently possess a plutonium production capability and must purchase its Pu fuel from foreign sources.

2.5.2 Additional SRO Mission Options and Trade Studies

Multiple trade studies were performed in an effort to reduce the total mass of the SRO spacecraft such that it might fit on a single existing launch vehicle. The trades considered a reduced number of science instruments, a smaller narrow angle camera (NAC), a shorter mission duration, and exploration over a narrower span of the rings.

The lightest option (Option #1 in Table 2.5.2-1) represents the minimum mission assessed in this study, and would have a spacecraft mass of ~9,200 kg. This SRO mission variant would carry only four instruments, comprised of the WAC, NAC, LIDAR and VISIR. The NAC would use smaller optics to decrease its mass even further, but at the expense of reduced resolution of the ring particles (2.5 cm/pixel versus the baseline 0.5 cm/pixel). The mission duration would be 10

years for the cruise phase, with a nominal 30-day science mission as compared to the baseline 1-year mission. The ring-traverse range would be reduced to 10,000 km, but would still include exploration of the A and B rings. This option would represent a significantly reduced science mission relative to the baseline, both in scope and duration.

The second option (Option #2) is similar to Option #1, but would include the higher resolution 0.5-cm/pixel NAC and a radar altimeter. The total spacecraft mass of this option would be approximately 10,700 kg. The impact on the science mission would be slightly less that that of Option #1, due primarily to the larger focal length NAC, but would still be significantly reduced from the baseline.

The third option (Option #3) would include the same instrument complement as the baseline mission (8 instruments including the 0.5 cm/pixel resolution NAC) and would operate for 1 year in Saturn orbit; however, it would include only enough fuel to traverse 10,000 km across the ring plane (similar to options #1 and #2) as compared with 18,000 km of the baseline mission. The total spacecraft mass of this option would be 12,600 kg. Though less area of the ring plane would be explored in this option, this mission could potentially meet all science objectives and thus would represent only a minimal descoping of the baseline mission.

Table 2.5.2-1. Alternate SRO Mission Concepts Explored within the SRO Trade Study

Option	Instruments	Science Mission Duration	Ring Traverse Range	Circularize Delta V (m/s)	Science Mission Delta V (m/s)	S/C Mass (kg)
Baseline	WAC, NAC (0.5 cm), LIDAR, VISIR, Mag., Langmuir, INMS, Dust	1 year	18,000 km	3650	2273	18,718
1	WAC, NAC (2.5 cm), LIDAR, VISIR	30 days	10,000 km	3650	750	9,200
2	WAC, NAC (0.5 cm), LIDAR, Radar Altimeter, VISIR	30 days	10,000 km	3650	750	10,700
3	WAC, NAC (0.5 cm), LIDAR, VISIR, Mag., Langmuir, INMS, Dust	1 year	10,000 km	3650	1535	12,600

The conclusion of the mass trade study is that the minimum SRO mission would require a LV with at least 30% more launch capability than those currently in existence (including the Delta IV-Heavy), and that the baseline mission would require over 3 times the current launch mass capability. New EELV-derived launch vehicle concepts being considered for future Mars, Moon and JIMO missions could potentially be used to launch any of four SRO mission options considered in this study. One LV concept [46] would have a 28,000 kg launch capability to a C_3 of 15 km^2/s^2, providing a 50% mass margin for the heaviest (baseline) option detailed herein. This additional mass margin could be used to add additional science payload, to further expand the mission duration and/or ring traverse distance of the SRO Orbiter, or to decrease the travel time to Saturn.

Analyses were performed to assess the mission impact of increasing the minimum operating height of the Orbiter above the ring plane. Increasing this height could be desirable from a safety perspective, as the Orbiter would then be less likely to encounter stray ring particles at higher elevations. The result is that increasing the minimum operating height from 1 km to 2 km would double the required amount of fuel needed for making ring hops. Increasing the height from 1

km to 3 km would likewise triple the required fuel quantity. For the baseline spacecraft configuration, increasing the minimum operating height to 3 km would effectively decrease the duration of the science mission to four months (Figure 2.5.2-1). Additionally, increasing the Orbiter hopping height would decrease the effective ring particle resolution obtained using the baseline narrow angle camera. The reduction in resolution would be proportionate to the increase in hop height; for example, a 2-km minimum hop height would yield a 1-cm/pixel resolution, and a 3-km height would provide a 1.5-cm/pixel resolution. This reduction in resolution would decrease the ability to the Orbiter to meet the science goals, particularly regarding the measurements of ring particle dynamics and kinematics. A larger NAC could be used to maintain the baseline 0.5-cm/pixel resolution at higher operating heights, but with an associated mass penalty due to the need for larger optics.

Another trade study assessed the effect of varying the total ring translation distance upon the duration of the science mission for the baseline SRO spacecraft. Decreasing the ring translation distance of the Orbiter would make additional fuel available for ring hops, thus permitting an extended duration science mission. For example, a two-year mission could be achieved were the translation distance reduced to approximately half (~9,000 km) of the baseline distance. Conversely, additional regions of the rings could be explored were one willing to trade away propellant nominally used for ring hops. Thus, one could obtain an additional 5,000 km of ring traverse range (23,000 km total) at the cost of reducing the science mission duration to about 6 months. The results of these trades are illustrated in Figure 2.5.2-1.

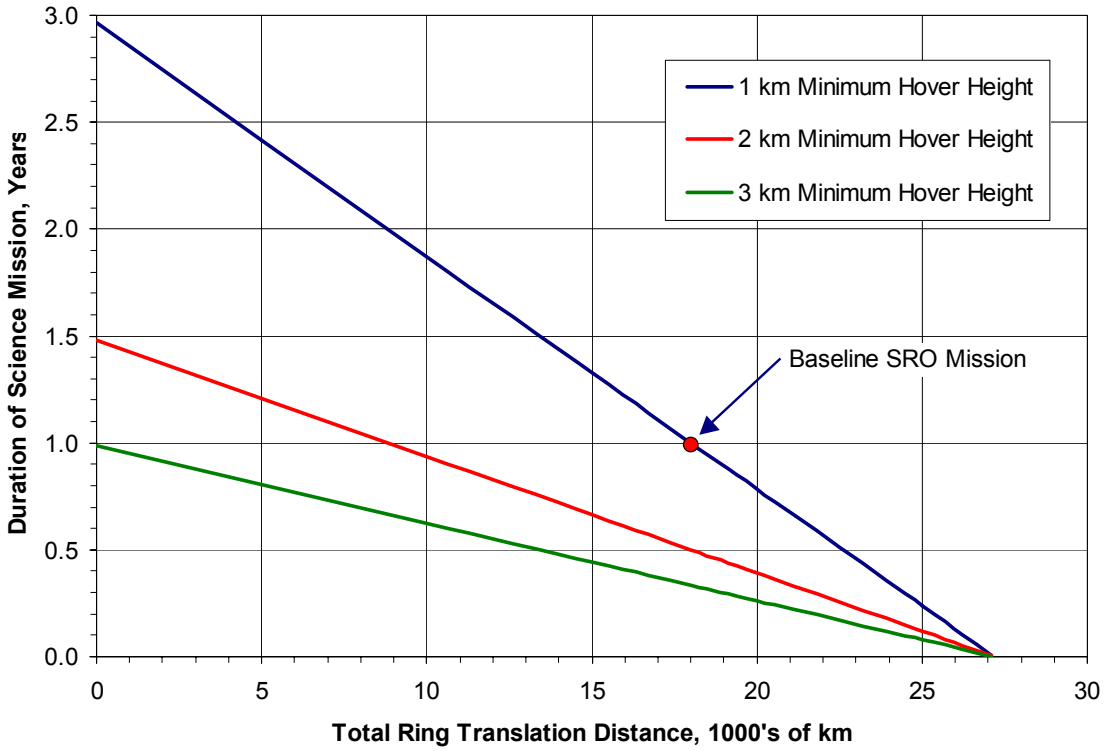

Figure 2.5.2-1. Trade of Science Mission Duration versus Ring Translation Distance and Minimum Hover Height for the Baseline SRO Orbiter Configuration.

2.5.3 SRO Summary and Conclusions

Saturn remains one of the most fascinating planets within the solar system. To better understand the complex ring structure of this planet, the SRO mission would spend one year in close proximity to Saturn's A and B rings and perform detailed observations and measurements of the ring particles and electric and magnetic fields. The SRO Orbiter would co-orbit close to the ring plane (1 to 1.4 km above the ring plane centerline), providing an unprecedented vantage point for making ring particle observations. These data would be used to enhance our understanding of the mechanisms of formation and evolution of planetary ring systems. Due to the long mission duration (11 years), low solar insolation at Saturn, and stringent spacecraft stability requirements, radioisotope power would be the only viable option for this mission. Three MMRTGs would be employed to provide 275 We (EOM) to power all instruments and subsystems, and would be augmented by lithium-ion batteries to provide load leveling during peak power usage. A natural follow-on to the Cassini-Huygens mission, SRO would be a challenging mission of significant scientific value.

This page is intentionally blank

3 POWER TECHNOLOGIES FOR STANDARD RPS SYSTEMS

The power conversion technologies considered for the standard-RPS mission studies were the Multi-Mission Radioisotope Thermoelectric Generator (MMRTG) and Stirling Radioisotope Generator (SRG). Both RPSs are designed to have similar performance characteristics in terms of power, lifetime, and operating environments, and both are planned to be available starting in 2009. The key differences between the MMRTG and SRG are their methods of converting thermal energy to electric power, the number of GPHS modules used to generate heat, and the associated conversion efficiencies.

This section presents the most current performance estimates of the MMRTG and SRG as of the time of this writing. However, both RPS systems are currently in development, and thus their performance values will evolve as their respective designs mature.

3.1 MULTI-MISSION RADIOISOTOPE THERMOELECTRIC GENERATOR (MMRTG)

The MMRTG is based on the thermoelectric converters used on the SNAP-19 RTG. The fundamental physical process involved in thermoelectric (TE) power conversion is the Seebeck effect, which is the electromotive force that arises between two dissimilar materials (i.e., metals or semi-conductors) when their electrical junction is subjected to a temperature difference. Thermocouples, used to measure temperature, are a common application of this effect. The electromotive force generated by the thermoelectric can be used to drive an electric circuit, or if large enough, a spacecraft power system. Thermoelectric converters are highly reliable, easily scalable, and can be designed to be highly redundant. Furthermore, TEs generate a power output that is load following and consequently easy to regulate, are compact, rugged, radiation resistant, and produce no noise, vibration or torque during operation. The disadvantage of thermoelectrics is their relatively modest conversion efficiency, resulting in lower power densities and greater fuel requirements compared to dynamic power converters.

The current MMRTG configuration is shown in Figure 3-1. It consists of three basic assemblies: the heat source, the converter, and the outer case/radiator. The heat source consists of eight GPHS modules similar to those used in the GPHS-RTG that was successfully flown on the Galileo and Cassini spacecraft.

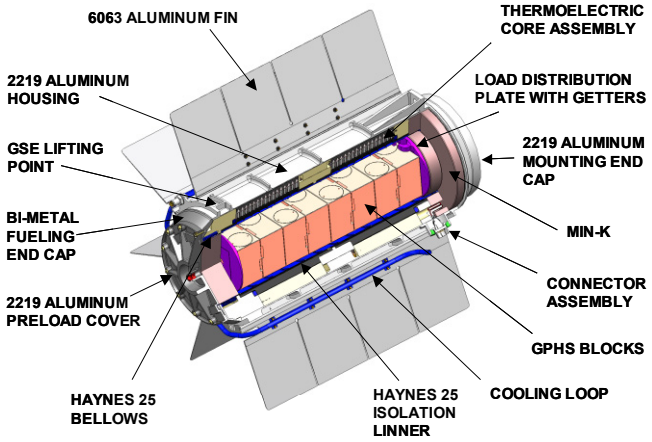

Figure 3-1. MMRTG Design Concept

The converter employs Lead-Telluride/Tellurides of Antimony, Germanium, and Silver (PbTe/TAGS) thermocouples, which have a history of use in diverse environments ranging from the oxidizing atmosphere of Mars to the vacuum of deep space. Much of the converter design, including the thermocouples, is based on the SNAP-19 RTG, which was successfully used on the Viking 1 and 2 Mars landers and the Pioneer 10 and 11 spacecraft. The outer case of the MMRTG and its integrated conduction fin radiator are made of aluminum.

Table 3-1. Current Top-Level Requirements for the MMRTG and SRG [10, 51, 52]

Requirement	MMRTG	SRG
Heat Source Quantity	8 GPHS Modules (~4 kg Pu^{238})	2 GPHS Modules (~1 kg Pu^{238})
Thermal Power at BOM	250 +/- 6 Wt per GPHS module	
Delivered Electrical Power	≥110 watts at BOM	
Environment	Operate in deep space and on surface of Mars. Deep Space thermal environment includes direct solar flux, and Earth albedo and IR at Earth departure (Table 3-2). The temperature of deep space is 4K. Mars surface is characterized as 5-10 torr CO_2 atmosphere with temperatures of 150-278K (Table 3-3). Identify impacts and approaches to withstand Titan atmosphere.	
Lifetime	Provide power for ≥14 years	
Voltage (Vdc)	Operate over a range of 22 – 36 Vdc and provide maximum power over the life of the mission with a spacecraft bus operating at 28 +/- 0.2 Vdc	
Reliability	Maximize reliability, including use of series-parallel circuitry for the MMRTG. Avoid single point failures.	
Mass	As small and lightweight as possible while maximizing specific power (W/kg)	
Power during launch	Maximize power during launch (e.g., produce ≥80% of nominal power during launch, returning to 100% of nominal power after end of launch sequence).	
Size	Fit within maximum acceptable envelope for DOE shipping container (USA/9904/B(U)-F-84 used to transport fueled systems.	
Operations	Allow use on missions involving multiple Venus gravity assist maneuvers.	
Random Vibration	Withstand the random vibration environment induced by the EELV, as defined in Table 3-4.	
Shock	Withstand the pyrotechnic shock induced by the payload fairing jettison and upper stage separation from the spacecraft, as defined in Table 3-5.	
Landing Loads	The maximum specified landing load is 30g, defined by airbag landing. The MMRTG is currently being designed to withstand 40g [52].	
EMI/EMC	Designed to EMI/EMC Standard 461C and meet magnetic requirements of 25 nT at 1-meter.	
Sterilization (Mars only)	NASA 4A or 4B	
Mission-specific Heat Rejection	Allow complete waste heat removal by cooling loops or by radiation heat transfer to space or any combination of both methods.	
Radiation Environment	Withstand radiation environments encountered on surface of Mars. Identify impacts and approaches to withstand total dose of up to 4 Mrads (Si) behind 100 mils of aluminum.	
Safety	Minimize impact to safety that components may have on integrity of GPHS modules and fuel clads during an accident. The generator design in and of itself shall not impede the free and clear release of GPHS modules under a reasonable range of inadvertent Earth reentry conditions established jointly by NASA and DOE. Use of passive design features to facilitate free and clear release of GPHS modules shall be considered.	

Table 3-2. Thermal Radiation Design Requirements [51]

Mission Phase	Solar Distance (AU)	Direct Solar Flux (W/m^2)	Reflected Solar (Albedo)	Planetary Infrared (W/m^2)	Atmosphere Attenuation (Tau)
Earth Orbit	1.01	0 to 1414	0 to 0.32	227 to 241	NA
Outbound Cruise	1.0 to 1.66	1414 to 490	N/A	N/A	N/A
Mars Arrival	1.6	0 to 710 (perihelion) 0 to 490 (aphelion)	0.332 (perihelion) 0.254 (aphelion)	128 (perihelion) 99 (aphelion)	0.2 to 0.5

Table 3-3. Mars Surface Thermal Environment [51]

Environment	Value
Radiation Sink Temperature	Sky: 123 to 172 K Ground: 150 to 304 K
Convective Environment	Atmosphere Temperature: 150 to 278 K Wind: Maximum of 30 m/sec Atmospheric Pressure: 5 to 10 torr
Surface Emissivity	0.6 to 0.8
Gas Composition	95.32% CO_2, 2.7% N_2, 1.6% Ar, 0.13% O_2, 0.07% CO, 0.03% H_2O)

Table 3-4. Random Vibration Requirements Due to EELV Launch Loads [51, 52]

Frequency, Hz	EELV	
	Qual Test	FA Test
20 - 50	+ 3 dB/Oct.	+ 3 dB/Oct.
50 - 250	0.20 g^2/Hz^*	0.10 g^2/Hz
250 - 350	- 6.0 dB/Oct.	- 6.0 dB/Oct.
350 - 1000	0.10 g^2/Hz	0.05 g^2/Hz
1000 - 2000	- 12 dB/Oct.	- 12 dB/Oct.
Overall	12.4 g_{rms}	8.7 g_{rms}
*Note: The MMRTG is being designed to 0.3 g^2/Hz (peak) and 15.1 g_{rms} (overall) in order to withstand the higher launch vibration loads of the Delta IV heavy.		

Table 3-5. Shock Requirements Due to EELV Pyrotechnic Loads [51]

Frequency (Hz)	Peak SRS Response (Q=10)
100	40 g
100 – 2,000	+ 10.0 dB/Oct.
2,000 – 10,000	6000 g

The MMRTG electrical output rate is a function of the cold shoe temperature of its thermoelectric modules that is driven by the ambient operating environment. The nominal MMRTG output power in deep space (DS) is currently predicted to be 125 We at BOM and 100 We after 14 years (Fig. 3-2), assuming a thermal output of 1984 watts (BOM) from eight GPHS modules [12]. For Mars applications, the power level is currently predicted to be 123 We at BOM and 98 We after 14 years assuming a Mars solar-noon temperature for the entire mission [12]. The corresponding expected system efficiencies at BOM are ~6.3% in deep space and ~6.2% on the surface of Mars.

The MMRTG power output degrades exponentially with time due to radioactive decay of the Pu fuel (~0.8%/year) and due to sublimation of the thermoelectric material (~0.8%/year). The electrical power degradation rate is the combination of the plutonium decay rate and the thermoelectric sublimation rate, and estimated at ~1.6%/year for the MMRTG.

As the MMRTG is still in development and its flight performance unverified, all mission studies herein conservatively assumed that it will generate 110 We (minimum specification value) and 2000 Wt at time of launch (i.e., BOM). This corresponds to a system efficiency of 5.5% at BOM. Additionally, it was conservatively assumed that the electrical power degradation rate was 1.7%/year, and the MMRTG would experience a 2-year storage and spacecraft integration duration between BOL and BOM. The MMRTG power levels used in the mission studies are presented in Table 3-6 as a function of time, and were assumed the same for both deep space and on the surface of Mars.

The mass of each MMRTG is currently estimated at ~43 kg, which includes the effect of design-

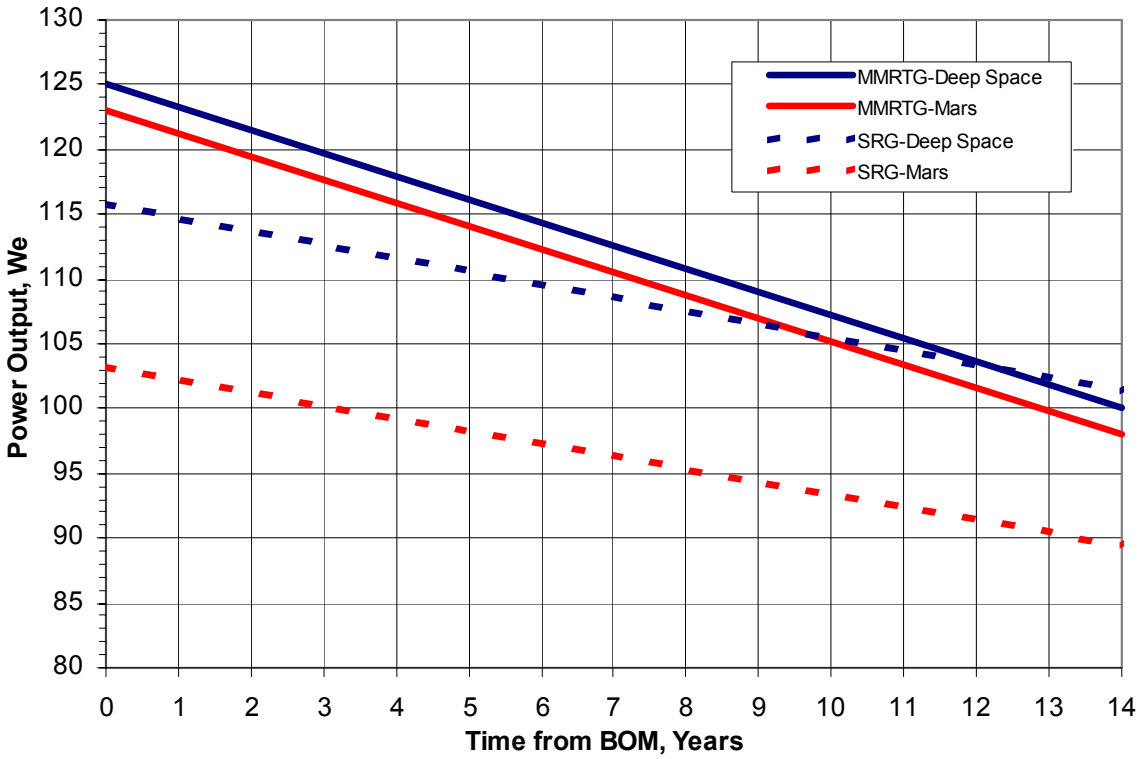

Figure 3-2. Predicted RPS Power Output in Deep Space as a Function of Time Relative to BOM [12, 13]

ing the MMRTG to withstand the higher launch loads of the Delta IV-heavy. The mass requirement of the MMRTG is ≤45 kg [52], which was assumed in the mission studies herein.

The MMRTG system is designed to operate over a voltage range of 22 to 36 Vdc, but is optimized to provide near maximum power to the spacecraft bus at 28 Vdc ± 0.2 over the design lifetime.

The MMRTG has eight thermally conductive fins located radially around the housing that are used to reject excess heat from the converter housing. The fins are coated with a high emissivity and low absorptivity material. A continuous auxiliary cooling tube runs axially along the base of each fin, which can be mated with an auxiliary heat removal system for mission phases in which active cooling is required. The dimensions of the MMRTG are provided in Figure 3-3.

Table 3-6. Estimated MMRTG Power Levels Assumed within the Mission Studies

Time from BOM (Yrs)	Thermal Power (Wt)	Electrical Power (We)
0	2000	110.0
1	1984	108.2
2	1969	106.4
3	1953	104.6
4	1938	102.9
5	1923	101.2
6	1907	99.5
7	1892	97.9
8	1878	96.3
9	1863	94.7
10	1848	93.1
11	1834	91.6
12	1819	90.1
13	1805	88.6
14	1791	87.1
15	1776	85.7
16	1763	84.3
17	1749	82.9
18	1735	81.5

The MMRTG EMI environment is composed of a DC magnetic field with a maximum magnetic field strength of 17 nT as measured off the centerline of the RTG (to one side) at a distance of 1 meter from the outer housing [54]. This satisfies the EMI requirement of ≤25 nT at 1-m distance.

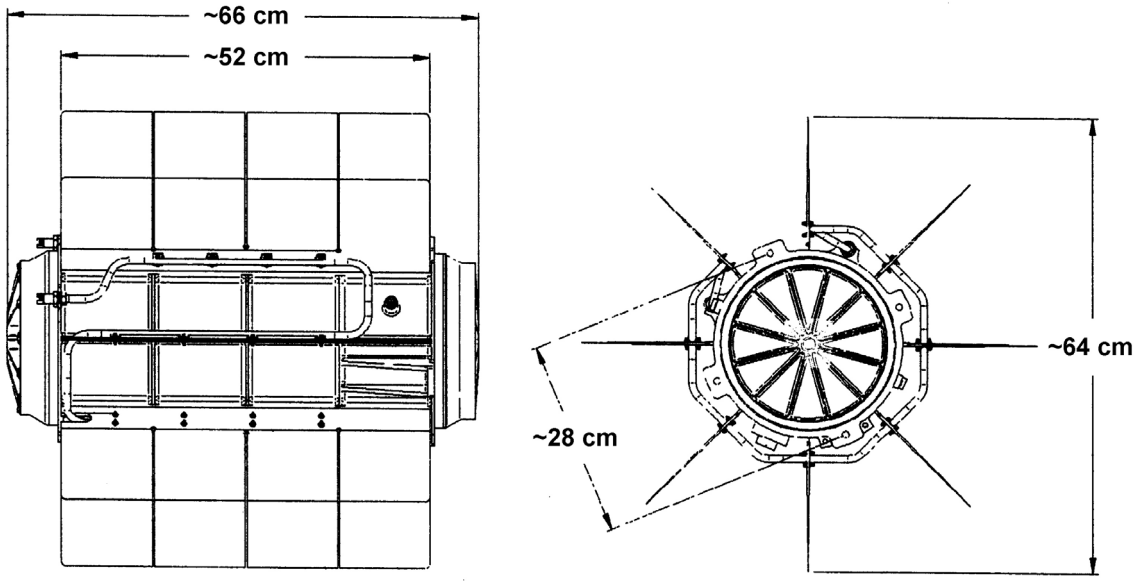

Figure 3-3. MMRTG Overall Dimensions [53]

3.2 STIRLING RADIOISOTOPE GENERATOR (SRG)

The SRG is similar to the MMRTG in terms of power output and multi-mission capability, but differs in that it employs a dynamic Stirling cycle for thermal-to-electric power conversion. This conversion process is roughly four times more efficient than thermoelectrics, resulting in each SRG requiring only two GPHS modules (one quarter that of the MMRTG) to produce a comparable power level.

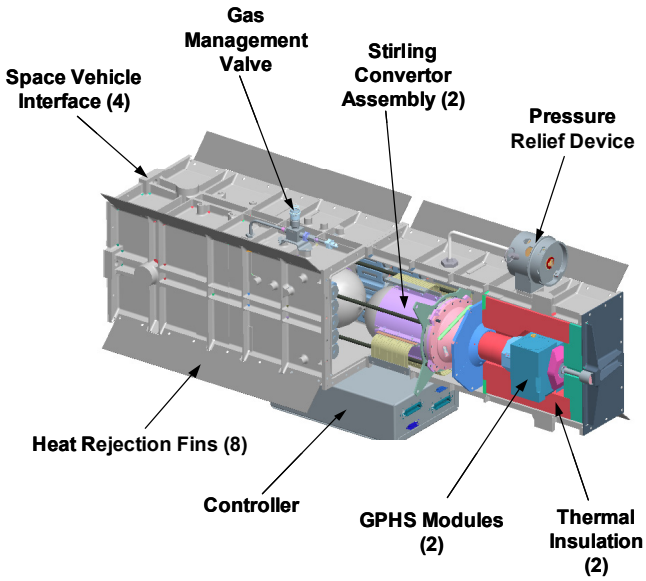

Figure 3-4. Stirling Radioisotope Generator [55]

The current SRG configuration, shown in Figure 3-4, consists of a beryllium housing, two Stirling converters, two GPHS modules located at either end surrounded by bulk thermal insulation, and an electronic controller and auxiliary components mounted on the housing exterior. Thermal-to-electric power conversion is performed by two free-piston Stirling engines, each integrated with a linear alternator within a common pressure vessel. Each closed-cycle Stirling engine converts the heat from one GPHS module into reciprocating motion with a linear alternator, thus producing an AC electrical power output that is then converted to DC power, yielding system efficiency between ~21% and 23% (BOM) depending on the ambient operating environment.

The SRG conversion efficiency is sensitive to the ambient environment, generating ~11% more electrical power in deep space versus that produced on the surface of Mars at BOM. The reduced electrical output on the Mars surface is due, in part, to the higher ambient temperature relative to deep space (resulting in lower Carnot efficiency), and to greater heat leakage from the converter due to thermal conduction and convection to the atmosphere. This results in less thermal energy available to be converted to electricity.

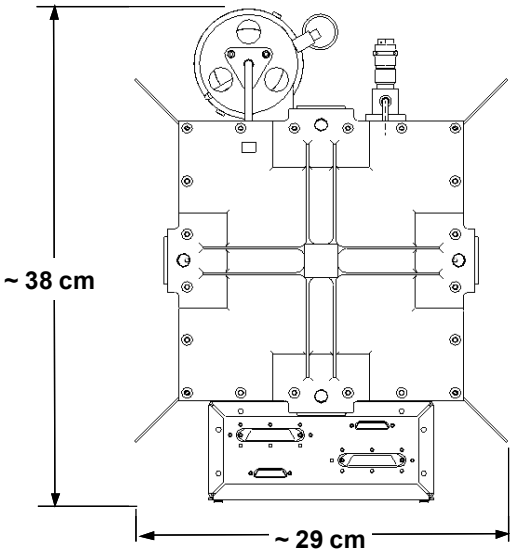

Figure 3-5. SRG Overall Dimensions [58]

The electrical output of the SRG is illustrated in Figure 3-3. In deep space (T_{amb}~4K), the SRG is currently predicted to deliver ~115.8 We at BOM and 101.4 We after 14 years with a nominal BOM thermal inventory of 496 Wt [13]. For Mars applications, the power level is currently predicted to be ~103.3 We at BOM and 89.6 We after 14 years [13]. This corresponds to system conversion efficiencies of approximately 23.3% in deep space and 20.8% on Mars at BOM.

As with the MMRTG, the SRG is still in development and its flight performance unverified. Therefore, the mission studies considered herein conservatively assumed the SRG electrical output in deep space to be 110 We at BOM (minimum specification value), with the time-dependent power output provided in Table 3-7. Within a Mars surface environment, the Lockheed Martin predicted values were assumed (Fig. 3-2 and Table 3-7). Electrical power output was assumed to degrade by a total of ~1%/year due to plutonium fuel decay (~0.8%/year) and degradation of the thermal insulation (~0.2%/year).

The mass of each individual SRG unit is currently estimated at 34 kg [57], which was assumed in the mission studies herein.

The SRG has four thermally conductive fins to reject excess heat from the converter housing. Located at the diagonal corners of the unit, each fin extends along the entire length of the 104-cm long SRG. The width (fin-tip to fin-tip) of the SRG is ~29 cm, and the height is ~38 cm (Fig. 3-5). An auxiliary cooling tube runs axially along the base of the unit, which can be mated with an auxiliary heat removal system for mission phases in which active cooling is required.

The EMI environment of the SRG remains to be fully characterized, and thus was not assessed in this study.

Table 3-7. Estimated SRG Power Levels Assumed in the RPS Mission Studies for Deep Space (DS) and Mars Environments

Time from BOM (Yrs)	Thermal Power (Wt)	Electrical Power in DS (We)	Electrical Power on Mars (We)
0	500	110.0	103.0
1	496	108.9	102.0
2	492	107.8	101.0
3	488	106.8	100.0
4	484	105.7	99.0
5	481	104.7	98.1
6	477	103.7	97.1
7	473	102.6	96.1
8	469	101.6	95.2
9	466	100.6	94.2
10	462	99.6	93.3
11	458	98.6	92.4
12	455	97.7	91.5
13	451	96.7	90.6
14	448	95.8	89.7
15	444	94.8	88.8
16	441	93.9	87.9
17	437	93.0	87.1
18	434	92.0	86.2

3.3 RPS PERFORMANCE COMPARISON MATRIX

The relative performance characteristics of the MMRTG and SRG are presented in Table 3-8 as a function of the operating location (deep space vs. surface of Mars) and as a function of the mission segment (beginning of mission vs. 14 years after BOM). The values in this table are believed to be the most accurate available at the time of this document, and are subject to change during the development cycle of both RPS units.

Table 3-8. Current Performance Parameters of the MMRTG and SRG [52, 59, 60]

RPS Parameters	MMRTG	SRG
General Characteristics		
Dimensions	66 cm (L) x 64 cm (W) x 64 cm (H)	104 cm (L) x 29 cm (W) x 38 cm (H)
Mass[1], kg	43	34
Number of GPHS Modules	8	2
Reference Thermal Inventory[2] at BOM, Wt	1984	496
T_{cold} at BOM, ^{o}C	208[3] / 189[4]	42[5] / 18[6]
Performance at BOM		
Deep Space		
Electrical power, We	125	116
Conversion Efficiency, (%)	6.3%	23.4%
Specific Power, We/kg	2.9	3.4
Mars Surface		
Electrical power, We	123	103
Conversion Efficiency, (%)	6.2%	20.7%
Specific Power, We/kg	2.9	3.0
Performance at 14 Years past BOM		
Deep Space		
Electrical power, We	100	101
Conversion Efficiency, (%)	5.5%[8]	22.8%[7]
Specific Power, We/kg	2.3	3.0
Mars Surface		
Electrical power, We	98	90
Conversion Efficiency, (%)	5.4%[8]	20.2%[7]
Specific Power, We/kg	2.3	2.6

Notes
1. Current estimates from Boeing and Lockheed Martin.
2. Reference thermal power numbers used to calculate system efficiencies for each RPS type.
3. Temperature at the MMRTG thermoelectric cold junction [52]
4. Temperature at the MMRTG fin root [52]
5. Temperature of the SRG SCA cold end [59]
6. Temperature of the SRG SCA alternator [59]
7. Data provided by [60]
8. Computed from MMRTG thermal inventory of 1805 Wt and indicated electrical output at 14 years.

4 ACKNOWLEDGEMENTS

The authors of this report gratefully acknowledge the follow individuals who contributed to the development of this document. All personnel are from JPL except where otherwise specified.

Section 1 to 2.2 Executive Summary and Mission Studies Introduction
Rob Abelson (Author)
Tibor Balint
John Elliott
Jim Randolph
George Schmidt, NASA HQ
Jim Shirley
Tom Spilker
Robert Wiley, DOE
Rebecca Richardson, DOE

Section 2.3 Lander Concepts
Tibor Balint (Author)
Jim Shirley (Co-Author)
Ellis Miner
New Product Development Team (NPDT)

Section 2.4.1 Mobility Concepts - Dual-Mode Lunar Rover Vehicle
John Elliott (Author)
Tim Schriener (Co-author)
Keith Coste (Co-author)
NPDT team
Ron Creel, SAIC

Section 2.4.2 Mobility Concepts - Aerobot
James Randolph (Author)
Wayne Zimmermann

Section 2.5 Satellite Concepts
Rob Abelson (Author)
Tom Spilker (Co-author)
Jim Shirley
Team X

Section 3 Power Technologies for Standard RPS Systems
Rob Abelson (Author)
Jack Chan, Lockheed Martin
Kip Dodge
Alan Harmon, DOE
Bill Otting, Boeing
Rebecca Richardson, DOE

Noel Sargent, GRC
George Schmidt, NASA HQ
Jeff Schreiber, GRC
Robert Wiley, DOE

New Product Development Team
Knut Oxnevad (Team Lead)
Kevin Anderson
Luther Beegle
Robert Carnright
Salvador Distefano
Raymond Ellyin
Nickolas Emis
David Hansen
Robert Haw
Michael D Henry
Timothy.Y.Ho
Steven D Keates
Daniel A Nigg
Guillermo Olarte
Cesar Sepulveda
Thomas I Valdez
Eric Woods

Team-X
Alan Hoffmann
Gene Bonfiglio
Richard Cowley
Adrian Downs
Ali Ghaneh
Bob Kinsey
Gerhard Klose
Brian Lewis
Jose Macias
Dennis Matthew
Jeff Padin
Partha Shakkottai
Bill Smythe
Paul Stella

Risk Communication
Mary Beth Murrill
Victoria Friedensen, NASA HQ
Sandy Dawson

5 REFERENCES

1. Burdick, G., “Multi-Mission Radioisotope Thermoelectric Generator (MMRTG) and Stirling Radioisotope Generator (SRG) Requirements Specification – Draft”, Jet Propulsion Laboratory, May 9, 2002.
2. NASA/GSFC Solar Probe Website, http://solarprobe.gsfc.nasa.gov/, September 2004.
3. Johns Hopkins University Applied Physics Lab, http://pluto.jhuapl.edu/mission.htm, November 2004.
4. Furlong, R. P., and E. J. Wahlquist, “U.S. Space Missions Using Radioisotope Power Systems”, Nuclear News, April 1999.
5. Nine Planets Website, http://www.nineplanets.org/, 2004.
6. Nine Planets Website, http://www.deepspace.ucsb.edu/ia/nineplanets/titan.html, 2004.
7. Shirley, J.H. and R.W. Fairbridge, *Encyclopedia of Planetary Sciences*, Chapman & Hall, London, 1997.
8. “New Frontiers in the Solar System—An Integrated Exploration Strategy,” National Research Council of the National Academies, 2003.
9. Bush, G. W., “A Renewed Spirit of Discovery”, http://www.whitehouse.gov/space/renewed_spirit.html, 2004.
10. Schmidt, G.R., “NASA’s Program for Radioisotope Power System Research and Development”, Solar System Exploration Division, Office of Space Science, NASA Headquarters, July 2004.`
11. Casani, J., et. al., “Report of the RPS Provisioning Strategy Team”, Jet Propulsion Laboratory, May 8, 2001.
12. Personal communication (e-mail) from Bill Otting, Boeing Rocketdyne, January 7, 2005.
13. Presentation chart provided by Jack Chan, Lockheed Martin, November 12, 2004.
14. Mehlem, K., Narvaez, P., “Magnetostatic Cleanliness of the Radioisotope Thermoelectric Generators (RTGs) of Cassini”, IEEE International Symposium on Electromagnetic Compatibility, Seattle, WA, August 2, 1999.
15. Sargent, N., Facca, L., Regan, T., “Magnetic Field Characterization Test of Free Piston 55W Stirling Engine Converter,” NASA GRC Test Report 55-008, May 29, 2002.
16. Winterhalter, D., Smith, E., Marquedant, R., “The Compact Electric and Magnetic Sensor”, Small Instruments for Space Physics, JPL Document D-12297, November 1993, pp. 2-33 to 2-39.
17. Website, http://en.wikipedia.org/wiki/Venus_(planet), September 2004.
18. Website, http://moon.pr.erau.edu/~holmesg/venus.html, September 2004.
19. Website, http://www.spacedaily.com/news/venus-04f.html, September 2004.
20. Benner, L.A.M., (1997) Triton. In *The Encyclopedia of Planetary Sciences*, J.H., Shirley & R.W. Fairbridge (Eds), Chapman & Hall (New York), 1997, pp. 836-840.
21. Website, http://www.solarviews.com/eng/triton.htm, September, 2003.
22. Website: http://www.nineplanets.org/triton.html, September, 2003
23. Watters, T.R., “Planets; Smithsonian Guides”, Macmillan, USA, 1995
24. Balint, T., "Europa Surface Science Package Feasibility Assessment", Report Number: JPL D-30050, Jet Propulsion Laboratory / California Institute of Technology; September 2004.
25. Mars Exploration Rovers Website, http://marsrovers.jpl.nasa.gov/home/index.html, NASA-JPL, 2004.

26. Balint, T. and J.F., Jordan, Jr., "Overview of NASA's Mars Exploration Program for the Next Decade", 2004 SAE Control & Guidance System Committee Meeting No. 94, Reno, Nevada, USA, November 2-4, 2004.
27. Anderson, P., "SRG110 Program Overview", Presented at the SRG-110 Program Briefing, Jet Propulsion Laboratory, Pasadena, CA, June 28, 2004.
28. Rovang, R., "Multi-Mission Radioisotope Thermoelectric Generator (MMRTG); MMRTG Preliminary Design Review Data Package", The Boeing Company, February 24, 2004.
29. Lipinski, R.J., et al., "Small Fission Power Systems for Mars", In El-Genk, M.S., (ed.), AIP Conference Proceedings #608, Space Technology and Applications International Forum (STAIF 2002), pp.1043-1053, Melville, NY, 2002.
30. Jun, I., "Peer review for radiation shielding approach", JIMO Technical Baseline Review-2, JIMO Government Study Team, January 29, 2004.
31. Noca, M, and R. W. Bailey, "Mission Trades for Aerocapture at Neptune", AIAA-2004-3843, AIAA/ASME/SAE/ASEE Joint Propulsion Conference and Exhibit, Fort Lauderdale, July 11-14, 2004.
32. Bailey, R., J. Hall, T. Spilker and N. Okong'o, "Neptune Aerocapture Mission and Spacecraft Design Overview", AIAA-2004-3842, AIAA/ASME/SAE/ASEE Joint Propulsion Conference and Exhibit, Fort Lauderdale, Florida, July 11-14, 2004.
33. Personal communications with Robert Haw, Jet Propulsion Laboratory, June 2004.
34. NASA-KSC, Launch vehicle database. Website: http://elvperf.ksc.nasa.gov/elvMap/.
35. Slaybaugh, J. C.. "Review of Dual-Mode Lunar Roving Vehicle (DLRV) Design Definition Study – Case 320", Bellcom, Inc., Washington D.C., October 29, 1969.
36. "Dual Mode Lunar Roving Vehicle Preliminary Design Study", Grumman Aerospace Corporation, February 1970.
37. Jun, I, "Design Cycle Two Review: Preliminary Radiation Environment", Jet Propulsion Laboratory Internal Document, June 13-14, 2002.
38. Jun, I, "Single Brick GPHS Total Dose Estimates", Jet Propulsion Laboratory Internal Document, December 23, 2003.
39. Manvi, R., W. Zimmerman, M. Quadrelli, S. Chao, A. Sengupta, C. Weisbin, "JPL Titan Design Study – RASC FY'03 Final Report", JPL Internal Document D-29084, 15 November 2003.
40. Kakuda, R. and T. Sweetzer, "Team X Titan Blimp Study", JPL Internal Document - Titan Blimp 01-06, June 4, 2001.
41. Abelson, R., et al., "Enabling exploration with Small Radioisotope Power Systems", JPL Pub 04-10, September 2004
42. Astrophysical Analogs Campaign Science Working Group (AACSWG).
43. Spilker, T.R., "Saturn Ring Observer", Acta Astronautica 52 (2003), 2002, pp. 259-265.
44. Website. http://solarsystem.nasa.gov/planets/profile.cfm?Object=Saturn&Display=Rings
45. Website. http://www.solarviews.com/eng/saturnrings.htm
46. Satter, C., et al., "Saturn/Titan Mission - JIMO Follow-On Mission Studies", Internal Team Prometheus Report, July 9, 2004, pp. 19.
47. "Why the Cassini Mission Cannot Use Solar Arrays", Jet Propulsion Laboratory, http://saturn.jpl.nasa.gov/spacecraft/safety/solar.pdf, November 1996.
48. Personnel Communication with Bernard Laub, Ames Research Center, May 2004.
49. Cassini Radiation Control Plan, PD 699-229, JPL D-8813, Jet Propulsion Laboratory, February 1993.

50. Personal correspondence with Alan Hoffmann, Cassini Environmental Requirements Engineer, Jet Propulsion Laboratory, August 2004.
51. Chan, J., "SRG110 Environmental Criteria and Test Requirements Specification – Revision 5.1", Lockheed Martin, August 11, 2004.
52. MMRTG Quarterly Management Review, Boeing, September 2004, pp. 17.
53. MMRTG Quarterly Review, Boeing, September 28, 2004, pp. 63.
54. MMRTG Magnetics Analysis Presentation, Boeing, June 4, 2004.
55. Personal Communication (e-mail) with Jack Chan, Lockheed Martin, November 19, 2004.
56. Personal Communication (e-mail) with Jack Chan, Lockheed Martin, November 2004.
57. SRG110 System Specification Rev. 3, Lockheed Martin, June 2004.
58. Personal Communication (e-mail) with Jack Chan, Lockheed Martin, November 19, 2004.
59. SRG EU PDR, Lockheed Martin, August 2004.
60. Personal Communication (e-mail) with Jack Chan, Lockheed Martin, November 22, 2004.

This page is intentionally blank

6 ACRONYMS AND ABBREVIATIONS

AC	Alternating Current
ACS	Attitude and Control System
AIMS	Acousto-Optic Imaging Spectrometer
AS	Active Sonde
ASTEP	Astrobiology Science and Technology for Exploring Planets
ASTID	Astrobiology Science and Technology Instrument Development
BOL	Beginning of Life
BOM	Beginning of Mission
C&DH	Command and Data Handling
CBE	Current Best Estimate
CCD	Charge Coupled Device
CDS	Command and Data System
CHAMP	Color Handlens Microscope
CTS	Communications Transfer Switch
DC	Direct Current
DOE	Department of Energy
DLVR	Dual Mode Lunar Rover
DMLRV	Dual Mode Lunar Rover Vehicle
DRDF	Directors Reasearch Discretionary Fund
DSN	Deep Space Network
DTE	Direct to Earth
EDL	Entry, Descent and Landing
EELV	Evolved Expendable Launch Vehicle
EMC	Electromagnetic Compatibility
EMI	Electromagnetic Interference
EOL	End of Life
EOM	End of Mission
FOV	Field of View
FPS	Frames Per Second

GC/MS	Gas Chromatograph/Mass Spectrometer
GCR	Galactic Cosmic Radiation
GPHS	General Purpose Heat Source
GPHS-RTG	General Purpose Heat Source – Radioisotope Thermoelectric Generator
GPR	Ground Penetrating Radar
GRC	Glenn Research Center
GRNS	Gamma Ray/Neutron Spectrometer
HGA	High Gain Antenna
HOMER	Heatpipe-Operated Mars Exploration Reactor
HXGR	Heat Exchanger
HYB	Hybrid
INMS	Ion and Neutral Mass Spectrometer
IMU	Inertial Measurement Unit
IR	Infra Red
I_{sp}	Specific Impulse
JIMO	Jupiter Icy Moons Orbiter
JPL	Jet Propulsion Laboratory
LADAR	Laser Detection and Ranging
LED	Light Emitting Diode
LGA	Low Gain Antenna
Li-Ion	Lithium Ion
LIBS	Laser Inducted Breakdown Spectroscopy
LIDAR	Light Detection and Ranging
LILT	Low Intensity Low Temperature
LV	Launch Vehicle
MER	Mars Exploration Rover
MGA	Medium Gain Antenna
MHW	Multi-Hundred Watt
MIDP	Mars Instrument Development Program
MMRTG	Multi-Mission Radioisotope Thermoelectric Generator

MLI	Multi Layer Insulation
MNFI	Microscopic Near Field Imager
MS	Mass Spectrometer
MSL	Mars Science Laboratory
NAC	Narrow Angle Camera
NASA	National Aeronautics and Space Administration
NEAR	Near Earth Asteroid Rendezvous
NEP	Nuclear Electric Propulsion
NIMO	Neptune Icy Moons Orbiter
NRC	National Research Council
NTO	Nitrogen Tetroxide
Pancam	Panoramic Camera
PCU	Power Converter Unit
PDU	Power Distribution Unit
PIDDP	Planetary Instrument Definition and Development Program
PNG	Passive Neutron Generator
Pu-238	Plutonium 238
PS	Passive Sonde
RAT	Rock Abrasion Tool
REP	Radioisotope Electric Propulsion
RPS	Radioisotope Power System
RTG	Radioisotope Thermoelectric Generator
SA	Solar Array
SDST	Small Deep Space Transponder
SEP	Solar Electric Propulsion
SPE	Solar Particle Event
SRG	Stirling Radioisotope Generator
SRO	Saturn Ring Observer
SNAP	Space Nuclear Auxiliary Power
TAGS	Tellurides of Antimony, Germanium and Silver
TCM	Trajectory Correction Maneuver

TCS	Thermal Control System
TEGA	Thermal and Evolved Gas Analyzer
TES	Thermal Emission Spectrometer
TM	Telemetry
TPS	Thermal Protection System
TRL	Technical Readiness Level
TWTA	Traveling Waveguide Tube Amplifier
ULF	Ultra Low Frequency
VDC	Volts (Direct Current)
VEEJGA	Venus Earth Earth Jupiter Gravity Assist
VJGA	Venus Jupiter Gravity Assist
VGA	Venus Gravity Assist
VISIR	Visual/Infrared
WAC	Wide Angle Camera
We	Watts (Electric)
Wt	Watts (Thermal)
WTS	Waveguide Transfer Switch